Life cycle environmental and economic assessments of zeolite 13X-based space heating systems

By

Tien Viet Tran

A thesis submitted in partial fulfilment of the requirements for the degree of

Master of Science

Department of Mechanical Engineering

University of Alberta

Abstract

The important role of a heat storage system in the transition to a low carbon economy is widely acknowledged in scientific literature. In cold regions like Canada, where fossil-based space heating systems are widely used, the associated greenhouse gas emissions (GHGs) are a major concern. The use of a zeolite 13X adsorbent heat storage system for space heating provides a promising alternative when integrated with renewable resources such as solar and wind. This study developed a bottom-up techno-economic and life cycle assessment models to understand the economic viability and environmental sustainability of the proposed heating system. The storage system is designed to replace a traditional 16 kW furnace installed in an average single detached house in Canada over a 20-year lifetime.

The life cycle greenhouse gas emissions are estimated to be 0.127 kg CO_2 eq per kWh of delivered heat. The largest contribution is due to energy consumption in the operational phase (71% of the total emissions). The material production stage accounts for 28%, primarily a result of the upstream emissions in the manufacturing of air solar collectors. The system is energy efficient due to its net energy ratio of 3.2. The ratio of adsorbent vessel length to diameter and the pallet diameter appear to be the most sensitive parameters both for GHG emissions and net energy ratio. The uncertainty analysis shows that GHG emissions and net energy ratio of the space heating system are in the range of 90.1-205.4 g CO_2 eq/kWh and 2.26-3.36, respectively. The low GHG emissions are a strong competitive aspect of zeolite-based space heating system.

At a cost of $0.05 to 0.06 per kWh of produced heat, the system appears to be competitive with existing space heating systems such as hot water heating electric boiler and hot water heating gas-fired boiler. Photovoltaic thermal air solar collectors are the largest portion of the capital investment, about 67% of the total system cost. Length-to-diameter ratio, zeolite pallet diameter, and solar collector potential were found to be most sensitive variables in Morris sensitivity analysis. Additionally, the system has a scale factor of 0.761, as developed in this study. The research highlights that adsorbent storage using solar heat for space heating is an economically feasible and environmentally sound alternative to conventional heating. The information developed in this study could be used to make investment decisions and formulate policy.

Preface

This thesis is original work by Tien Viet Tran under the supervision of Dr. Amit Kumar. Chapter 2, "Developing a framework to evaluate the life cycle energy and greenhouse gas emissions of space heating system using zeolite 13X as an adsorbent material" by Tien Viet Tran, Eskinder Gemechu, Abayomi Olufemi Oni, Ye Carrier, Handan Tezel, and Amit Kumar, has been submitted to *Journal of Energy Storage*. Chapter 3, "Developing a techno-economic model to evaluate the cost performance of a zeolite 13X-based space heating system" by Tien Viet Tran, Abayomi Olufemi Oni, Eskinder Gemechu, Handan Tezel, and Amit Kumar, has been submitted to *Energy Conversion and Management*. I was responsible for concept formulation, data collection and analysis, model development, and manuscript composition. Dr. E. Gemechu and Dr. A.O. Oni provided guidance to conduct the research and reviewed the papers. Dr. T. Handan and Dr. Y. Carrier provided data for designing the technical model for the studied system. Dr. A. Kumar was the supervisory author and was involved with the concept formation, result assessment, and manuscript composition.

Acknowledgements

I would like to thank Dr. Amit Kumar for his valuable guidance and support throughout my research. I have come to understand under Dr. Kumar that it is never too late to acquire knowledge in any field.

I appreciate the support of the NSERC Energy Storage Technology (NEST) Network (RYERU NSERC 468468 Kumar) and the University of Alberta (UOFAB VPRGRF NEST KUMAR) for the financial support provided to carry out this research. I am grateful to the NSERC/Cenovus/Alberta Innovates Associate Industrial Research Chair in Energy and Environmental Systems Engineering and the Cenovus Energy Endowed Chair in Environmental Engineering for providing financial support for this project.

The research brought me opportunities to work with professors and experts in different fields and understand their perspectives on specific topics. Being a part of the Hydrogen/Life cycle Assessment Group with great colleagues enhanced the quality of my work and broadened my understanding of energy systems. I would like to express my gratitude to my group leads, Dr. Abayomi Olufemi Oni and Dr. Eskinder Gemechu, for the continuous guidance throughout the course of my study. I am also thankful to Dr. T. Handan and Dr. Y. Carrier for providing experimental data on the zeolite 13X adsorbent heat storage system. Additionally, I really appreciate the dedicated editorial assistance from Astrid Blodgett on the papers.

I am very thankful for the unconditional love and support from my family over the years. I am also grateful for the help in both the research and daily life I received from my friends and colleagues during these years. It has been short but memorable time completing a master’s degree at the University of Alberta.

Table of Contents

List of Tables

List of Figures

Acronyms

Al-Fum	Aluminium fumarate
BTU	British thermal unit
CAD	Canadian dollar
CAU-10-H	Aluminium hydroxide isophthalate
CO_2	Carbon dioxide
eq	Equivalent
FAH	Force air heating
ft	Foot or feet
GHG	Greenhouse gas
GWP	Global warming potential
HP	Horsepower
hr	Hour
HRV	Heat recovery ventilator
HWH	Hot water heating
in	Inch
ISO	International Organization for Standardization
kg	Kilogram
kJ	Kilojoule
km	Kilometer
kW	Kilowatt
kWh	Kilowatt hour
L/D	Length/Diameter

LCA	Life cycle assessment
LiCl	Lithium chloride
m	Meter
m^2	Square meter
m^3	Cubic meter
mc-Si	Multicrystalline silicon
MJ	Megajoule
mm	Millimeter
mmBTU	One million British thermal units
NER	Net energy ratio
^oC	Degree Celsius
Pa	Pascal
poly-Si	Polycrystalline silicon
PV	Photovoltaic
PVT	Photovoltaic thermal
s	Second
SAPO	Silicoaluminumphosphates
sqft	Square foot or square feet
TCS	Traction control system
TEA	Techno-economic assessment
TES	Thermal energy storage
US$ and USD	United States of America dollar
W	Watt

yr	year

Nomenclature

m_1	Mass flow rate (kg/s) of stream 1
h_1	Enthalpy (kJ/kg) of stream 1
w_1	Humidity ratio (g/kg) of stream 1
ρ_{da}	Dry air density
ρ	Density
x	Humidity ratio
T	Temperature
Re	Reynolds number
V	Velocity
μ	Dynamic viscosity
e	Roughness (ft)
D	Diameter of duct (ft)
f	Friction factor
μ_o	Dynamic viscosity at the reference absolute temperature
T_0	Reference absolute temperature
C	Sutherland constant

Δp	Pressure drop
L	Length of zeolite vessel
ϵ	Void fraction of the bed
v_s	Superficial velocity
D_p	Equivalent spherical diameter of the packing
T_c	Temperature in Celsius
t	Zeolite vessel thickness
C_c	Allowance for corrosion
P	Maximum allowable internal pressure
r_i	Inside radius of zeolite vessel
S	Maximum allowable working stress
E_j	Efficiency of joints
C_n	Cost of new facility
C_r	Cost for reference size Q_r
Q_n	Capacity of new facility
Q_r	Reference size
m	Correlation exponent

f_m Installation factor

f_p Gage pressure

Q Flow rate (KSCFM)

Chapter 1
Introduction

1.1 Background

Canada is situated in a cold climate; many of its provinces experience daily average temperatures around -15 ºC in winter (Weather & Climate 2019), which results in a space heating intensity of more than 0.49 GJ/m^2 per year (Natural Resources Canada 2019). The most common heating system in North America is the forced air system, which uses a furnace and a blower fan to deliver air through a network of ducts (Formisano 2019). Natural gas is the main furnace fuel consumed; liquid propane, fuel oil, and electricity are occasionally used (Service Champions 2018). Another option for space heating is the natural gas boiler, which is efficient and compact (Formisano 2019). These systems are popular because of the low-cost, reliable gas technology and the abundance of natural gas resources in North America (Home Guide 2019). According to Statistics Canada, natural gas only accounts for 6% household energy use in Quebec but is the principle household energy source of other provinces like Alberta (72%), Saskatchewan (68%), Ontario (62%), and British Columbia (54%) (Statistics Canada 2011). Given that most space heating technologies rely heavily on fossil fuels, space heating contributed to more than 60% of end-use energy and made up the second highest share of GHG emissions in the Canadian residential sector in 2016 (Lemghalef and Sager 2019).

The Canadian Net-Zero Emissions Accountability Act introduced in Parliament in November 2020 confirms Canada's goal of net-zero emissions by 2050 (Government of Canada 2021). Achieving this target requires transforming the energy system, i.e., increasing energy efficiency, reducing the use of fossil fuels, switching to renewable energy resources and carbon capture and storage (Melillo et al. 2014; Environment and Climate Change Canada 2019). For the residential sector, replacing traditional fossil fuel systems with greener space heating systems is a key to substantially reducing GHG emissions in this sector.

One promising solution is to integrate renewable systems by harvesting renewable resources and storing excess energy in residential homes. In regions where electricity is generated from renewable energy sources such as hydro, solar, or wind, heat converted from electricity by electric furnace, boiler, or another system would be ideal. The energy efficiency resulting in reduced energy bills and the associated capital cost are critical factors in consumers' decisions. Incentives available for the mitigation of GHG emissions are also attractive to consumers. In regions with less severe climates and higher GHG emissions from electricity generation, a popular choice is the heat pump, which is energy efficient (Formisano 2019). A heat pump can be used for both heating and cooling by extracting heat from outdoor air or ground sources (Formisano 2019). In regions with high GHG emissions in the electricity generation sector and abundant solar irradiation, solar-based heating systems are an option. Liquid-based active solar heating and room air heaters are examples of harvesting and using energy at the household level (U.S. Department of Energy 2020). The advantage of these systems is reduced dependency on grid electricity.

Because of the intermittent nature of solar energy, a storage system is required with solar collectors or panels providing heat when required, even when solar irradiation is absent. Energy storage is an important bridge to overcome the intermittency issue and stabilize renewable energy production. Energy storage systems retain excess energy when renewable energy resources are abundant and regenerate the stored energy during downtimes or intermittency periods. Energy storage systems can be categorized as electro-chemical, mechanical, or thermal storage. Common mechanical energy storage includes flywheel, pumped hydro energy, and compressed air energy storage. Hydrogen energy storage is a typical example chemical energy storage. However, thermal energy storage systems have significant potential and are the focus of this research. More specifically, the study investigates zeolite 13X (an adsorbent) storage for space heating in residential homes.

Thermal energy storage (TES) stores heat for both short-term use and seasonal applications. TES is categorized into sensible, latent, and thermochemical storage. Zeolite 13X belongs to the thermochemical category, in which heat is stored as chemical energy or a chemical bond. Zeolite, a porous material made of hydrous silicates, is commonly used as an adsorbent or a catalyst in different industries including as ion-exchange water softeners, dishwasher detergents, CO_2 capture, and odor control (Krishna et al. 2002; Jänchen et al. 2004; Jänchen et al. 2012; Schumann et al. 2012; Woodford 2019; Sandomierski et al. 2020). The zeolite structure resembles a cage that accepts water molecules into its framework and generates heat as a product (Jänchen et al. 2004). Zeolite is categorized by its three-dimensional crystal structure as type A or type X (Burkes 2020). Zeolite 13X is usually applied through an air separation process with high purity oxygen. Zeolite 13X and water were chosen for the space heating system in this study because they are not toxic to humans and the chemical formula of each substance stays the same during the operation phase.

Zeolite 13X thermochemical storage is still in the research and development stage, and its sustainability is a topic of concern. Hence, for this research a life cycle assessment (LCA) model was developed to assess GHG emissions. In addition, a techno-economic model of the zeolite 13X heating system connected to solar collectors was developed to assess cost. The GHG emissions model provides insights into the GHG emissions from the different life cycle stages (extraction, production, manufacturing, operation, and recycling) of individual components as well as the whole system. The model is a powerful tool that can identify and address areas of greatest environmental impact. Another useful application of life cycle assessment is the comparison of the environmental impact of different technologies. This comparison can help policymakers, investors, and consumers understand whether to develop new technologies or use existing technology.

A critical aspect of sustainable development is the economics of a new technology. The techno-economic assessment (TEA) model in this research was built from the bottom up with a scalable model for each component. The levelized cost of generated heat was calculated so that technologies can be compared. Therefore, this research provides necessary information for the sustainable development of the proposed zeolite 13X system for space heating purposes.

1.2 Literature review

Research on adsorbent materials such as zeolite 13X focuses on screening or improving the energy density of adsorbent pairs to reduce their physical footprints while achieving safe and stable interactions during the operation phase. For example, Hua et al. tested the energy density of various adsorbent materials under low regeneration temperatures and relative humidity to simulate partial charging (2019). A study by Lefebvre et al. experimented on new synthesized adsorbents and developed a model to simulate adsorbent reactions in the storage vessel based on various adsorbent properties and engineering fundamentals (2016). Tatsidjodoung et al. also performed an experimental and numerical study on prototype zeolite 13X and water-based adsorbent for space heating (2016). An average 38 ºC temperature increase during 8 hours of discharge was achieved with an inlet air flow rate of 180 m^3/hour and specific air humidity of 10 g/kg (Tatsidjodoung et al. 2016). Similarly, Johannes et al. designed and conducted experiments with a 2,000W zeolite open reactor system that supplied heat for a 2-hour period (2015). The authors found that lower humidity during hydration and reduced air flow rate lowered the maximum power released. Finck et al. researched a zeolite system delivering 800W of heating power (2014). The authors concluded that the decrease in temperature between desorption (charging) and condensing (discharging) from 100K to 80K reduced energy density by 30% (Finck et al. 2014). Van Alebeek et al. reported a delivered power of 4.4 kW and capacity of 52 kWh from a 250 L zeolite 13X system (2018). Lowering the pressure drop in the system increases the thermal performance of the storage system (Van Alebeek et al. 2018). Zettl et al. achieved a temperature increase of 36K with approximately 12 kWh of stored energy in a 50 kg zeolite rotating reactor (2014). de Boer et al. developed a 150 kg zeolite 13X prototype to verify the feasibility of the long-term thermochemical storage (TCS) and the capacity to deliver thermal energy at temperatures useful for domestic application (2014). Many researchers have proposed the use of adsorbent storage for space heating, but they have not explored means of integrating the storage into space heating systems at a residential scale. Moreover, in the absence of a system design, the environmental performance and economic feasibility are not known. These are critical gaps in the literature.

Research exploring the applications and environmental performance of adsorbents such as zeolite 13X for space heating is scarce. Horn et al. compared the environmental impacts of innovative materials for thermal storage in buildings such as phase change and thermochemical materials (2018). The study showed that thermochemical materials have higher global warming potential than phase change materials, which is mainly due to the high energy requirement during the production and manufacturing stages of thermochemical materials. Nienborg et al. also performed a comparative assessment of silica gel, silicoaluminumphosphates (SAPO-34), zeolite 13X, CAU-10-H, aluminium fumarate MOF (Al-Fum), and lithium chloride (LiCl)-vermiculate (2018). This thesis, therefore, aims to fill the aforementioned knowledge gaps by developing an LCA model to extensively evaluate the environmental benefits of integrating zeolite-based storage with air solar collectors to supply space heating for residents in cold climate regions such as Canada. Moreover, analysing the energy efficiency of the whole life cycle through the perspective of the net energy ratio will provide a good understanding of system energy management and is also focus of this study.

Another knowledge gap in the literature on adsorbent storage for space heating system is related to the economic feasibility and the scale factor of the various components of the system. Scapino et al. studied the techno-economic optimization of a sorption system in different energy markets (2020). The system included two heat exchangers, a heat recovery device, sorption reactor, humidification unit, and valves. The authors concluded that the sorption thermal energy storage integration would increase system profits by 41% in certain scenarios in the UK market. The paper focused on large-scale heat storage that provides heat to a district heating system. A rough economic evaluation by Hauer for a 7,000 kg zeolite 13X system that covers a heat load of 95kW over a period of 14 hours is about 60,000 Euro (2007). A humidifier, water tank, control unit, and three modules of zeolite 13X are the main components in this model. Hauer developed a system to provide additional heating and cooling for a school. Zondag et al. determined investment costs to be around 10200 Euro and 28000 Euro for solar collectors integrated with 7000 kg low-cost sorption materials and zeolite, respectively (2010). The authors considered low-cost sorption materials, storage casing, vacuum tube collectors, collectors system components, heat exchangers, and the bore hole. Installation, operating, and maintenance costs were included in the model. All of this research focuses on large-scale heating systems and does not consider costs for small, residential household storage. Moreover, the economies of scale and the impact of variability of the input parameters on the outputs are not well addressed in the existing literature. Therefore, this thesis addresses these gaps by developing a comprehensive techno-economic assessment model of a zeolite 13X thermal storage system with a photovoltaic thermal (PVT) air system. The model was developed from the bottom up based on the main components necessary for the adsorbent system. Additionally, uncertainty and sensitivity analyses were conducted to improve the accuracy of estimates and to understand the effects of key input parameters on the results.

1.3 Research gaps

The following are the key knowledge gaps the thesis aims to address:

- There is very limited information in the literature on integrating adsorbent storage into space heating systems. Most of the research is at laboratory scale with little emphasis on how the system would fit into residential heating systems. To fill this gap, engineering design is used to simulate a space heating system and characterize the process flow. Information from the system design is used in life cycle assessment and techno-economic modelling.
- There is no system-based quantification of the life cycle GHG emissions of the whole adsorbent heating system. Environmental performance data is necessary as it is a crucial indicator of the sustainability of a new proposed system and for comparisons among technologies.
- The energy performance of adsorbent-based space heating system in terms of net energy ratio is unknown. The net energy ratio helps to understand whether a technology delivers energy efficiently and can be used to prioritize renewable energy systems for future development.
- Most techno-economic studies are on large-scale or district heating systems; none have been done for individual households. As for the economic aspect, to precisely quantify the

life cycle cost in terms of $ per kWh, an appropriate system design is required. A techno-economic assessment helps understand the economic viability of an energy system and make reasonable comparisons with existing space heating systems.

- No scale factor for the zeolite-based heating system has been developed. The scale factor indicates a system's economies of scale and helps us understand its cost advantages at different capacities. Using the base case as a reference, this can help in predicting cost of the proposed system at different capacities.
- Most of the studies do not include sensitivity and uncertainty analyses and hence do not provide information on the parameters that have the most influence on the results. Hence, refining the critical parameters and performing sensitivity and uncertainty analyses can help enhance the precision and accuracy of the results of both LCA and TEA models.

1.4 Objectives

The overall objective of the thesis is to develop bottom-up life cycle and techno-economic assessment models for zeolite 13X storage connected to solar collectors for space heating purposes. The main objective is met by accomplishing the following specific objectives:

- Designing a zeolite 13X and solar thermal collector heating system with a capacity of 16 kW of heat for 8 hours discharge.
- Developing an LCA model to evaluate the environmental performance of the heating system by estimating its life cycle GHG emissions and net energy ratio.
- Developing a techno-economic model to assess the levelized cost of energy delivery and the economies of scale of the zeolite-based heating system.

- Comparing the GHG emissions throughout the lifespan and the levelized cost of heat released with existing conventional heating systems.
- Conducting detailed sensitivity and uncertainty analyses to provide insights into critical factors and the uncertain parameters.
- Using the developed models to conduct a case study for Alberta, Canada.

1.5 Scope and limitations

Many working pairs in thermochemical storage, such as activated alumina with water and magnesium oxide with carbon dioxide, have been studied experimentally. This study focuses on designing a heating system around a commonly used working pair, zeolite 13X and water. The region of study is Alberta, Canada, where cold weather is present most of the year. Bottom-up LCA and techno-economic assessment models were developed for zeolite 13X storage connected to a PVT collector for space heating. Most of the data used in the models was taken from published sources, and some was obtained from manufactures. The main stages in the LCA are material extraction, production, manufacturing, operation, and recycling. The functional unit used in the LCA model is kWh of heat generated for space heating, and the energy and material requirements throughout the life cycle are translated to grams of carbon dioxide per the functional unit (g CO_2 eq/kWh). The techno-economic assessment is based on the individual equipment, which has its own scalable correlation. Thus, the scale factor of the whole system indicates how the investment cost will change relative to system capacity. The levelized cost of electricity delivery, expressed as $/kWh, is used a cost indicator in the techno-economic assessment. Uncertainty analysis was performed to capture the uncertainties in the data that led inconsistencies in studies, for instance in zeolite energy density or electricity grid emissions, and sensitivity analysis to understand the impact of each parameter and further refine the LCA and TEA models. Different heating systems are compared to provide policymakers and consumers the insights necessary to make decisions.

Assumptions made during the design phase led to certain limitations in the model. The zeolite storage was designed to raise the air temperature in a house from 15 to 25 ºC, so a lower initial room temperature (e.g., below 15 ºC) would shorten the duration of discharge, or the room would not reach 25 ºC. Hence, sufficient solar irradiation is an important factor to maintain daytime indoor temperature above 15 ºC and charge the zeolite 13X system for 8 hours of use during the night. Although air is a common transfer fluid for solar collectors, it was challenging to obtain up-to-date data on solar collectors both for the LCA and the techno-economic assessments. Hence, the data for air solar collectors in this paper is from 2005. For this study, the current price of solar collectors was estimated. Moreover, it is assumed that the zeolite would be obtained in North America and the heating system would be assembled on the continent as well. Finally, the outputs of the system were evaluated based on grid emissions, electricity price, water price, and solar irradiation in Alberta, Canada. These parameters should be adjusted accordingly if the system is used elsewhere.

1.6 Organization of the thesis

The paper-based thesis comprises four chapters that should be read independently. The chapters share some common information needed for the development of the models, so repetition is unavoidable. The outline of the thesis is as follows:

Chapter 1, Introduction: The chapter presents the motivation, the current status of the proposed technology, and general information about the study.

Chapter 2 describes the development of the life cycle assessment framework used to evaluate the energy and GHG emissions performance of space heating using zeolite 13X as an adsorbent material. In order to perform GHG emissions analysis, a zeolite-based heating system was designed to meet certain heating requirements; this designed model forms the base case of the research. Information from the model is used as input in developing the LCA model to quantify the amount of CO_2 released per kWh of heat during the lifespan of the system. The energy inputs and outputs were used to calculate net energy ratio in order to determine the energy efficiency of the heating system. Uncertainty and sensitivity analyses were carried out to understand the critical components of the model inputs. Finally, heating systems were compared to predict the feasibility and competitiveness of the designed system.

Chapter 3 presents the techno-economic evaluation of a space heating system using the adsorbent material zeolite 13X. A framework was developed to guide the modelling of the techno-economic performance of the system. The functional unit for ease of comparison is $ per kWh heat delivered. Investment costs from different life cycle phases provide valuable information that helps in estimating system costs. The economies of scale of the proposed system were developed to see how the cost is affected by changing production capacity. The space heating system was compared with other heating systems on the market to determine its competitiveness. Finally, sensitivity and uncertainty analyses were performed to identify input parameters that have significant impacts on the overall results and determine the likely range of the outputs.

Chapter 4 summarizes the new contributions from the research and the key highlights. The main conclusions are shared and recommendations for future work are proposed.

References

Burkes, K. 2020. 3A, 4A, 5A, 13X… What's the difference? HengYe Inc. https://hengyeinc.com/3a-4a-5a-13x-whats-the-difference/ (Date accessed: March 18, 2020).

Carbon Dioxide Information Analysis Center. 2017. CDIAC Data. https://cdiac.ess-dive.lbl.gov/ (Date accessed: August 6, 2020).

Center for Climate and Energy Solutions. 2019. Global Emissions. https://www.c2es.org/content/international-emissions/#:~:text=Globally%2C%20the%20primary%20sources%20of,72%20percent%20of%20all%20emissions. (Date accessed: July 20, 2020).

de Boer, R., S. Smeding, H. Zondag and G. Krol. 2014. Development of a prototype system for seasonal solar heat storage using an open sorption process, Petten: ECN.

Environment and Climate Change Canada. 2019. Government of Canada releases emissions projections, showing progress towards climate target,. https://www.canada.ca/en/environment-climate-change/news/2019/12/government-of-canada-releases-emissions-projections-showing-progress-towards-climate-target.html (Date accessed: August 6, 2020).

Environment and Natural Resources. 2020. Greenhouse gas emissions. https://www.canada.ca/en/environment-climate-change/services/environmental-indicators/greenhouse-gas-emissions.html (Date accessed: August 4, 2020).

Finck, C., E. Henquet, C. van Soest, H. Oversloot, A.-J. de Jong, R. Cuypers and H. Van T'Spijker. 2014. Experimental results of a 3 kWh thermochemical heat storage module for space heating application. Energy Procedia **48**(0): 320-326.

Formisano, B. 2019. Types of Home Heating Systems. The Spruce. https://www.thespruce.com/types-of-home-heating-systems-1824772 (Date accessed: March 18, 2020).

Government of Canada. 2021. Net-Zero Emissions by 2050. https://www.canada.ca/en/services/environment/weather/climatechange/climate-plan/net-zero-emissions-2050.html (Date accessed: April 24, 2021).

Hauer, A. 2007. Adsorption systems for TES—design and demonstration projects. Thermal energy storage for sustainable energy consumption**:** 409-427, Springer.

Home Guide. 2019. How Much Does a New Furnace Replacement Cost? https://homeguide.com/costs/new-furnace-replacement-cost (Date accessed: April 21, 2020).

Horn, R., M. Burr, D. Fröhlich, S. Gschwander, M. Held, J. P. Lindner, G. Munz, B. Nienborg and P. Schossig. 2018. Life cycle assessment of innovative materials for thermal energy storage in buildings. Procedia CIRP **69**: 206-211.

Hua, Y., B. Ugur and F. H. Tezel. 2019. Adsorbent screening for thermal energy storage application. Solar Energy Materials and Solar Cells **196**: 119-123.

International Energy Agency. 2019. World Energy Outlook 2019. (Date accessed: August 6, 2020).

International Energy Agency. 2020. Global CO2 emissions in 2019. https://www.iea.org/articles/global-co2-emissions-in-2019 (Date accessed: June 25, 2020).

Jänchen, J., D. Ackermann, H. Stach and W. Brösicke. 2004. Studies of the water adsorption on zeolites and modified mesoporous materials for seasonal storage of solar heat. Solar Energy **76**(1-3): 339-344.

Jänchen, J., K. Schumann, E. Thrun, A. Brandt, B. Unger and U. Hellwig. 2012. Preparation, hydrothermal stability and thermal adsorption storage properties of binderless zeolite beads. International Journal of Low-Carbon Technologies **7**(4): 275-279.

Johannes, K., F. Kuznik, J.-L. Hubert, F. Durier and C. Obrecht. 2015. Design and characterisation of a high powered energy dense zeolite thermal energy storage system for buildings. Applied Energy **159**: 80-86.

Krishna, R., B. Smit and S. Calero. 2002. Entropy effects during sorption of alkanes in zeolites. Chemical Society Reviews **31**(3): 185-194.

Lefebvre, D., P. Amyot, B. Ugur and F. H. Tezel. 2016. Adsorption prediction and modeling of thermal energy storage systems: a parametric study. Industrial & Engineering Chemistry Research **55**(16): 4760-4772.

Lemghalef, L. and J. Sager. 2019. The future of home heating: Hybrid home heating systems offer energy savings and reduce GHG emissions. Natural Resources Canada. https://www.nrcan.gc.ca/simply-science/future-home-heating-hybrid-home-heating-systems-offer-energy-savings-and-reduce-ghg-emissions/22236 (Date accessed: March 18, 2020).

Melillo, J. M, T. T. C. Richmond and G. W. Yohe. 2014. Climate Change Impacts in the United States: The Third National Climate Assessment. United States of America, U.S. Global Change Research Program.

Natural Resources Canada. 2019. Energy Efficiency Trends in Canada 1990 to 2013. Office of Energy Efficiency. https://www.nrcan.gc.ca/energy/publications/19030 (Date accessed: October 31, 2019).

Nienborg, B., T. Helling, D. Fröhlich, R. Horn, G. Munz and P. Schossig. 2018. Closed adsorption heat storage—A life cycle assessment on material and component levels. Energies **11**(12): 3421.

Sandomierski, M., B. Strzemiecka and A. Voelkel. 2020. The influence of ion exchange in zeolite X on the properties of phenol-formaldehyde composites. International Journal of Adhesion and Adhesives: 102625.

Scapino, L., C. De Servi, H. A. Zondag, J. Diriken, C. C. Rindt and A. Sciacovelli. 2020. Techno-economic optimization of an energy system with sorption thermal energy storage in different energy markets. Applied Energy **258**: 114063.

Schumann, K., B. Unger, A. Brandt and F. Scheffler. 2012. Investigation on the pore structure of binderless zeolite 13× shapes. Microporous and Mesoporous Materials **154**: 119-123.

Service Champions. 2018. 7 Home Heating System Types. https://www.servicechampions.net/blog/7-home-heating-system-types/ (Date accessed: March 18, 2020).

Statistics Canada. 2011. Households and the Environment: Energy Use. https://www150.statcan.gc.ca/n1/en/pub/11-526-s/11-526-s2013002-eng.pdf?st=rCDt1deo (Date accessed: December 20, 2020).

Tatsidjodoung, P., N. Le Pierrès, J. Heintz, D. Lagre, L. Luo and F. Durier. 2016. Experimental and numerical investigations of a zeolite 13X/water reactor for solar heat storage in buildings. Energy Conversion and Management **108**: 488-500.

The United Nations. 2016. The Paris Agreement. https://unfccc.int/process-and-meetings/the-paris-agreement/the-paris-agreement (Date accessed: June 27, 2019).

U.S. Department of Energy. 2020. Active Solar Heating. https://www.energy.gov/energysaver/home-heating-systems/active-solar-heating (Date accessed: August 6, 2020).

Van Alebeek, R., L. Scapino, M. Beving, M. Gaeini, C. Rindt and H. Zondag. 2018. Investigation of a household-scale open sorption energy storage system based on the zeolite 13X/water reacting pair. Applied Thermal Engineering **139**: 325-333.

Weather & Climate. 2019. Climate and Average Weather in Canada. https://weather-and-climate.com/average-monthly-Rainfall-Temperature-Sunshine-in-Canada (Date accessed: June 25, 2020).

Woodford, C. 2019. Zeolites. https://www.explainthatstuff.com/zeolites.html (Date accessed: March 18, 2020).

World Resources Institute. 2017. Climate Analysis Indicators Tool. http://cait.wri.org/ (Date accessed: August 6, 2020).

Zettl, B., G. Englmair and G. Steinmaurer. 2014. Development of a revolving drum reactor for open-sorption heat storage processes. Applied thermal engineering **70**(1): 42-49.

Zondag, H., V. van Essen, M. Bakker and P. Bach. 2010. An evaluation of the economical feasibility of seasonal sorption heat storage, Petten: ECN.

Chapter 2

Developing a framework to evaluate the life cycle energy and greenhouse gas emissions of space heating system using zeolite 13X as an adsorbent material

1. Introduction

There is growing global consensus on the adverse impacts of global warming due to anthropogenic greenhouse gas (GHG) emissions. More than ninety-seven percent of climate scientists agree that the global warming trend has a strong correlation with human activities (NASA 2020). As a global response, the Paris Agreement was established in order to limit the earth's average temperature rise well below 2 ^{o}C (The United Nations 2016). Several pathways have been suggested to transform the global energy system to meet the reduction target. Among the pathways are energy efficiency improvement, carbon capture and storage technologies, and a shift towards renewable and low carbon energy sources such as bioenergy, nuclear power, and solar and wind energy (Kriegler et al. 2014; Rogelj et al. 2015; Child et al. 2018; Kalair et al. 2020). Renewable energy sources such as solar and wind are intermittent and these needs to be stored for continuous supply of energy.

Heat and electricity storage systems have important roles in the decarbonization of the energy system as they help increase the share of renewable energy sources in electricity generation. Integrating thermal energy storage (TES) with renewable energy provides a viable solution to the intermittent nature of solar and wind energy systems by storing excess energy when there is an abundance and discharging when the renewable source is not available (Díaz-González et al. 2012; Zhang et al. 2016). Thermal energy can be contained in various media under different mechanisms such as sensible, latent, and thermochemical storages (Socaciu 2011; Cabeza (ed.) 2014). Sensible heat storage such as molten salts is used for electricity generation but it requires a high operating temperature (Thaker et al. 2017). Latent heat storage, which is still under research and development, has a relatively high energy density but suffers from poor heat transfer, substantial heat loss, and supercooling (Mehari et al. 2020). Thermochemical storage such as adsorbents does not require an extremely high charging temperature. Adsorbent storage integrated with solar collectors could be used for space heating for a home, office, or warehouse. While both adsorbents and solar collectors have been well studied for different applications, the combined use of the two for space heating purposes has not been investigated. This research, therefore, aims to provide a novel contribution by designing an integrated system and evaluating its environmental and economic performance.

Most of the studies related to adsorbent materials focus on improving the energy density as well as developing models to monitor the storage performances. Hua et al. investigated the energy density of various adsorbent materials under low regeneration temperature and relative humidity (2019). The research by Lefebvre et al. synthesized new adsorbent materials and developed simulation models to predict the performances of adsorbents (2016). Studies by Dicaire and Tezel showed a high regeneration potential of adsorbents such as alumina/zeolite 13X with no loss in performance, which is an ideal characteristic for renewable energy storage applications (Dicaire and Tezel 2011, 2013). Horn et al. compared the environmental impacts of innovative materials for thermal storage in buildings such as phase change and thermochemical materials (2018). Nienborg et al. also performed a high level comparative assessment of storage materials (2018). Research exploring the application and environmental performance of adsorbents such as zeolite 13X for space heating is scarce. This paper aims to fill these knowledge gaps by developing an

LCA framework to extensively evaluate the GHG emissions of integrating zeolite-based storage with air solar collectors to supply space heating in cold climates.

A heating system is an essential part of every household in locations with cold climate. Space heating accounted for 61% of end-use energy and contributed the second highest GHG emissions in the Canadian residential sector in 2016 (Lemghalef and Sager 2019). Within same year, residential buildings in the world totaled to 10.9% emissions including GHG from fossil fuel combustion and electricity usage (Climate Watch 2016; Ge and Friedrich 2020). Forced air systems using a furnace and a blower fan to deliver air to rooms through a network of ducts is the most widely used heating system (Formisano 2019). Natural gas is the typical fuel for furnaces in North America and Europe, and liquid propane, fuel oil, and electricity are the main alternatives (Service Champions 2018). The relatively inexpensive gas furnace combined with the abundance of natural gas makes it affordable (Home Guide 2019). Another choice for space heating systems is a hot water boiler with radiator distribution, often used in less severe climates. Modern boilers are highly energy efficient and maintain air quality, compared to the dry air from a forced-air heating system (Formisano 2019). Heat pumps are also installed to provide both heating and cooling in places where the temperature rarely dips below the freezing point (Service Champions 2018). Heat pumps use waste heat from the surrounding environment and are highly efficient in warmer climates (Formisano 2019). While economic viability is still an important factor when considering a heating system, environmental aspects are becoming a key measurement of the technology's sustainability. Because the residential sector is one of the demand sectors which is responsible for a significant portion of GHG emissions globally, it is worth looking for environmentally sustainable alternatives to the conventional heating systems. In this context, this research looks at how zeolite 13X absorbent thermochemical storage integrated with solar collectors could be used for space heating in residential homes and what the GHG emissions are compared with the natural gas, liquid propane, fuel oil, and electricity-based furnaces widely used.

Zeolite, a porous material made of hydrous silicates, is commonly used for adsorbents or catalysts including as ion-exchange water softeners, dishwasher detergents, CO_2 capture, and odor control (Krishna et al. 2002; Jänchen et al. 2004; Jänchen et al. 2012; Schumann et al. 2012; Woodford 2019; Sandomierski et al. 2020). It has a cage-like structure that allows water molecules to enter the framework and generate heat as a side product (Jänchen et al. 2004). Zeolites are grown in three-dimensional crystal structures as Type A or Type X (Burkes 2020). Zeolite 13X is usually used in air separation processes with high purity oxygen. The working pair of zeolite 13X and water was chosen for space heating systems because it is not toxic to humans and no additional chemicals are produced during operation phase. The materials with non-toxic properties are commonly used in different applications but the environmental concerns relating to the whole system involving adsorbent have not been investigated extensively.

Tatsidjodoung et al. performed an experimental and numerical study on prototype zeolite 13X and water-based adsorbent for space heating (2016). A 38 ºC average lift temperature with 8 hours discharge was achieved with an inlet air flow rate of 180 m^3/hour and specific air humidity of 10 g/kg (Tatsidjodoung et al. 2016). Similarly, Johannes et al. designed and characterized a zeolite thermal energy storage system that supplied 2,000 W sensible heat power for 2 hours (2015). Significant temperature lift can be observed in the experimental results, 38 ºC with 8 hours of discharging (Johannes et al. 2015). Finck et al. researched a zeolite system delivering 800 W of heating power and found that decreasing temperature between desorption (charging) and condensing (discharging) from 100 K to 80 K lowered the energy density by 30% (Finck et al. 2014). Van Alebeek et al. reported a delivered power of 4.4 kW and capacity of 52 kWh from a

250L of zeolite 13X system (2018). Lowering the pressure drop in the system would increase the thermal performance of the storage system (Van Alebeek et al. 2018). However, the environmental sustainability of these new systems has not been widely studied. Hence, this paper aims to fill the knowledge and literature gaps by developing a bottom-up LCA model to estimate the GHG and net energy ratio of a zeolite 13X-based thermal storage system integrated with solar thermal collectors for space heating. The specific objectives of the study are to:

- Design a simulation model for space heating system using zeolite 13X and solar thermal collectors with a capacity of 16 kW of heat for 8 hours discharge;
- Use an LCA framework to estimate the life cycle GHG emissions and net energy ratio of the heating system;
- Perform sensitivity and uncertainty analyses to provide insights into critical factors and uncertain parameters which affect the life cycle GHG emissions;
- A case of Canada, a cold climate, for implementation of this system was conducted.

2. Method

Figure 2.1 presents the framework developed in this research. The framework comprises a system review, engineering design, and environmental assessment. The system review stage involves defining the heating system, identifying the key components, and setting the workflow and system boundary. A system of interest was designed based on the existing literature and developed information. In this study, the heating system is designed to determine the size of each component. The GHG emissions is based on LCA concept. Each component of the framework is discussed in detail in the following section.

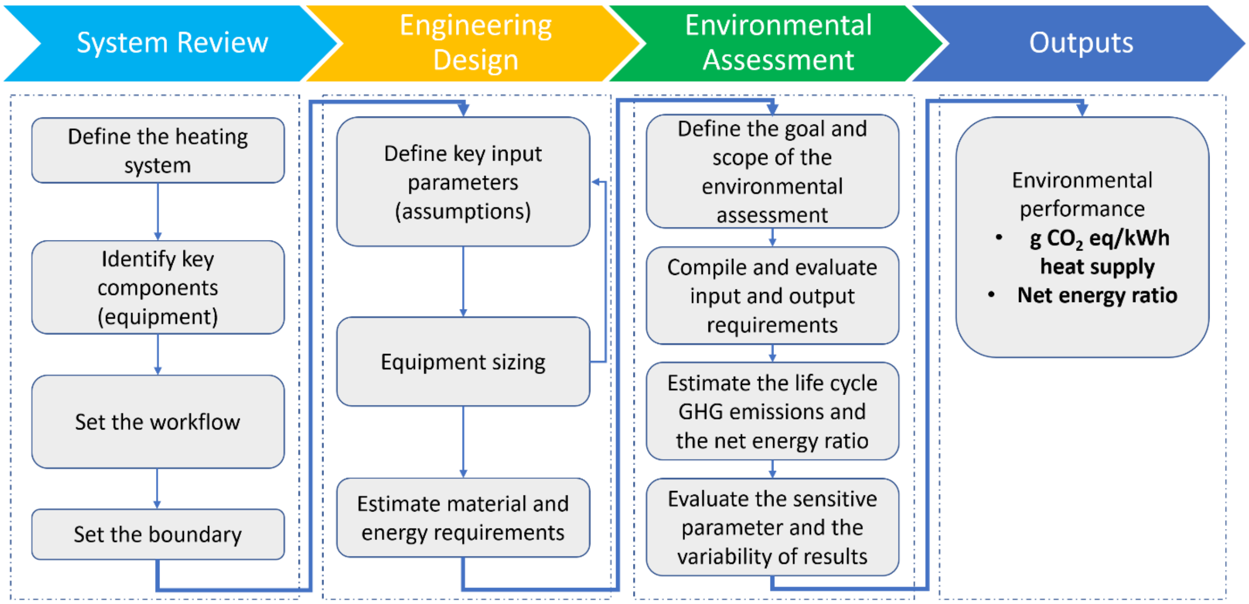

Fig. 2.1: **Developed framework for the study**

2.1 System review

Figure 2.2 illustrates the open-cycle zeolite 13X space heating system with solar collectors. The chosen working pair is zeolite 13X and water as both are poison-free and do not generate toxic chemicals during the operating phase. The heating system mainly comprises an insulated vessel, two fans, two humidifiers, ductwork, and solar collectors.

There are repetitive cycles of charging and discharging during the operational phase. For the charging cycle, the intake air from outside the house (or inside the building) is heated by being passed through a heat source, solar air collectors in this case. The hot air flows through the storage container and evaporates water molecules attached to the adsorbent pellets. The outlet humid air is disposed of outside. During the discharging cycle, high humidity air at room temperature is passed through the adsorbent bed to extract heat from the thermal storage. As water molecules in the airstream form weak bonds with the adsorbent material in the storage, heat is released through an exothermic reaction. The hot dry air from the outlet is used for space heating with the assistance of other equipment to adjust the relative humidity.

The charging phase requires the fans (1a and 1b) as shown in Fig. 2.2, heat source, storage container (6), and solar collectors (4) to be on active mode. The fan regulates the air flow rate through the solar heat source and storage container before the air is released outdoors. All the devices except the heat source run during the discharging cycle. Humidifier 2a (Fig. 2.2) increases the relative humidity of the airstream from fan 1a to above 90%. This saturated air passes through the container where it absorbs heat to increase the temperature while dehumidifying the stream. Fan 1b and humidifier 2b are used to modify the hot dry air from the adsorbent bed to a comfortable heat level distributed to rooms.

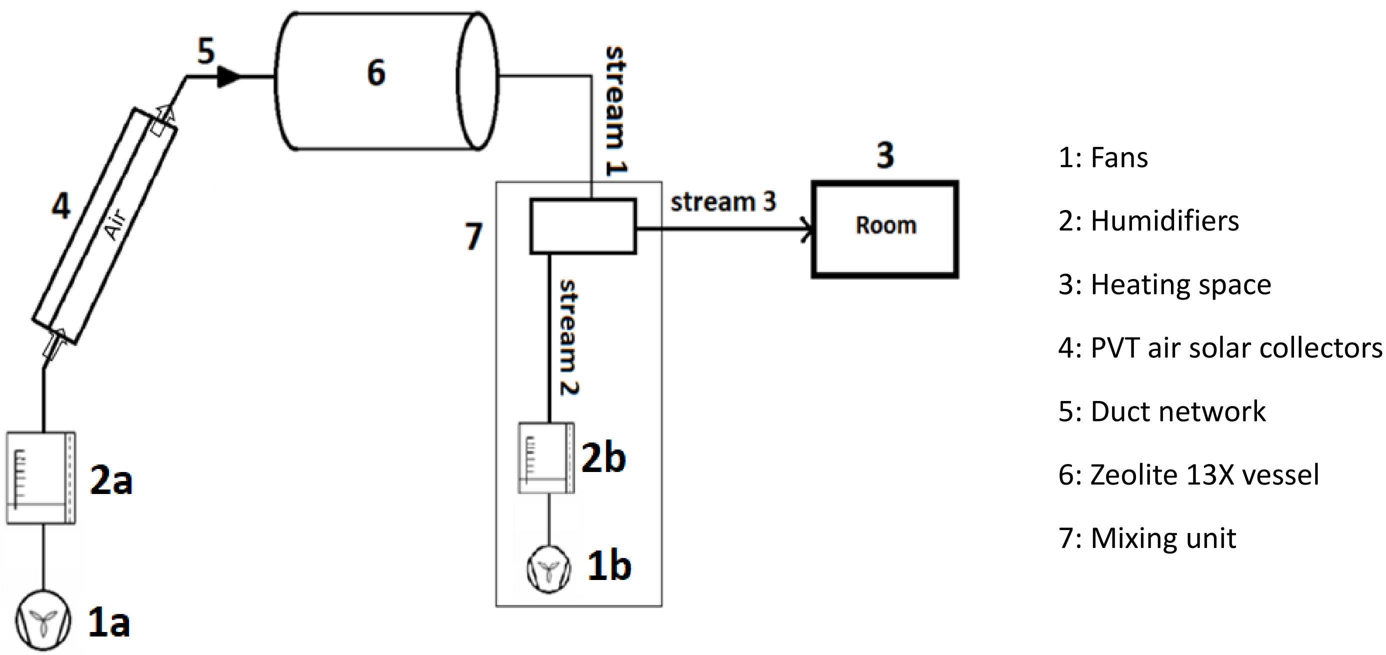

Fig. 2.2: Heating system

2.2 Engineering design

2.2.1 Design inputs and assumptions

A detached home with 1200 to 1500 square feet built before 1980 would need a gas furnace with a capacity of 55,000 British thermal units (BTUs) per hour (or 16 kW) (Furnace Depot 2016). Hence the base case system is sized to deliver 16 kW of heat for 8 hours. With the relative humidity and temperature of the hot airstream (stream 1) and the desirable qualities of the output to the rooms (stream 3), the relative humidity of stream 2 and the flow rate of each inlet stream can be calculated through the adiabatic mixing rules described in Eq. 1 and the psychrometric chart (Balmer 2011; Mugdha 2019). The recommended temperature is between 16 ºC and 19 ºC during the daytime when the system is on standby mode and the house is not occupied. Airstream 2 is chosen with the conservative 15 ºC as the initial indoor inlet air temperature. The comfortable temperature for living is around 21-22 ºC so the distributing air (airstream 3) is designed to have the ability to reach 25 ºC from an initial temperature (input temperature) of 15 ºC (Direct Energy 2020). The design is to accommodate the maximum capacity, but daily use would not require the system to operate at its maximum.

$$\frac{m_1}{m_2} = \frac{h_3 - h_2}{h_1 - h_3} = \frac{w_3 - w_2}{w_1 - w_3} \qquad \text{Eq. 1}$$

m is the mass flow rate in kg/s, *h* is the enthalpy in kJ/kg, and *w* is the humidity ratio (g/kg). The subscripts 1, 2, and 3 represent incoming streams 1 and 2 and the resulting stream 3, respectively, as described in Fig. 2.2.

The adsorbent storage volume (m^3) is estimated by considering the required total energy output and the energy density of the adsorbent. Zeolite 13X is assumed to have an energy density of 154 kWh/m^3 (Dicaire and Tezel 2013). The energy density range found in the uncertainty analysis is discussed in Section 3.3 for all the recorded zeolite 13X values from the literature.

The dimensions of the storage vessel are evaluated based on adsorbent volume and L/D. The total length of the duct system, which includes the connections between all the main components and additional ducts connected to the solar system, is designed to keep the pressure drop to less than 0.1 inch of water per 100 feet. The length of the duct system depends on the usable area, which was assumed to be 124 ft for a 1350 sq ft house. The Colebrook-White Equation (A3 in Appendix) and the Darcy laminar friction factor (Eq. A4 in Appendix) are used to find the friction factor of the airstream in the ducts when the flow is either turbulent (when the Reynolds number is above 2,000) or laminar (Toth and Bobok 2016).

The pressure drop value through a spherical packed bed was calculated from the Ergun's equation (Eq. A6 in Appendix) (Coker 2014). Equation A6 requires dynamic viscosity (μ), which is provided by Sutherland's Equation A5 in Appendix (Montgomery 1947). The significant head loss from the pipe is addressed through Equation A7 in Appendix with additional gravitational acceleration parameters (McDonald and Magande 2012). With the known flow rates and total pressure drop, we assessed the motor power of both fans using Equation A13 in Appendix (Engineering ToolBox 2003). For the humidifier, the total water mass flow rate required to saturate the air was found through the actual air flow rate needed and the saturated vapor density (Eq. A14 in Appendix) (Nave 2017). To determine the power consumed by the humidifiers, we developed a correlation by collecting capacity and power rating data from vendors (Fig. A1 in the Appendix). From the figure, Eq. 2 was established with 6 data points between 10 kg/hr to 72 kg/hr flow rate and is used to approximate the power rating (in W) that is needed. The operating temperature of the humidifier is assumed to be 20 ºC, which is the average temperature of airstream 2 (inlet) and airstream 3 (outlet). Table 2.1 shows all assumptions and reference values for model inputs.

$$Humidifier\ Power\ Rating = 50 * \ Required\ Flowrate \qquad \text{Eq. 2}$$

Table 2.1: Input parameters for the designed model

COMPONENT	Parameter	Value	Units	Reference/Comments
Stream 1	Air temperature	50	ºC	(Dicaire and Tezel 2011)
	Relative humidity	0	%	(Dicaire and Tezel 2011)
Stream 2	Air temperature	15	ºC	The temperature on the low side when people are absent from the house before the furnace starts
Stream 3	Air temperature	25	ºC	The high-end house temperature for comfort.
	Relative humidity	35	%	(Unsdorfer 2015)
Adsorbent energy density	Zeolite 13X	154	kWh/m^3	(Dicaire and Tezel 2013)
	Zeolite density	704	kg/m^3	(Nienborg et al. 2018)
	Porosity	0.4		(Lefebvre et al. 2016)
	Pellet diameter	0.01	m	(Lefebvre et al. 2016)
Hot air properties	Dynamic viscosity	0.01963	cP	(Montgomery 1947)
	Density	1.2461	kg/m^3	(Engineering ToolBox 2004)
Container/Vessel	Allowance for Corrosion	0.003	m	(Sőlken ; Wadkar et al. 2015)
	Maximum allowable working pressure	103000	kPa	(CIS GmbH Consulting Inspection Services 2020)
	Efficiency of joints	0.8		(Peters et al. 1968)
Ductwork	Roughness	0.0005	ft	(Engineering ToolBox 2003)
	Length	124	ft	Ductwork length varies. A small- to average-size house would have the assumed length.
Fan	Efficiency	50	%	(Engineering ToolBox 2003)

COMPONENT	Parameter	Value	Units	Reference/Comments
Humidifier	Operating temperature	20	ºC	The average of the high and low temperature range of the house
Thermal conductivity	Galvanized steel	18	W/mK	(Bennaji et al. 2010)
	Fiberglass	0.040	W/mK	(Hammond 2008)

The thickness of the container (*t*) is estimated by taking into account allowance for corrosion (C_c,) maximum allowable internal pressure (*P)*, inside radius *(*r_i*)*, maximum allowable working stress (*S)*, and efficiency of joints (E_j*)*, as described in Equation A15 in Appendix, derived from Peters et al. (Peters et al. 1968). The gage of the ducts is assigned according to the recommendation gage for circular ducts for heating and general ventilation work (Engineering ToolBox 2008). The insulation thickness of the duct and container are designed with a maximum heat loss of 5%. This prevents the rooms closest to the furnace from overheating and insufficient heat being delivered to the further rooms. Reducing the charging temperature results in less energy stored (Finck et al. 2014). Hence, a 20% margin of safety on sizing zeolite volume is considered to ensure sufficient heat is produced and provide compensation for heat loss during the operating phase while not overheating the house.

Knowing the maximum energy can be stored in the adsorbent, we calculated the solar collector's area required to provide on average the minimum energy to fully charge the storage system daily. In this paper, the solar collector is assumed to harvest 806 kWh/m^2 per year (Tripanagnostopoulos et al. 2006). The assumption is based on the fact that the solar potential in Alberta, Canada, a jurisdiction with cold climate, is relatively similar to Italy's, where Tripanagnostopoulos et al. conducted a solar collector experiment (Global Solar Atlas v2.2 2020). The GHG emissions from the solar system, therefore, are estimated from the quantity used from the solar collector.

2.2.2 Simulation model outputs

To provide 16 kW of heat for 8 hours, a 1 m^3 container 3.7 mm thick is required. Only two pieces of equipment, fans and humidifiers, consume electricity during the operating phase. Large capacity humidifiers are needed to either boost relative humidity to above 90% during discharging mode or control the relative humidity to the room. The power ratings of humidifiers 2a and 2b are 0.68 kW and 1.13 kW, respectively. Small fan motors (0.23 kW and 0.08 kW) are needed to overcome the total pressure and to provide the desirable output flow rate. The capacity of the fan depends heavily on the size of the zeolite pellets. Table 2.2 lists additional outputs obtained from the simulation model. All of the main components have relatively small footprints, so it is feasible to fit the heating system in a conventional furnace room.

Table 2.2: Output from the simulation model

COMPONENTS	PARAMETER	VALUE	UNITS
Stream 1	Volumetric flow rate	0.2933	m^3/s
Stream 2	Volumetric flow rate	0.5594	m^3/s
	Relative humidity	89 %	
Zeolite	Volume	1.005	m^3
Container/Vessel	Diameter	1.086	m
	Length	1.086	m
	Pressure drop	250.22	Pa
	Thickness	0.00370	m
Fan	Total pressure loss	1.42	in of water
	Fan 1 power rating	0.30	HP
	Fan 2 power rating	0.12	HP
Humidifier	Humidifier 1 capacity	13.7	kg/hr
	Humidifier 1 power rating	683.0	W
	Humidifier 2 capacity	20.4	kg/hr
	Humidifier 2 power rating	1129.3	W
Insulation	Thickness	0.015	m
Solar collectors	Total area needed	38.9	m^2

2.3 Life cycle assessment of the storage system

LCA, according to the International Organization for Standardization (ISO) guidelines and framework, is an environmental framework used to evaluate life cycle GHG emissions and net energy ratio (International Organization for Standardization 2006a, 2006b). LCA has four phases: goal and scope definition, inventory analysis, impact assessment, and interpretation. Each phase is equally important and should be clearly defined for meaningful comparisons as well as further research purposes.

The overall objective of this study's LCA is to develop a bottom-up model to understand the GHG emissions and net energy performance of zeolite 13X-based thermal storage in a residential space heating application. Such an assessment will provide insights into the use of solar-integrated adsorbent as an environmentally sustainable alternative to the conventional heating systems available in the market. 1 kWh of heat generated from zeolite storage is considered the functional unit. The functional unit is the reference unit to which all input and output requirements are normalized. It is used as a base to have a meaningful comparison among different technologies with the same function. GHG emissions and net energy ratio are the environmental indicators.

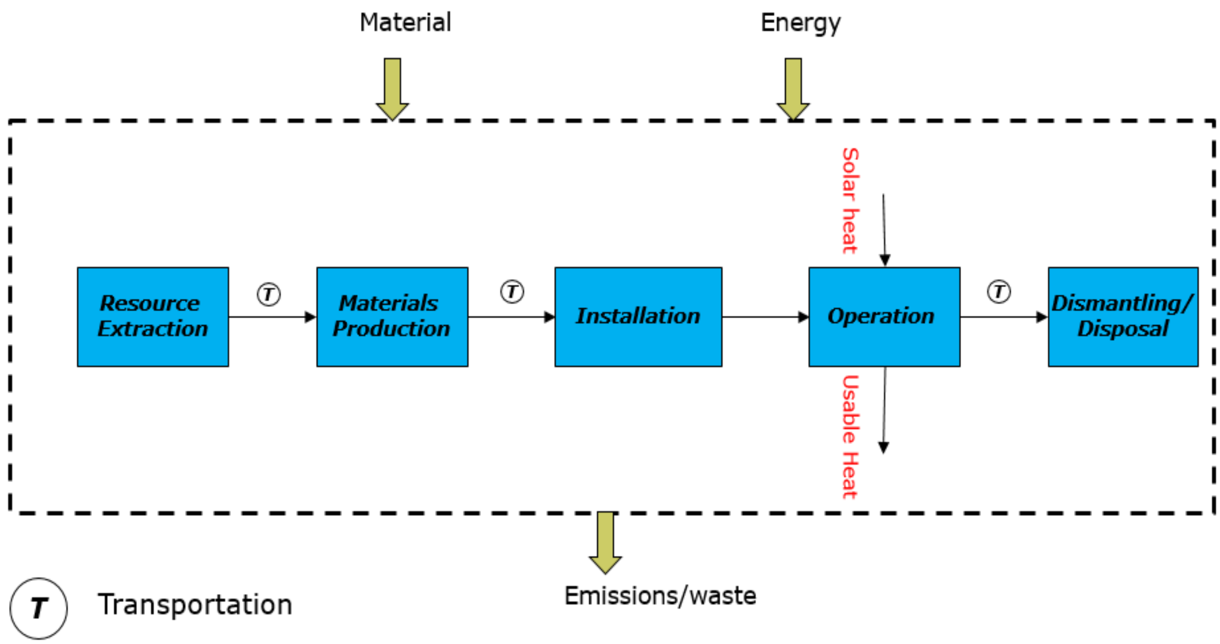

Fig. 2.3: System boundary diagram

Figure 2.3 depicts the system boundary considered for the life cycle assessment. The system boundary includes material extraction, manufacturing, transportation, operation, and end of life (recycling). Energy and material requirements at each stage of the life cycle are estimated and translated into GHG emissions. Resource extraction considers the emissions of equipment and fuel needed to extract ore from mines and on-site washing to remove impurities. Material production emissions occur in the refinery where raw materials needed for equipment are produced through chemical reactions, melting, and so on. The installation process includes the assembly or shaping of materials to produce a device. Emissions from fuel consumption, i.e., fossil fuel combustion, are considered in the operation stage. Finally, the disposal process involves mainly the recycling of materials. Assigning recyclable material GHG emissions a value from 0% to 100% in the sensitivity and uncertainty analyses generates a range of GHG emissions results for the system, should the material be recycled.

2.3.1 Inventory analysis

Inventory analysis involves input and output data compilation and calculation at each stage of the life cycle of the product system. Energy inputs are heat from fossil fuels, petroleum, electricity, and solar heat. Material requirements are materials used to make each component and include steel (galvanized steel, carbon steel, and stainless steel), aluminum, zeolite 13X, fiberglass, and water. During discharging, electricity is required for the adsorbent storage system. The upstream emissions for electricity production are considered based on the grid mix. The outputs of the system are heat for space heating and water vapour in the air to regulate the humidity. Table 2.3 lists the main materials used in each component. The data is based on engineering design and from vendor listings.

Table 2.3: Material inventory list for a system of capacity 16 kW

Components	Materials	Weights (kg)	Notes/Comments
Vessel	Carbon steel	156.3	The thickness, from Eq. A15 in the Appendix, and the density of material were used to calculate the weight
Storage core	Zeolite 13X	424.4	With the output energy and energy density of zeolite, we obtained total weight of zeolite.
Duct network	Galvanized steel	126.5	A similar calculation to the vessel but with a chosen gauge for ductwork and the density of steel
Humidifier 2a	Stainless steel	22	We used the correlation developed in Figure A3

Components	Materials	Weights (kg)	Notes/Comments
Humidifier 2b	Stainless steel	37	We used the correlation developed in Figure A3
Fan 1a	Stainless steel	5.79	We used the correlation developed in Figure A2 and a percentage allocation for the materials
	Aluminium	1.45	
Fan 1b	Stainless steel	1.26	We used the correlation developed in Figure A2 and percentage allocation for the materials
	Aluminium	0.32	
Dampers and Valves	Galvanized steel	3.22	We used the correlation developed in Figure A4
Insulation	Fibreglass	15.5	The thickness and insulation weight were evaluated assuming percentage heat loss

Once the sizes of the heating system components were known, we constructed the LCA model to reflect the environmental footprint of the system. Most of the global warming potential (GWP) emissions data was obtained from the literature and the rest from other sources with regional modifications to account for the fact that the system is used in North America. We segregated each piece of equipment by material in order to perform a bottom-up GHG emissions assessment. The solar air collector system was evaluated separately and integrated directly into the designed model. Regression correlations for the fans and the humidifiers were developed to obtain their weights (Figs. A2 & A3 in Appendix). Since the construction material of the humidifiers is mostly stainless steel (according to the vendor listings), we assumed 100% of the equipment was stainless steel by weight. For fans, the materials vary greatly by type, capacity, and scenario. Therefore, this study assumes the fans are 80% stainless steel by weight and the rest is aluminum. The percentage can be varied in the uncertainty analysis to change the results.

Table 2.4: Emissions from materials and grids

MATERIALS	VALUE	UNITS	REFERENCE	NOTES
Galvanized steel	3163.7	gCO_2 eq/kg	(Wang 2018)	
Aluminum	6828.5	gCO_2 eq/kg	(Wang 2018)	
Stainless steel	2068.1	gCO_2 eq/kg	(Wang 2018)	
Carbon steel	2984.2	gCO_2 eq/kg	(Wang 2018)	
Zeolite 13X	5738.9	gCO_2 eq/kg	(Horn et al. 2018; Nienborg et al. 2018)	This value is adjusted with Alberta grid emission
Fiberglass	1350.0	gCO_2 eq/kg	(Hammond 2008)	
Alberta grid emissions	163.8	gCO_2 eq/MJ	(Heaps 2012)	
Germany grid emissions	90.3	gCO_2 eq/MJ	(ElectricityMap Live 2019)	The emissions are used to adjust material production emissions
Fuel (diesel)	86373.72	gCO_2 eq/mmBTU	(Wang 2018)	
Solar collectors (GWP100)	397	gCO_2 eq/m^2	(Tripanagnostopoulos et al. 2006)	This value is adjusted with Alberta grid emission

Dampers and valves weights are evaluated using correlations taken from information from commercial products. The correlation between weight and diameter of a damper was obtained from various vendor data and is given in Fig. A4 in the Appendix. The life of the system is considered to be 20 years because it is recommended that a regular gas furnace be changed after about that length of time (Petro Home Service 2020; Sedgwick 2020; Tonkens 2020). The GHGs considered during the lifespan are those emitted throughout the whole process from manufacturing the materials, the assembly process to create devices, the transportation, and the electricity consumption during the use phase. The recycle phase can be considered by varying the proportion of virgin material and recycled material.

2.3.2 Net energy ratio

The net energy ratio is the ratio between total energy output and total non-renewable energy input (calculated through Eq. 2). For thermal energy storage, it is a measure of total useful heat generated per unit of fossil fuel input (Miller and Kumar 2013; Kapila et al. 2019). The value represents how efficient the storage system is compared to other technology and how much energy gain the storage provides. If the value is less than 1, the system releases less energy than the total non-renewable energy that is put into it. Therefore, storage that works well with renewable energy sources would have much better NER than other storage systems. If the value is greater than 1, the system is providing more useful energy output than the total non-renewable energy input.

$$Net\ Energy\ Ratio\ (NER) = \frac{Total\ energy\ output}{Non-renewable\ energy\ input} \qquad \text{Eq. 2}$$

The non-renewable energy value required to produce common metals and transportation fuel (e.g., galvanized steel, stainless steel, aluminium, diesel) was collected from the literature. The energy consumption to produce 1 kg of zeolite 13X in this simulation is 66 MJ/kg, which is the average number of non-renewable primary energy values obtained from Nienborg et al. and Horn et al.. The energy requirement to make 1 kg of insulation is 19.7 MJ/kg (Schmidt et al. 2004).

2.3.3 Sensitivity and uncertainty analyses

Sensitivity analysis helps the user find input parameters that have great effects on the outcomes and uncertainty analysis provides a range of likely outcomes from the given input ranges. The model uses the Morris sensitivity analysis to determine the most sensitive input data (Di Lullo et al. 2020). Uncertainty analysis is performed by running a Monte Carlo simulation up to a hundred thousand times, depending on the accuracy needed. The simulation helps to point out the most likely scenario for the chosen base case. The precise and accuracy of a single point estimate is always a concern when developing new technology and, hence, uncertainty analysis would provide a more realistic range with high confidence for investors or policymakers to consider.

Table 2.5 presents the ranges of input parameters used in the uncertainty analysis. Other studies give different energy densities of zeolite 13X and zeolite systems because of the different conditions when charging and discharging the storage. The range recorded in published studies is between 106 and 250 kWh/m^3 (Gantenbein et al. 2001; Dawoud et al. 2007; Hauer 2007; Scapino et al. 2017a, 2017b). Laboratory experiments were performed with L/D of 0.1 to 2.8 (Ugur 2013; Kuznik et al. 2020). Another physical property of zeolite 13X that can affect the model outcome is the pellet diameter. The upper range of 3 mm to 8 mm was chosen because the small diameter would increase the pressure drop and the power rating of the equipment in the system (Zhengzhou Gold Mountain Science and Technique Co. Ltd 2019). Depending on the condition of the galvanized steel duct system, the roughness of the inside surface could range from 0.0001967 to 0.0009836 ft (Ratnayaka et al. 2009). The range of duct length is generated by adding and subtracting a margin of safety from the developed correlation between the usable area and the duct length. Here, a safety factor of 20% was chosen conservatively compared to the error from the model with the collected data (less than 5% error). Although fan blower efficiency can be higher, in this study, the fan efficiency was varied between 40% and 84% (Brendel 2010; Mathson and Ivanovich 2011). The fan can be made from many material, including steel, aluminium, and zinc. The construction materials chosen here are steel and aluminium and the percentage contribution of each was varied to see the influence on the results (Air Turbine Propeller Co. 2015). The GHG emissions provided in papers by Horn et al. and Nienborg et al. were used to form a possible range of zeolite 13X emissions (Horn et al. 2018; Nienborg et al. 2018). As for the electricity mix, the high end of the emissions range is from using more than 95% coal-fired electricity and the lower end is the average Canadian electricity emissions from all provinces in 2013 (U.S. Energy Information Administration ; Bull Frog Power 2015; Sharp 2019). The energy harvest is based on the solar potential and the efficiency of the solar collector. The lower limit is the same efficiency and solar potential as Italy's and the upper limit is the lowest daily average in the year in Alberta, Canada (Tripanagnostopoulos et al. 2006; Athaudage Dona 2014).

Table 2.5: Sensitivity and uncertainty inputs

Variables	Min	Max	Unit	Reference/Comments
Zeolite energy density	106	250	kWh/m^3	(Gantenbein et al. 2001; Dawoud et al. 2007; Hauer 2007; Scapino et al. 2017a, 2017b)
Length-to-diameter ratio	0.1	2.8		(Ugur 2013; Kuznik et al. 2020)
Zeolite pellet diameter	0.003	0.008	m	(Zhengzhou Gold Mountain Science and Technique Co. Ltd 2019)
Pipe roughness	0.06	0.03	mm	(Ratnayaka et al. 2009)
Length of duct system	30.4	44.5	m	Assumed

Variables	Min	Max	Unit	Reference/Comments
Fan efficiency	40%	84%		(Brendel 2010; Mathson and Ivanovich 2011)
Percentage of aluminium Fan 1a	0%	100%		(Air Turbine Propeller Co. 2015)
Percentage of aluminium Fan 1b	0%	100%		(Air Turbine Propeller Co. 2015)
Zeolite 13X emissions	6454.2	6520.8	gCO_2 eq/kg	(Horn et al. 2018; Nienborg et al. 2018)
Alberta grid emissions	50	266.5	gCO_2 eq/MJ	(U.S. Energy Information Administration ; Bull Frog Power 2015; Sharp 2019)
Solar collector potential	806.5	1000	kWh/m^2-yr	(Tripanagnostopoulos et al. 2006; Athaudage Dona 2014)

Variables	Min	Max	Unit	Reference/Comments
Transportation distance	1100	5000	km	Assumed. The lowest value in the transportation range is the distance from Alberta, Canada to British Columbia, Canada (Canada's west coast) and the highest is the stretch between Alberta and Newfoundland, Canada (Canada's east coast). This is an assumption to show the range of distances of transportation.

3. Results and discussion

3.1 Life cycle GHG emissions phases

Figure 2.4 presents the GHG emissions of the heating system by life cycle stage. The system generates 0.127 $kgCO_2$ eq per kWh (heat). The operational phase has the largest emissions contribution, approximately 71% of the total. Humidifier and fan electricity consumption along with high intensity grid emissions make up the highest share. The results are consistent with other studies on fans and similar motors, which show the operation phase contributes as much as 98.5% of the GHG emissions while production, distribution, and end of life contribute 1.4%, 0.02%, and 0.06%, respectively (Andrada et al. 2012; Orlova et al. 2016). The material extraction and component manufacturing stages account for around 28% of the total GHG emissions. The main contribution is from the material and energy requirements to manufacture the solar collectors (roughly 23%) and adsorbent bed (5%). The photovoltaic (PV) modules, heat recovery unit glaze, and reflectors account for 67%, 19%, and 7% of GHG emissions from the solar collector system (Fu et al. 2015). More specifically, PV cells and glazed covering are the key contributors to the high emissions number of the PV module component. A brief study showed that the production process of solar-grade poly-Si makes up approximately 50% of PV cell GWP due to intensive electricity and steam consumption (Fu et al. 2015). Improvement in these areas would substantially reduce the overall emissions from the whole heating system. With respect to the adsorbent bed, the largest impact is from the fabrication of zeolite 13X due to high electricity consumption. Acquiring sodium silicate makes up the largest share in the extraction stage (Seo et al. 2019). Some studies pointed out that zeolite 13X is not affected by charging cycles, which could potentially improve the environmental performance of the material. More studies need to be conducted to understand the lifetime, charging/discharging properties, and recyclable characteristics of this material. The recycling of zeolite was assessed through a range of GHG emissions values in the sensitivity and uncertainty analyses. However, it was found that the recycling process does not have a great impact on the GHG emissions per unit heat generated (the values can be seen in sensitivity and uncertainty analyses results below). Steel manufacturing makes a large contribution to GHG emissions through the basic oxygen furnace (including ladles and casters), the main energy and GHG emissions intensive process. Although recycled steel has lower GHG emissions than virgin steel (Wang 2018), the overall influence in the life cycle of a zeolite space heating system is insignificant since the relative contribution of steel is small. The life cycle GHG emissions from assembly and transportation are negligible.

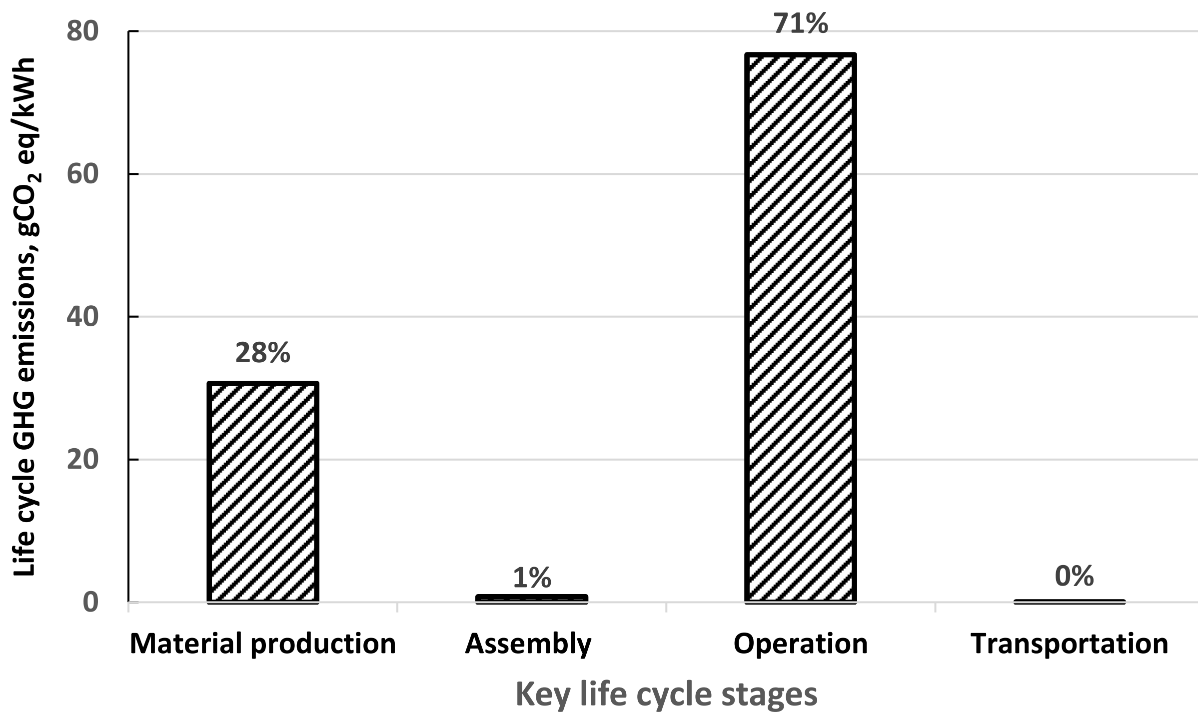

Fig. 2.4: Life cycle GHG emissions

3.2 Environmental performance of the zeolite heating system in several provinces

Since the highest life cycle GHG emissions are due to electricity consumption during the operational phase, it is worth considering how the outcome (gCO_2 eq/kWh) could be sensitive to a change in the source of electricity, i.e., when the heating system is used elsewhere. Figure 2.5 shows the relative GHG performances of the zeolite 13X-based heating system in several Canadian provinces. The greatest impact occurs when the heating system is used in GHG-intensive regions (i.e., Alberta, Nova Scotia, and Saskatchewan). Electricity generation in those provinces is heavily dependent on fossil fuel. The electricity grid in Alberta, a western province in Canada with a large fossil fuel-based energy source, emits the highest GHG emissions per kWh in Canada. This is due to the high dependence on fossil fuel, especially coal, which provides affordable and constant electricity supply to energy-intensive industries and large consumer demand. Manitoba, British Columbia, Ontario, Quebec, and Newfoundland and Labrador have very low electricity grid emissions. For example, when the zeolite 13X heating system is used in Quebec, the life cycle GHG emissions could be as low as 32.5 gCO_2 eq/kWh, almost four times lower than using the same system in Alberta. In this case, the material production stage has the largest share of life cycle GHG emissions and hence it is the area to focus on to further improve environmental performance. The Canadian government is planning to phase out coal by 2030, which would greatly impact the grid GHG emissions factor for fossil-dominant provinces such as Saskatchewan, Alberta, and Nova Scotia (Environment and Climate Change Canada 2018). For instance, if Alberta's grid GHG emissions fall from 589.8 gCO_2 eq/kWh in 2018 to 359 gCO_2 eq/kWh in 2030 (Heaps 2012), the life cycle GHG emissions from the proposed system would decrease by 30%. This signifies the importance of selecting suitable space heating systems for an existing grid mix and considering regional factors before implementing new technologies.

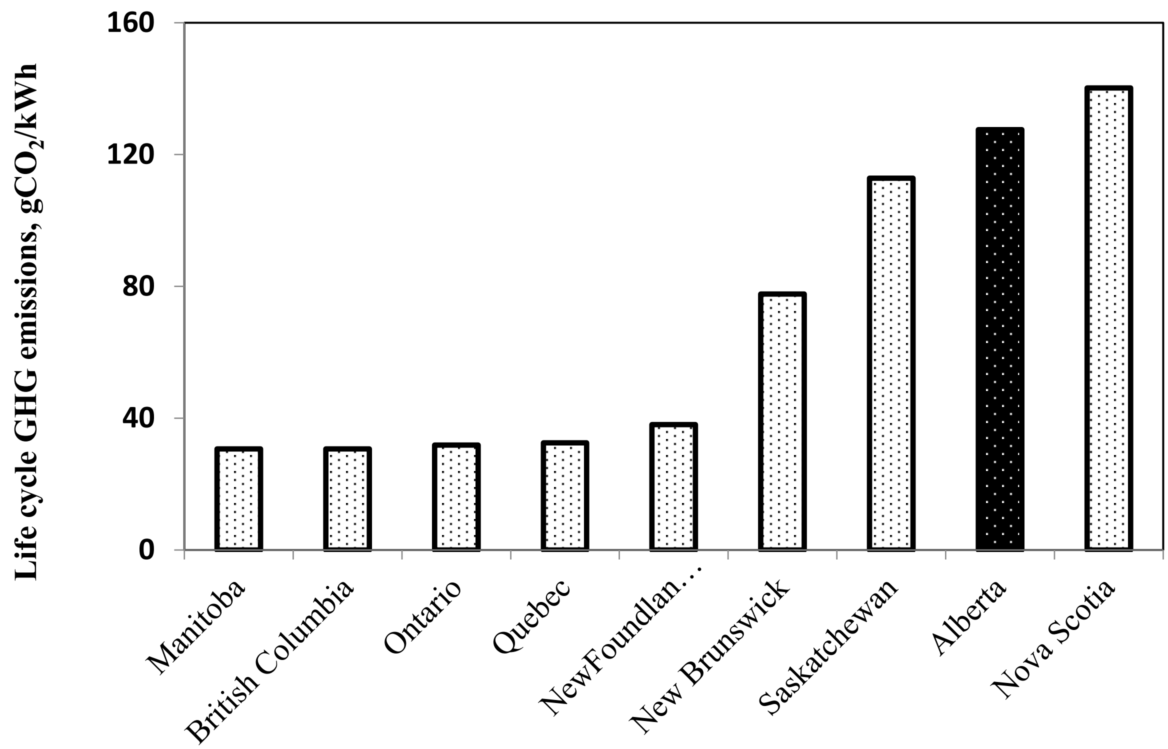

Fig. 2.5: **Base case with different provincial grid emissions in Canada**

3.3 Environmental performance of various heating systems

It is also important to compare the environmental impacts of the zeolite 13X heating system with other furnaces that are available on the market and have been studied. Yang et al. researched the environmental performance of the electric boiler, gas-fired boiler, electric furnace, and gas-fired furnace in Quebec (2008). To assess the sustainability of these systems in Alberta, we adjusted the results from Yang et al.'s paper by applying the Alberta grid emissions to all the space heating systems studied here. The results are presented in Fig. 2.6. In Yang et al.'s paper, the electric boiler and electric furnace are preferred in Quebec because of their low emissions during the operating phase, which lead to low overall GHG emissions. However, in Alberta and Saskatchewan, these same heating systems performed the worst environmentally. As Fig. 2.6 shows, surprisingly, the gas furnace performs much better than the electric furnace, and the adsorbent system is the best of all the systems. This once again confirms the importance of heating system selection based on grid emissions.

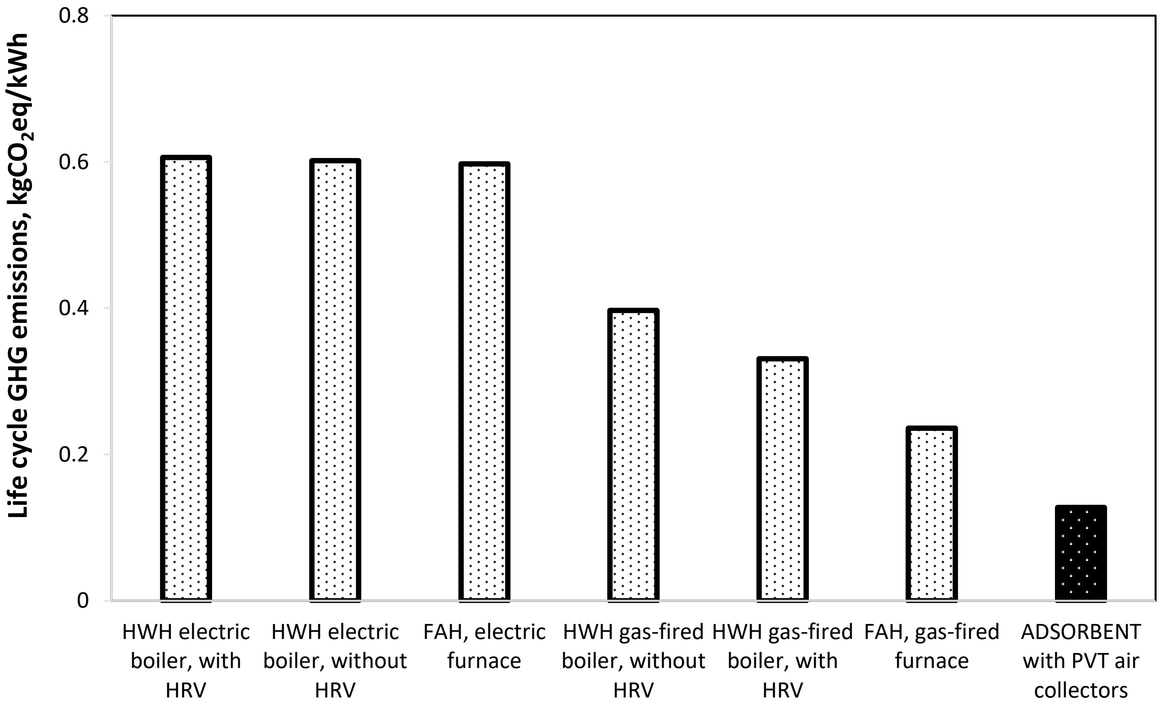

Fig. 2.6: GHG emissions comparison among different heating systems

3.4 Net energy ratio

As mentioned, the NER is an important indicator for renewable energy systems. The net energy ratio of the zeolite 13X heating system is approximately 3.2, which means that every 1 kWh of fossil fuel input, the designed system generates 3.2 kWh of heat energy for use. An NER higher than 1 indicates that the system is a net energy producer. The relatively large NER of the system is due to the use of a clean energy source, solar irradiation, for the charging process. The main non-renewable energy input, which makes up the largest share, is Alberta's grid electricity, used by the electric fans and humidifiers during the operating stage. The energy performance of the heating system can be improved further by using a cleaner electricity mix. A zeolite 13X-based heating system has a higher NER than the low temperature geothermal installation, which has an NER of nearly 2 (Arrizabalaga et al. 2012). However, the NER of renewable technologies such as a solar water heating installation (NER = 4 to 16) or a photovoltaic installation (NER = 4) has a great advantage over energy generation compared to the proposed system (Battisti and Corrado 2005; Fthenakis and Alsema 2006). Colclough and McGrath reported an NER of 5 for solar-based domestic hot water (DHW) and 3.6 for a large-scale solar-based DHW and space heating system (2015). The study also showed that integrating aqueous seasonal thermal energy storage or a PV solar array to a heating system results in lower NERs, 2.5 and 2.4, respectively (Colclough and McGrath 2015). The zeolite 13X heating system, hence, appears to have a relatively higher energy performance than other renewable energy systems.

3.5 Sensitivity and uncertainty analysis

Figures 2.7 and 2.8 present the sensitivity analysis results for GHG emissions and NER, respectively. The L/D of the zeolite vessel and grid electricity emissions profile are the parameters that most influence the overall system GHG emissions. A small change in the L/D could contribute to a significant change in the sizing of the fans and humidifiers. These are the devices with the largest impact because they consume electricity during their operating lifetime. Electricity grid emissions, hence, are also an important parameter with a great influence on the output. Pellet diameter and fan efficiency are sensitive parameters since more powerful motors are needed to overcome the internal pressure drop in the system. The last sensitive parameter worth mentioning is the energy density, which determines physical dimensions and weight. With higher energy density, less material is needed to pack the same amount of required heat. Pellet diameter and L/D are the inputs with greatest influence on the output of the NER (Fig. 2.8). These parameters are properties of the storage that determine the size of each piece of equipment in the system. Energy density and fan efficiency are also crucial parameters that affect the output results.

Figure 2.9 displays the range of emissions following a Monte Carlo simulation with 100,000 runs. With a 90% confidence interval, the life cycle GHG emissions value ranges from 90.1 g CO_2 eq/kWh to 205 g CO_2 eq/kWh. Even the high end of the range for the space heating model (205 gCO_2 eq/kWh) is a very competitive system environmentally compared to the gas furnace and the electric boiler. The simulated mean value of GHG emissions and the most probable value are 141 gCO_2 eq/kWh and 138 gCO_2 eq/kWh. As for the NER (Fig. 2.10), the uncertainty assessment result has a narrower range, 2.26 to 3.36 with a 90% confidence interval. The mean and the probable values are about 2.93, and 3.0, respectively. It is certain that the attachment of energy storage to a renewable source such as solar collectors would result in positive energy return.

Despite some successful initial results, there are some limitations to this study. First, the proposed system was designed based on engineering principles without performing real experiments. Some aspects of the real system cannot be foreseen. Second, the desorption of zeolite from the heat generated by the sun should be researched to quantify the actual energy density zeolite can achieve. Finally, further studies are needed to assess the environmental impact and the efficiency of air solar collectors for space heating because of the limited information available on such systems.

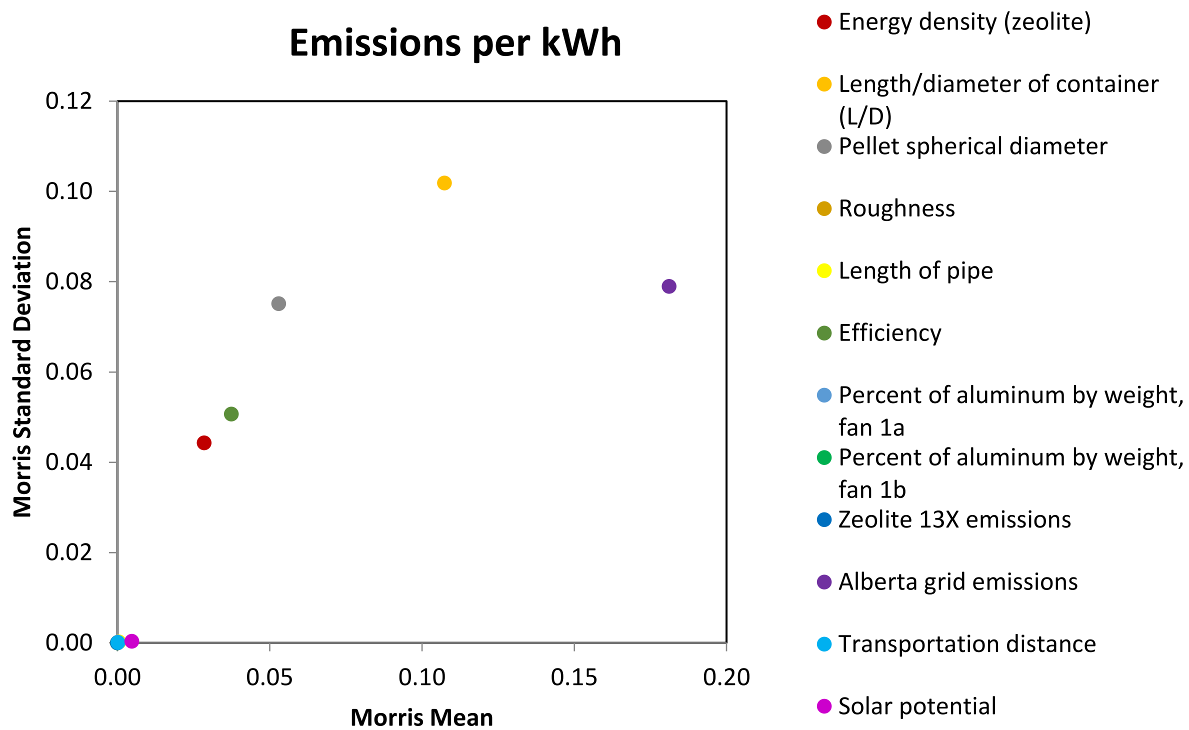

Fig. 2.7: Morris sensitivity analysis for space heating system emissions

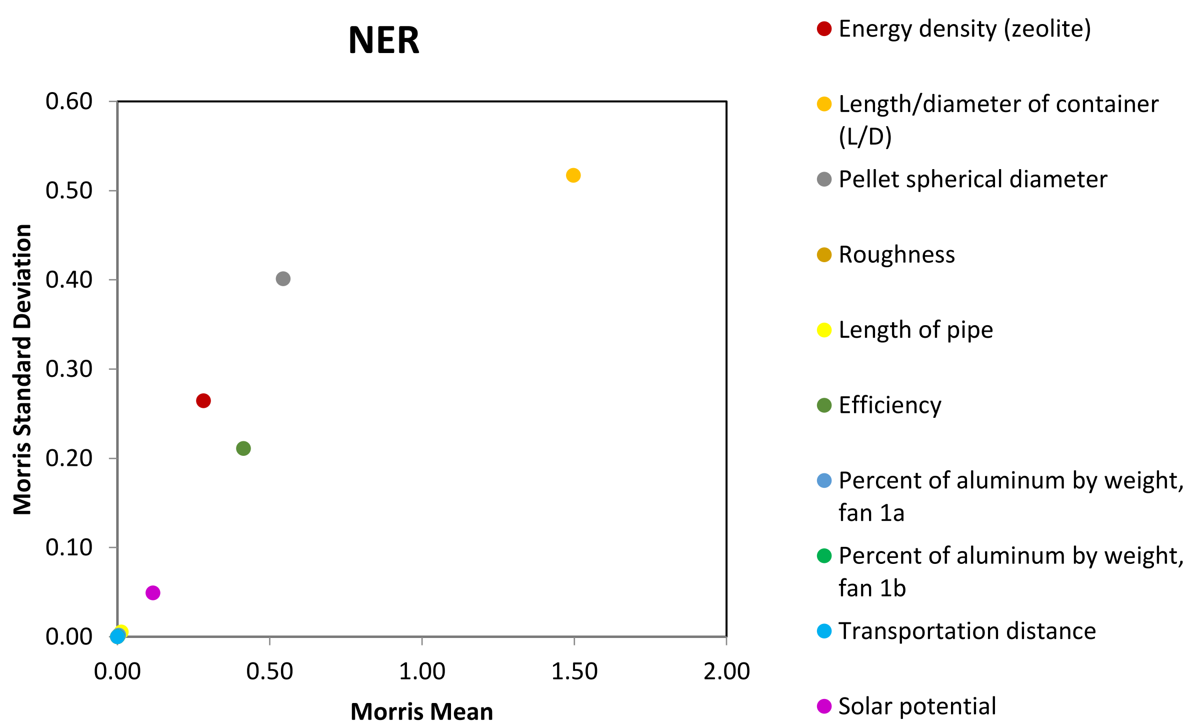

Fig. 2.8: Morris sensitivity analysis for space heating system NER

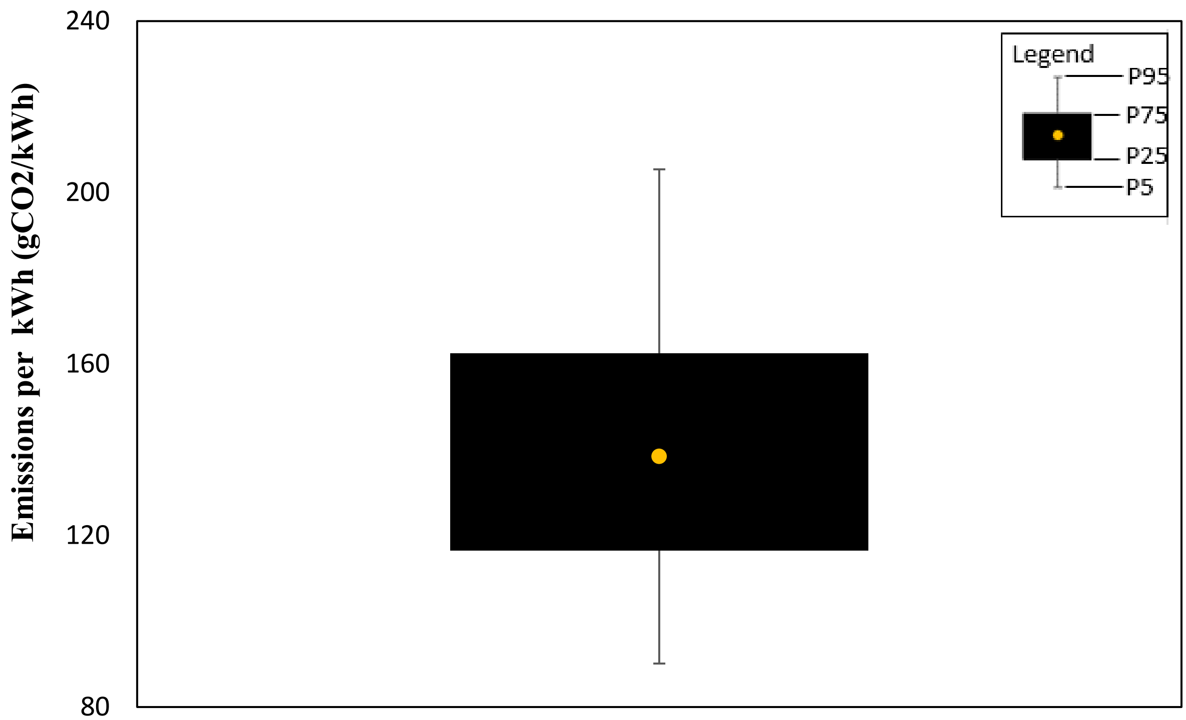

Fig. 2.9: Uncertainty analysis for the emissions per kWh

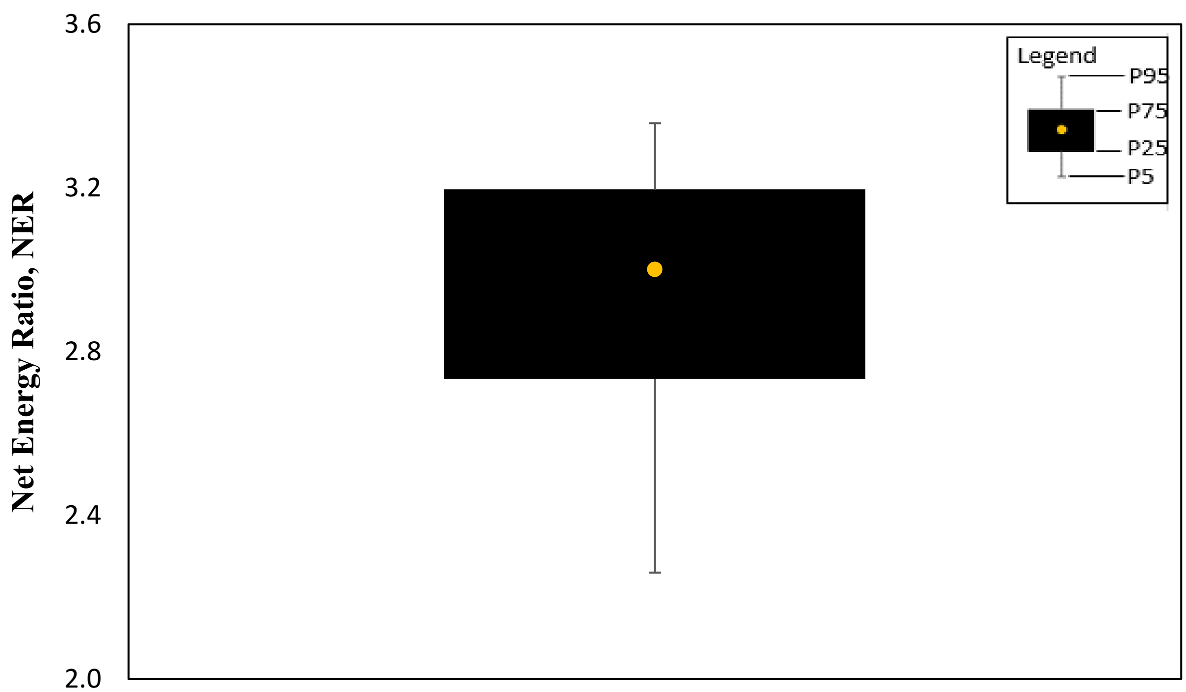

Fig. 2.10: Uncertainty analysis for the NER

4. Conclusion

Increased energy demand poses a significant environmental burden because of high fossil fuel use. There is a need to shift to clean energy technologies such as solar and wind. The role of heat and electricity storage systems in increasing the share of solar and wind energy and decarbonizing the global energy system has been widely acknowledged in scientific literature. The space heating sector is one of the highest GHG emissions contributors and hence environmental measures are required in the sector. Alternative pathways to reduce space heating GHG emissions include thermal energy storage integrated with solar energy, which could be used in residential homes, offices, or warehouses. The overall objective of this study is to develop a framework to evaluate the energy and GHG emission performances of zeolite 13X-based adsorbent integrated with air solar collectors to supply space heating in cold climates and conduct a case study for Canada. The framework integrates engineering system design and life cycle assessment. The designed 16 kW adsorbent storage would generate around 128 g CO_2 eq per kWh of heat supplied over a 20-year lifetime. The GHG emissions and the NER values would likely to fall in the ranges of 90.1-205.4 g CO_2 eq per kWh and 2.26-3.36, respectively, with a 90% confidence interval. The highest share of the life cycle GHG emissions and total energy input in the system comes from the electricity requirement during the operating phase. Therefore, the carbon intensity of the electricity grid has a great impact on the environmental performance of the system. The Canadian government's plan to phase out coal would make the zeolite 13X system more favorable, given its lower grid emissions, in the future. The adsorbent system would emit the lowest GHGs over the lifetime even at its high-end value compared to the electric boiler and gas furnace in provinces with high grid emissions. The adsorbent L/D, electricity emission factor, and pellet diameter are among the most sensitive parameters in terms of both GHG emissions and NER. The key observation from the study is that adsorbent storage using a solar heat source for space heating is an environmentally promising technology. The information developed in this study would be useful for industry and government in making investment decisions and policy formulation.

References

Air Turbine Propeller Co. 2015. Fan Materials & Finishes. http://www.airturbine.com/fan-materials-finishes (Date accessed: April 24, 2020).

Andrada, P., B. Blanqué, E. Martínez, J. Perat, J. Sánchez and M. Torrent. 2012. Environmental and life cycle cost analysis of one switched reluctance motor drive and two inverter-fed induction motor drives. IET Electric Power Applications **6**(7): 390-398.

Arrizabalaga, E., P. Hernandez, X. Oregi, L. Mabe and B. Sanchez. 2012. Net energy analysis of geothermal energy installations. Building Sustainability Assessment 2012. Portugal.

Athaudage Dona, N. 2014. Performance of the solar thermal hot water system at the southland leisure centre. Unpublished master's thesis, University of Calgary.

Balmer, R. T. 2011. Modern Engineering Thermodynamics. United State of America, Academic Press.

Battisti, R. and A. Corrado. 2005. Evaluation of technical improvements of photovoltaic systems through life cycle assessment methodology. Energy **30**(7): 952-967.

Bennaji, N., I. Mellouki and N. Yacoubi. 2010. Thermal properties of metals alloy by electrical pyroelectric method (EPE). Journal of Physics: Conference Series (Vol. 214, p. 012138). IOP Publishing.

Brendel, M. 2010. The Role of Fan Efficiency in Reducing HVAC Energy Consumption. https://www.amca.org/assets/resources/public/userfiles/file/AMCA_Spring2010RoleOfFE.pdf (Date accessed: April 24, 2020).

Bull Frog Power. 2015. Canadian Emission Factors for Grid Electricity. https://www.bullfrogpower.com/wp-content/uploads/2015/09/2015_bullfrog_power_electricity_emission_calculator.pdf (Date accessed: April 24, 2020).

Burkes, K. 2020. 3A, 4A, 5A, 13X… What's the difference? HengYe Inc. https://hengyeinc.com/3a-4a-5a-13x-whats-the-difference/ (Date accessed: March 18, 2020).

Cabeza, L. F. (ed.) 2014. Advances in thermal energy storage systems: Methods and applications. United Kingdom, Woodhead Publishing Series in Energy 66.

Child, M., D. Bogdanov and C. Breyer. 2018. The role of storage technologies for the transition to a 100% renewable energy system in Europe. Energy Procedia **155**: 44-60.

CIS GmbH Consulting Inspection Services. 2020. Some examples for allowable stress values "S" of typical carbon steels according to Section II, Part D, Table 1A, metric. https://www.cis-inspector.com/asme-code-calculation-allowable-stresses.html (Date accessed: October 7, 2019).

Climate Watch. 2016. Historical GHG Emissions. https://www.wri.org/blog/2020/02/greenhouse-gas-emissions-by-country-sector#:~:text=Global%20annual%20greenhouse%20gas%20emissions,rose%20each%20year%20since%20then. (Date accessed: December 10, 2020).

Coker, A. K. 2014. Ludwig's Applied Process Design for Chemical and Petrochemical Plants, Gulf Professional Publishing.

Colclough, S. and T. McGrath. 2015. Net energy analysis of a solar combi system with Seasonal Thermal Energy Store. Applied Energy **147**: 611-616.

Dawoud, B., E. H. Amer and D. M. Gross. 2007. Experimental investigation of an adsorptive thermal energy storage. International Journal of Energy Research **31**(2): 135-147.

Di Lullo, G., E. Gemechu, A. O. Oni and A. Kumar. 2020. Extending sensitivity analysis using regression to effectively disseminate life cycle assessment results. The International Journal of Life Cycle Assessment **25**(2): 222-239.

Díaz-González, F., A. Sumper, O. Gomis-Bellmunt and R. Villafáfila-Robles. 2012. A review of energy storage technologies for wind power applications. Renewable and Sustainable Energy Reviews **16**(4): 2154-2171.

Dicaire, D. and F. H. Tezel. 2011. Regeneration and efficiency characterization of hybrid adsorbent for thermal energy storage of excess and solar heat. Renewable Energy **36**(3): 986-992.

Dicaire, D. and F. H. Tezel. 2013. Use of adsorbents for thermal energy storage of solar or excess heat: improvement of energy density. International Journal of Energy Research **37**(9): 1059-1068.

Direct Energy. 2020. Recommended Thermostat Settings in the Winter. Energy Efficiency. https://www.directenergy.com/learning-center/energy-efficiency/recommended-thermostat-settings-winter (Date accessed: April 22, 2020).

Direct Energy. 2020. Your Average House Temperature. https://www.directenergy.ca/learn/recommended-thermostat-settings-winter (Date accessed: Aprill 22, 2020).

ElectricityMap Live. 2019. Climate Impact by Area. https://www.electricitymap.org/?page=map&solar=false&remote=true&wind=false (Date accessed: October 7, 2019).

Engineering ToolBox. 2003. Fans - Efficiency and Power Consumption. https://www.engineeringtoolbox.com/fans-efficiency-power-consumption-d_197.html (Date accessed: October 7, 2019).

Engineering ToolBox. 2003. Ventilation Ducts - Roughness & Surface Coefficients. https://www.engineeringtoolbox.com/surface-roughness-ventilation-ducts-d_209.html (Date accessed: October 7, 2019).

Engineering ToolBox. 2004. Density of Moist Humid Air. https://www.engineeringtoolbox.com/density-air-d_680.html (Date accessed: October 7, 2019).

Engineering ToolBox. 2008. Ducts - Sheet Metal Gauges. https://www.engineeringtoolbox.com/ductwork-sheet-metal-gauges-d_1157.html (Date accessed: October 8, 2019).

Environment and Climate Change Canada. 2018. Canada's coal power phase-out reaches another milestone. https://www.canada.ca/en/environment-climate-change/news/2018/12/canadas-coal-power-phase-out-reaches-another-milestone.html (Date accessed: May 14, 2020).

Finck, C., E. Henquet, C. van Soest, H. Oversloot, A.-J. de Jong, R. Cuypers and H. Van T'Spijker. 2014. Experimental results of a 3 kWh thermochemical heat storage module for space heating application. Energy Procedia **48**(0): 320-326.

Formisano, B. 2019. Types of Home Heating Systems. The Spruce. https://www.thespruce.com/types-of-home-heating-systems-1824772 (Date accessed: March 18, 2020).

Fthenakis, V. and E. Alsema. 2006. Photovoltaics energy payback times, greenhouse gas emissions and external costs: 2004–early 2005 status. Progress in Photovoltaics: Research and Applications **14**(3): 275-280.

Fu, Y., X. Liu and Z. Yuan. 2015. Life-cycle assessment of multi-crystalline photovoltaic (PV) systems in China. Journal of Cleaner Production **86**: 180-190.

Furnace Depot. 2016. BTU Charts. http://furnacedepot.ca/btu-charts/ (Date accessed: September 26, 2019).

Gantenbein, P., S. Brunold, F. Flückiger and U. Frei. 2001. Sorbtion materials for application in solar heat energy storage. Rapperswill, Switzerland: University of Applied Science.

Ge, M. and J. Friedrich. 2020. 4 Charts Explain Greenhouse Gas Emissions by Countries and Sectors. World Resources Institute. https://www.wri.org/blog/2020/02/greenhouse-gas-emissions-by-country-sector#:~:text=Global%20annual%20greenhouse%20gas%20emissions,rose%20each%20year%20since%20then. (Date accessed: December 10, 2020).

Global Solar Atlas v2.2. 2020. https://globalsolaratlas.info/map?s=51.845617,-112.148438&m=site&c=11.609193,8.4375,3 (Date accessed: April 22, 2020).

Hauer, A. 2007. Evaluation of adsorbent materials for heat pump and thermal energy storage applications in open systems. Adsorption **13**(3-4): 399-405.

Heaps, C. 2012. Somerville, MA, USA. Long-range Energy Alternatives Planning (LEAP) system. Stockholm Environment Institute. [Software version 2017.0. 4.0]. http://sei-us.org/Publications_PDF/SEI-LEAP-brochure-Jan2012.pdf (Date accessed: May 5, 2019).

Home Guide. 2019. How Much Does a New Furnace Replacement Cost? https://homeguide.com/costs/new-furnace-replacement-cost (Date accessed: April 21, 2020).

Horn, R., M. Burr, D. Fröhlich, S. Gschwander, M. Held, J. P. Lindner, G. Munz, B. Nienborg and P. Schossig. 2018. Life cycle assessment of innovative materials for thermal energy storage in buildings. Procedia CIRP **69**: 206-211.

Hua, Y., B. Ugur and F. H. Tezel. 2019. Adsorbent screening for thermal energy storage application. Solar Energy Materials and Solar Cells **196**: 119-123.

International Organization for Standardization. 2006a. ISO 14040 International Standard-Environmental Management-Life Cycle Assessment-Principles and Framework, Geneva, Switzerland. https://www.iso.org/obp/ui/#iso:std:iso:14040:ed-2:v1:en (Date accessed: September 1, 2019).

International Organization for Standardization. 2006b. Environmental Management: Life Cycle Assessment; Requirements and Guidelines. ISO Geneva. https://www.iso.org/obp/ui/#iso:std:iso:14044:ed-1:v1:en (Date accessed: September 1, 2019).

Jänchen, J., D. Ackermann, H. Stach and W. Brösicke. 2004. Studies of the water adsorption on zeolites and modified mesoporous materials for seasonal storage of solar heat. Solar Energy **76**(1-3): 339-344.

Jänchen, J., K. Schumann, E. Thrun, A. Brandt, B. Unger and U. Hellwig. 2012. Preparation, hydrothermal stability and thermal adsorption storage properties of binderless zeolite beads. International Journal of Low-Carbon Technologies **7**(4): 275-279.

Jelle, B. P. 2016. Nano-based thermal insulation for energy-efficient buildings. Start-Up Creation**:** 129-181, Elsevier.

Johannes, K., F. Kuznik, J.-L. Hubert, F. Durier and C. Obrecht. 2015. Design and characterisation of a high powered energy dense zeolite thermal energy storage system for buildings. Applied Energy **159**: 80-86.

Kalair, A., N. Abas, M. S. Saleem, A. R. Kalair and N. Khan. 2020. Role of energy storage systems in energy transition from fossil fuels to renewables. Energy Storage: e135.

Kapila, S., A. Oni, E. Gemechu and A. Kumar. 2019. Development of net energy ratios and life cycle greenhouse gas emissions of large-scale mechanical energy storage systems. Energy **170**: 592-603.

Kriegler, E., J. P. Weyant, G. J. Blanford, V. Krey, L. Clarke, J. Edmonds, A. Fawcett, G. Luderer, K. Riahi and R. Richels. 2014. The role of technology for achieving climate policy objectives: overview of the EMF 27 study on global technology and climate policy strategies. Climatic Change **123**(3-4): 353-367.

Krishna, R., B. Smit and S. Calero. 2002. Entropy effects during sorption of alkanes in zeolites. Chemical Society Reviews **31**(3): 185-194.

Kuznik, F., D. Gondre, K. Johannes, C. Obrecht and D. David. 2020. Sensitivity analysis of a zeolite energy storage model: Impact of parameters on heat storage density and discharge power density. Renewable Energy **149**: 468-478.

Lefebvre, D., P. Amyot, B. Ugur and F. H. Tezel. 2016. Adsorption prediction and modeling of thermal energy storage systems: a parametric study. Industrial & Engineering Chemistry Research **55**(16): 4760-4772.

Lemghalef, L. and J. Sager. 2019. The future of home heating: Hybrid home heating systems offer energy savings and reduce GHG emissions. Natural Resources Canada. https://www.nrcan.gc.ca/simply-science/future-home-heating-hybrid-home-heating-systems-offer-energy-savings-and-reduce-ghg-emissions/22236 (Date accessed: March 18, 2020).

Mathson, T. and M. Ivanovich. 2011. AMCA's Fan Efficiency Grades: Answers to Frequently Asked Questions. AMCA International 2011: 1-12. https://www.amca.org/assets/resources/public/userfiles/file/Nospreads_FanEfficGrades.pdf (Date accessed: April 24, 2020).

McDonald, A. G. and H. Magande. 2012. Introduction to Thermo-fluids Systems Design. United States of America, John Wiley & Sons.

Mehari, A., Z. Xu and R. Wang. 2020. Thermal energy storage using absorption cycle and system: a comprehensive review. Energy Conversion and Management **206**: 112482.

Miller, P. and A. Kumar. 2013. Development of emission parameters and net energy ratio for renewable diesel from Canola and Camelina. Energy **58**: 426-437.

Montgomery, R. 1947. Viscosity and thermal conductivity of air and diffusivity of water vapor in air. Journal of Meteorology **4**(6): 193-196.

Mugdha, P. 2019. Psychrometric Process (with chart)|Air Conditioning|Thermal Engineering. http://www.engineeringenotes.com/mechanical-engineering/air-conditioning/psychrometric-process-with-chart-air-conditioning-thermal-engineering/50038 (Date accessed: October 3, 2019).

NASA. 2020. Climate Change: How Do We Know? National Aeronautics and Space Administration (NASA). https://climate.nasa.gov/evidence/ (Date accessed: June 27, 2019).

Nave, R. 2017. Relative Humidity. http://hyperphysics.phy-astr.gsu.edu/hbase/Kinetic/relhum.html (Date accessed: October 4, 2019).

Nienborg, B., T. Helling, D. Fröhlich, R. Horn, G. Munz and P. Schossig. 2018. Closed adsorption heat storage—A life cycle assessment on material and component levels. Energies **11**(12): 3421.

Orlova, S., A. Rassõlkin, A. Kallaste, T. Vaimann and A. Belahcen. 2016. Lifecycle analysis of different motors from the standpoint of environmental impact. Latvian Journal of Physics and Technical Sciences **53**(6): 37-46.

Peters, M. S., K. D. Timmerhaus, R. E. West, K. Timmerhaus and R. West. 1968. Plant Design and Economics for Chemical Engineers, McGraw-Hill New York.

Petro Home Service. 2020. When is it time to replace your oil or natural gas furnace? https://www.petro.com/heating/is-it-time-for-a-new-furnace (Date accessed: October 7, 2019).

Ratnayaka, D. D., M. J. Brandt and K. M. Johnson. 2009. Chapter 12 - Hydraulics. Water Supply (Sixth Edition)**:** 463-498. Boston, Butterworth-Heinemann.

Rogelj, J., G. Luderer, R. C. Pietzcker, E. Kriegler, M. Schaeffer, V. Krey and K. Riahi. 2015. Energy system transformations for limiting end-of-century warming to below 1.5 C. Nature Climate Change **5**(6): 519.

Sandomierski, M., B. Strzemiecka and A. Voelkel. 2020. The influence of ion exchange in zeolite X on the properties of phenol-formaldehyde composites. International Journal of Adhesion and Adhesives: 102625.

Scapino, L., H. A. Zondag, J. Van Bael, J. Diriken and C. C. Rindt. 2017a. Energy density and storage capacity cost comparison of conceptual solid and liquid sorption seasonal heat storage systems for low-temperature space heating. Renewable and Sustainable Energy Reviews **76**: 1314-1331.

Scapino, L., H. A. Zondag, J. Van Bael, J. Diriken and C. C. Rindt. 2017b. Sorption heat storage for long-term low-temperature applications: A review on the advancements at material and prototype scale. Applied Energy **190**: 920-948.

Schumann, K., B. Unger, A. Brandt and F. Scheffler. 2012. Investigation on the pore structure of binderless zeolite 13× shapes. Microporous and Mesoporous Materials **154**: 119-123.

Sedgwick. 2020. How Long Does It Take to Replace a Furnace & When to Replace It? https://www.sedgwickheating.com/long-furnace-last-know-replace/#:~:text=The%20average%20lifespan%20of%20a,is%20approximately%2015%2D20%20years (Date accessed: December 10, 2020).

Seo, Y., M. Suzuki, T. Takagi and K. Dowaki. 2019. Life-cycle assessment of adsorbents for biohydrogen production. Resources **8**(1): 52.

Service Champions. 2018. 7 Home Heating System Types. https://www.servicechampions.net/blog/7-home-heating-system-types/ (Date accessed: March 18, 2020).

Sharp, A. 2019. Alberta's NDP government says emissions reductions prove carbon pricing works. The National Observer. https://www.nationalobserver.com/2019/02/20/news/albertas-ndp-government-says-emissions-reductions-prove-carbon-pricing-works (Date accessed: April 24, 2020).

Socaciu, L. G. 2011. Seasonal sensible thermal energy storage solutions. Leonardo Electronic Journal of Practices and Technologies **19**: 49-68.

Sőlken, W. Effects & Economic impact of Corrosion. Explore the World of Piping. http://www.wermac.org/materials/corrosion_allowance.html#:~:text=The%20corrosion%20allowance%20is%20a,reached%20its%20end%20of%20life. (Date accessed: October 7, 2019).

Tatsidjodoung, P., N. Le Pierrès, J. Heintz, D. Lagre, L. Luo and F. Durier. 2016. Experimental and numerical investigations of a zeolite 13X/water reactor for solar heat storage in buildings. Energy Conversion and Management **108**: 488-500.

Thaker, S., A. O. Oni and A. Kumar. 2017. Techno-economic evaluation of solar-based thermal energy storage systems. Energy Conversion and Management **153**: 423-434.

The United Nations. 2016. The Paris Agreement. https://unfccc.int/process-and-meetings/the-paris-agreement/the-paris-agreement (Date accessed: June 27, 2019).

Tonkens, A. 2020. How Long Does a Furnace Last in Canada? Cansumer. https://cansumer.ca/how-long-does-a-furnace-last-canada/ (Date accessed: December 10, 2020).

Toth, A. and E. Bobok. 2016. Flow and Heat Transfer in Geothermal Systems: Basic Equations for Describing and Modeling Geothermal Phenomena and Technologies, Elsevier.

Tripanagnostopoulos, Y., M. Souliotis, R. Battisti and A. Corrado. 2006. Performance, cost and life-cycle assessment study of hybrid PVT/AIR solar systems. Progress in Photovoltaics: Research and Applications **14**(1): 65-76.

U.S. Energy Information Administration. How much carbon dioxide is produced per kilowatthour of U.S. electricity generation? EIA. https://www.eia.gov/tools/faqs/faq.php?id=74&t=11 (Date accessed: April 24, 2020).

Ugur, B. 2013. Thermal energy storage in adsorbent beds. Master of Applied Science, University of Ottawa.

Unsdorfer, S. 2015. Managing Ideal Indoor Humidity for Maximum Comfort. Central Heating & Air Conditioning. https://www.centralhtg.com/blog/managing-home-humidity-for-maximum-comfort (Date accessed: October 7, 2019).

Van Alebeek, R., L. Scapino, M. Beving, M. Gaeini, C. Rindt and H. Zondag. 2018. Investigation of a household-scale open sorption energy storage system based on the zeolite 13X/water reacting pair. Applied Thermal Engineering **139**: 325-333.

Wadkar, V., S. Malgave, D. Patil, H. Bhore and P. Gavade. 2015. Design and analysis of pressure vessel using ANSYS. Journal of Mechanical Engineering and Technology (JMET) **3**(2): 01-13.

Wang, M. 2018. Argonne National Laboratory. Fuel Cell GREET1 Model. Center for Transportation Research. https://greet.es.anl.gov/ (Date accessed: October 7, 2019).

Woodford, C. 2019. Zeolites. https://www.explainthatstuff.com/zeolites.html (Date accessed: March 18, 2020).

Yang, L., R. Zmeureanu and H. Rivard. 2008. Comparison of environmental impacts of two residential heating systems. Building and Environment **43**(6): 1072-1081.

Zhang, H., J. Baeyens, G. Caceres, J. Degreve and Y. Lv. 2016. Thermal energy storage: Recent developments and practical aspects. Progress in Energy and Combustion Science **53**: 1-40.

Zhengzhou Gold Mountain Science and Technique Co. Ltd. 2019. Molecular Sieve Zeolite 13X. http://www.adsorbentcn.com/13x.htm (Date accessed: April 24, 2020).

Chapter 3

Developing a techno-economic model to evaluate the cost performance of a zeolite 13X-based space heating system

1. Introduction

Renewable energy installation capacity has been growing substantially over the years and now makes up three-quarters of the new installation capacity around the world (International Renewable Energy Agency 2020). However, renewable energy has faced several economical, social, and technological challenges (Lu et al. 2020). One of the common geographical barriers in the use of renewable energy such as solar and wind is intermittent supply, a result of, for example, the unpredictability of solar irradiation and wind speed. Storage technology is a promising solution to resolve the intermittency problem. Thermal energy storage (TES) can store excess heat for a long period of time with minimal loss of energy to the surrounding environment (Prieto et al. 2016), thus it has been widely investigated as a means of providing excess industrial sector energy to the residential sector. Space heating is one of the highest contributors to greenhouse gases (GHGs). Hence there is a need to develop a feasible solution such as thermal energy storage connected to solar collectors.

A space heating system is an essential part of buildings in cold climatic regions like Canada and major parts of the US. Forced air is the most popular space heating system on the continent; it uses a furnace and a blower fan to deliver conditioned air to rooms through a duct network (Formisano 2019). Natural gas is widely used as an energy source; other fuels like liquid propane, fuel oil, and electricity are less popular (Service Champions 2018). A natural gas forced air system is commonly used because its design is simple and it uses cheap fuel (Home Guide 2019), but it emits large amounts of GHG emissions while it is operating. In 2016, space heating accounts for more than 60% of the energy consumption in residential appliance energy use, making it the second largest contributor to GHG emissions in Canada (Lemghalef and Sager 2019; Natural Resources Canada 2020). Globally, residential buildings accounted for 10.9% total emissions due to fossil fuel combustion and electricity usage in 2016 (Climate Watch 2016; Ge and Friedrich 2020). Other space heating systems, electric boilers, and heat pumps have better environmental performance but are not as versatile as a natural gas furnace (Nitkiewicz and Sekret 2014; Craig 2019). However, regional factors such as provincial regulations and available resources facilitate the use of specific space heating systems. The GHG emissions from the space heating systems could be reduced if these are based on renewable energy sources like solar energy integrated with energy storage systems.

A thermochemical heat storage system using adsorbent material like zeolite not only stores heat for seasonal use but has a lower energy density than other thermal storage systems such as latent heat (Kylili and Fokaides 2016). Zeolite comprises hydrous silicates, which are commonly used as adsorbents or catalysts in different applications including ion-exchange water softeners, dishwasher detergents, CO_2 capture, and odor control (Woodford 2019). Zeolite 13X has a cage-like structure that allows it to capture water molecules and generate heat as a product (Jänchen et al. 2004). Type A and X are the two categories of zeolite, classified based on the compound’s three-dimensional crystal structure (Burkes 2020). The working pair of zeolite 13X and water is chosen for residential thermal storage because no harmful product is generated during the operating phase and the substances are stable at a wide range of temperatures.

The concept of adsorbent thermochemical storage has been around for a long time, but current research on the use of zeolite-based adsorbent for space heating systems has three major gaps. First, most studies on zeolite 13X modules are in the experimental stages and mainly aim to understand the physical and chemical characteristics and key parameters; these do not suggest how to integrate the storage system into the space heating system. Finck et al. experimented with a 3 kWh traction control system (TCS) module, focussing on space heating with a temperature lift of 20 K (2014). Van Alebeek et al. designed 4 separate segments with 62.5 L of zeolite each to understand how to use the sorption TCS for a household (2018). The module delivered 4.4 kW power with a total stored energy of 54 kWh. Zettl et al. conducted an experimental study with zeolite in a rotating reactor. The temperature lift of process air is up to 36 K with approximately 12 kWh of stored energy in 50 kg of zeolite (2014). de Boer et al. developed a 150 kg zeolite 13X prototype to verify the feasibility of a long-term TCS and the capacity to deliver thermal energy at temperatures useful for domestic application (2014). However, sustainability of the proposed technology has not been investigated.

Second, although there is very limited research on the techno-economic performance of zeolite 13X for large-scale heating systems. There are few studies that evaluate the economic feasibility for just smaller storage in residential households. Scapino et al. studied the techno-economic optimization of the sorption system in different energy markets (2020). The system includes two heat exchangers, a heat recovery device, sorption reactor, humidification unit, and valves. The authors concluded that sorption thermal energy storage integration would increase overall system profits by 41% in certain scenarios in the United Kingdom's market. The paper focuses on heat storage to provide heat to district heating systems. A rough economic evaluation by Hauer for a 7,000 kg zeolite 13X system that covers a heat load of 95 kW over a period of 14 hours is about 60,000 Euro (2007). A humidifier, water tank, control unit, and three zeolite 13X modules are the main components. The system was developed to provide additional heating and cooling for a school. Zondag et al. estimated investment costs of around 10200 Euro and 28000 Euro for solar collectors integrated with 7000 kg low-cost sorption materials and zeolite, respectively (2010). The authors considered low-cost sorption materials, storage casing, vacuum tube collectors, collector system components, heat exchangers, and the bore hole.

The third significant gap in studies of zeolite-based adsorbent for space heating systems is very limited focus on development of scale factor to understand the impact on capital cost of the system with a change in the size of the system due to economies of scale.

This research, therefore, aims to fill the research and knowledge gaps by conducting a comprehensive techno-economic assessment of the zeolite 13X thermal storage system with a PVT air system. The model was developed from the bottom up with the incorporation of various components necessary for the adsorbent system. The specific objectives of the study are to:

- Design and simulate a PVT-charged zeolite 13X storage for a space heating system in the residential sector;
- Develop a techno-economic model to compute the levelized cost of energy for zeolite 13X storage for small-scale buildings such as houses;
- Compare the levelized cost of heat released with that of existing conventional heating systems;
- Develop scale factors for the cost components to understand the economies of scale of the zeolite heating system for different climates and usable sizes;
- Conduct a case study for Alberta, a western Canadian province and cold climate jurisdiction;
- Conduct a detailed sensitivity and uncertainty analysis to provide insights into critical factors and uncertain parameters.

2. Method

A framework provides guidelines through which to execute research. This research has four parts: system review, engineering design, techno-economic assessment, and model output and results interpretation. First, a review was performed to identify space heating systems and their components. Second, an engineering model was developed to size the equipment/devices in the space heating system proposed for this study. Third, the techno-economic model was developed to assess the feasibility of the proposed system. Finally, the outputs of the model were interpreted and discussed.

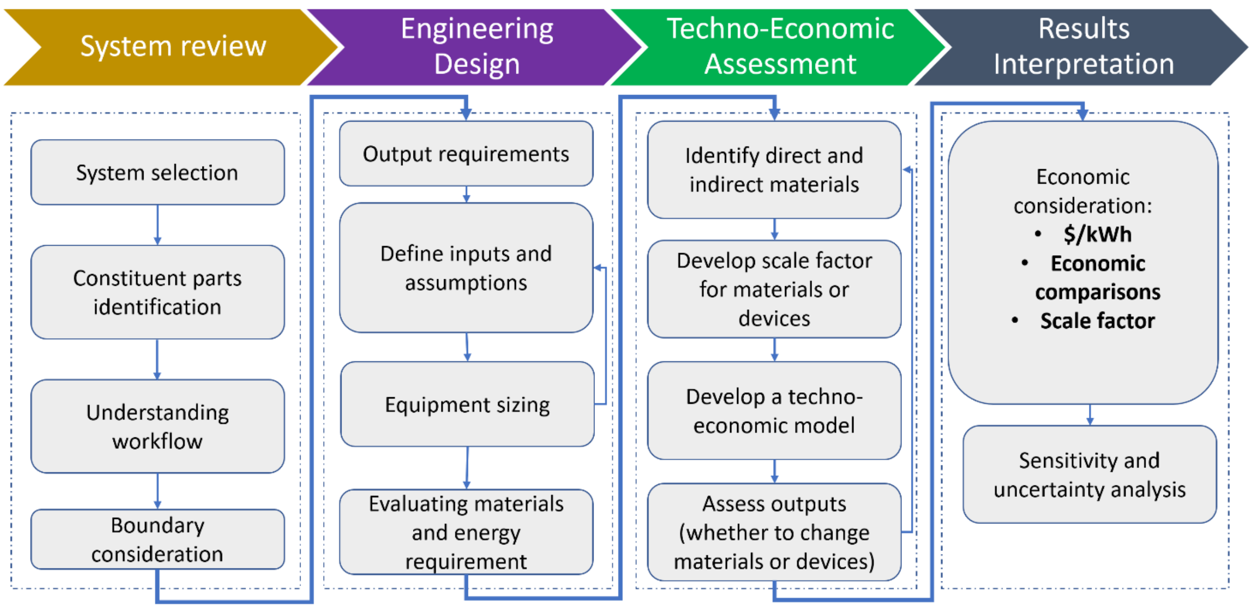

Fig. 3.1: Methodological framework

2.1 System review

System selection

Many working pairs (A and B) were investigated with the aim of achieving high energy density as well as stability, low environmental impact, and low cost:

$$AB + \text{heat} \leftrightarrow A + B$$

We conducted a brief review to identify adsorbent pairs of interest. Many processes have the potential to become a heat storage medium, i.e., the dehydration of salt hydrate, metal hydrides, and hydroxides, the de-ammoniation of ammonium chlorides, and the decarboxylation of metal carbonates (Kerskes 2016). The working pair of zeolite 13X and water has many advantages over other processes. Some reports suggest that zeolite 13X's energy density does not degrade over charging and discharging cycles. In radioactive waste management, the zeolites were utilized more than 25 years, which is longer than a 20-year lifespan considered in this study (UKEssays 2018). Zeolite 13X is reusable, so the environmental impacts of manufacturing it would be low. Additionally, during the operating phase, the material does not emit any GHGs or toxic chemicals. Therefore, water and zeolite 13X were chosen for the space heating system.

System description

The main components of the space heating system are blower fans, humidifiers, solar collectors, adsorbent vessel, zeolite 13X, a duct network, insulation, filters, and valves. Fan 1a (as labelled in Fig. 3.2), the solar collectors, and the zeolite vessels are active during the charging cycle, while all the equipment except the solar collectors operate during the discharging phase.

To charge the system, cold air (or room air) is taken in by the fan and passed through solar collectors to be heated. The heated air provides sufficient energy to break the bond between water and zeolite 13X. The output air would therefore have higher humidity than the inflow air. This air is safe to use for space heating directly if needed. For discharging, when there is no solar available, the humidifier (2a in Fig. 3.2) is turned on to increase the air's relative humidity to nearly 100%. Fan 1a will regulate the flow rate of the humidified air entering the adsorbent vessel. Because of the reaction between water and zeolite, the heat generated will increase the temperature of the air flowing through. The result of this process creates a hot dry airstream that can be used for space heating in households. Fan 1b and Humidifier 2b are used to adjust the temperature and relative humidity for comfort purposes before air is delivered to rooms through a duct network.

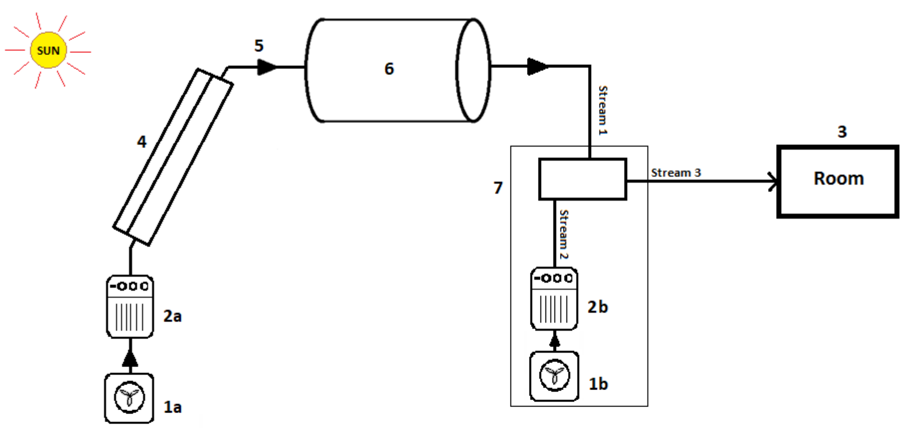

1: Fan

2: Humidifier

3: House or rooms

4: Solar heat source

5: Duct system

6: Adsorbent bed

7: Air mixing unit

Fig. 3.2: Space heating system with PVT air solar collectors

2.2 Engineering design

The main parameters used in the design phase of the research for a zeolite 13x space heating system are displayed in Table 3.1. The data was taken from various sources including published papers and online industrial websites. The parameters are crucial in developing the base case for the proposed system.

Table 3.1: Techno-economic model inputs for the heating system

COMPONENT	PARAMETER	UNITS	VALUE	REFERENCE/NOTES
House sizing	Usable area	125	m^2	This number is the average of median above-grade living area of a single detach (Statistics Canada 2019)
Capacity	Output energy	kW	16	With the area, the furnace sizer is chosen for specific condition
	Operating duration	hrs	8	The hours are chosen to meet the nighttime heating needs
Stream 1	Air temperature	ºC	50	(Dicaire and Tezel 2011)
	Relative humidity	%	0	(Dicaire and Tezel 2011)
Stream 2	Air temperature	ºC	15	The temperature on the low side when people are absence from the house before furnace started
Stream 3	Air temperature	ºC	25	Ductwork length varies. A small to average size house would have around the assumed length
	Relative humidity	%	35	(Unsdorfer 2015)
Adsorbent energy density	Zeolite 13X	kWh/m^3	154	(Dicaire and Tezel 2013)
	Zeolite density	kg/m^3	704	(Nienborg et al. 2018)
	Porosity		0.4	(Lefebvre et al. 2016)
	Pellet diameter	m	0.01	(Lefebvre et al. 2016)
Hot air properties	Dynamic viscosity	cP	0.01963	(Montgomery 1947)
	Density	kg/m^3	1.2461	(Engineering ToolBox 2004)
Container/Vessel	Allowance for corrosion	m	0.003	(Sőlken 2020)
	Maximum allowable working pressure	kPa	103,000	(CIS GmbH Consulting Inspection Services 2020)
	Efficiency of joints		0.8	(Peters et al. 1968)
Ductwork	Roughness	ft	0.0005	(Engineering ToolBox 2003)
	Length	ft	30	Assumed

COMPONENT	PARAMETER	UNITS	VALUE	REFERENCE/NOTES
Fan	Efficiency	%	50	(Engineering ToolBox 2003)
Humidifier	Operating Temperature	ºC	20	The average of the high and low temperature range of the house
Thermal conductivity	Galvanized steel	W/mK	18	(Bennaji et al. 2010)
	Fiberglass	W/mK	0.040	(Hammond 2008)

The base case of the space heating system needs to deliver 16 kW of heat over 8 hours. For a 125 m^2 usable area with a 2.44 m ceiling height and an air exchange of up to 9 times per hour, the output of the system (Stream 3) is designed to achieve a flow rate of 1800 cubic feet per minute. The delivered air would be 25ºC with a relative humidity of 35%. These values were chosen because the comfortable temperature and humidity for living are around 20-22ºC and 30-60% (Acurite 2017; Direct Energy 2019, 2020). The temperature and relative humidity of the calculated stream (e.g., Stream 3 in Fig. 3.2) can be calculated from the qualities of the two other streams by applying adiabatic mixing rules (through Equation A11 in Appendix) or a psychometric chart (Balmer 2011; Mugdha 2019).

The volume of zeolite 13X was obtained using the total energy output (kWh) and the energy density of material (kWh/m^3), which was obtained from literature. The thickness of the vessel is found by applying Equation A15 in Appendix, derived from Peters et al. (Peters et al. 1968).. The pressure drop across the zeolite 13X bed was estimated by Ergun's equation (Equation A6 in Appendix) (Coker 2014).

The total pressure loss of the system is an essential parameter in sizing the blower fan motor. The humidifiers were sized based on the maximum flow rate and vapour density (or capacity) needed to increase the air's relative humidity to above 90%. Insulation is considered to contribute no more than 5% heat loss to the whole system, including the vessel and duct network. We assumed there was no heat loss to rooms close to the furnace and that heat would be distributed unevenly throughout the house. Finally, we deduced the physical area of solar collectors based on the heating demand requirement and the available solar irradiation. Our study used data from an earlier study conducted of 806 kWh/m^2 per year for PVT – because Alberta has similar solar potential (Tripanagnostopoulos et al. 2006; Global Solar Atlas v2.2 2020).

2.3 Techno-economic assessment

Materials and components of the heating system were modelled as a function of both cost and size to account for economies of scale (Eq. 1). With the scale factor of 1, the equation becomes a straight line and the cost increases proportionally with the capacity. If the scale factor is less than 1, the rate of capital cost increase is less than the growing rate of capacity. This means less capital cost is needed for the additional capacity (Sultana et al. 2010). For instance, steel cost was calculated using Equation 5 (Moore 1959) in which 0.65 is the scale factor for steel production (Pootakham and Kumar 2010) and the cost of a short tonne of carbon steel is US$716 in 2019 (Wallace 2018; World Steel Prices 2019). The cost of galvanized steel, the main material in the duct network, is approximately $1320 per short tonne (Wallace 2018; World Steel Prices 2019).

$$C_n = C_r(\frac{Q_n}{Q_r})^m \quad \text{(Eq. 1)}$$

Here, C_n is the cost of a product at a capacity Q_n, C_r is the known cost for the reference capacity Q_r, and m is the correlation exponent ($0<m<1$).

The volume and weight of zeolite required for the system were estimated with the available information on zeolite energy density. A correlation (shown in Fig. 3.3) was developed between the weight of zeolite and the investment cost as found in commercial data.

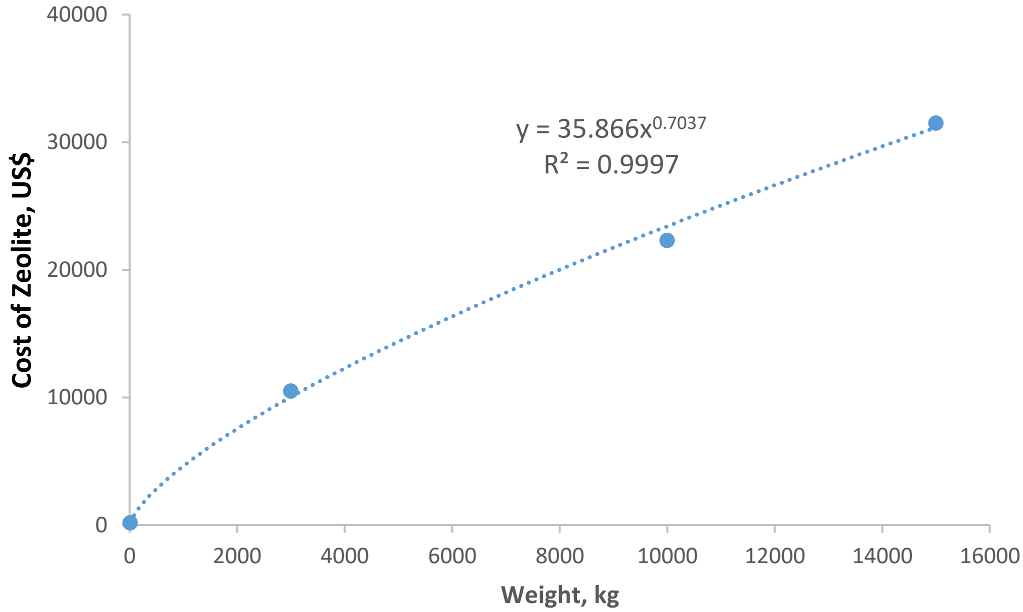

Fig. 3.3: Weight vs cost correlation for zeolite 13X

The heating system comprises two fans and two blowers. Each fan was designed to have enough power to overcome the internal pressure developed inside the system due to packed zeolite, friction on the ducts, and filters. The cost formula of the fan with a motor is described through Eq. 2 (Couper et al. 2010). Carbon steel is the material chosen for the installation factor and the fan is a propeller with guide vanes.

$$C = 1.218 f_m f_p \exp[a + b * lnQ + c * (lnQ)^2] \quad \text{(Eq. 2)}$$

Here, f_m is the installation factor, which determines the materials used, f_p is the gage pressure required, a, b, and c are constants for fan type and can be radial blades, backward curved, propeller, or propellers with guide vanes.

Another important component in the model is the humidifier. One humidifier is critical in the discharging process to release the stored heat and the other is necessary to change the humidity level. The correlation given in Fig. 3.4 was created based on the vendor cost data available online (Guangzhou Dongao Electrical Co. 2019).

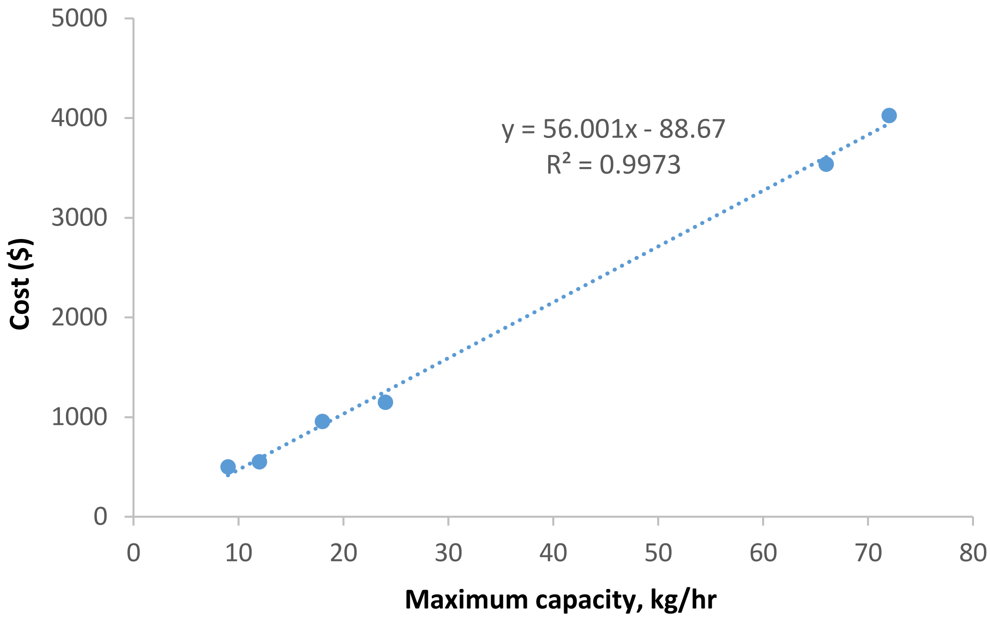

Fig. 3.4: Maximum capacity vs cost for humidifiers

Transportation cost was determined with the weight of all the materials in the system and the transportation distance. A tractor-trailer operating in uncongested conditions would cost roughly 0.244 CAD per tonne-km (Ray Barton & Associates 2006). For the base case, the transportation distance is assumed to be 1100 km.

The installation cost is primarily affected by the usable area of a residential house since the area determines the size of the furnace and the cost of the duct system. Fig. 3.5 shows the developed correlation between the usable area and the installation cost. The data was retrieved from a vendor on space heating (PickHvac 2020). Fibreglass was chosen for both the zeolite vessel and the duct network insulation. The relationship between weight and cost per kg was generated based on data available from a manufacturer and is shown in Fig. 3.6 (Buy Insulation Products 2020). Miscellaneous items such as the damper and valves were also considered in the initial investment.

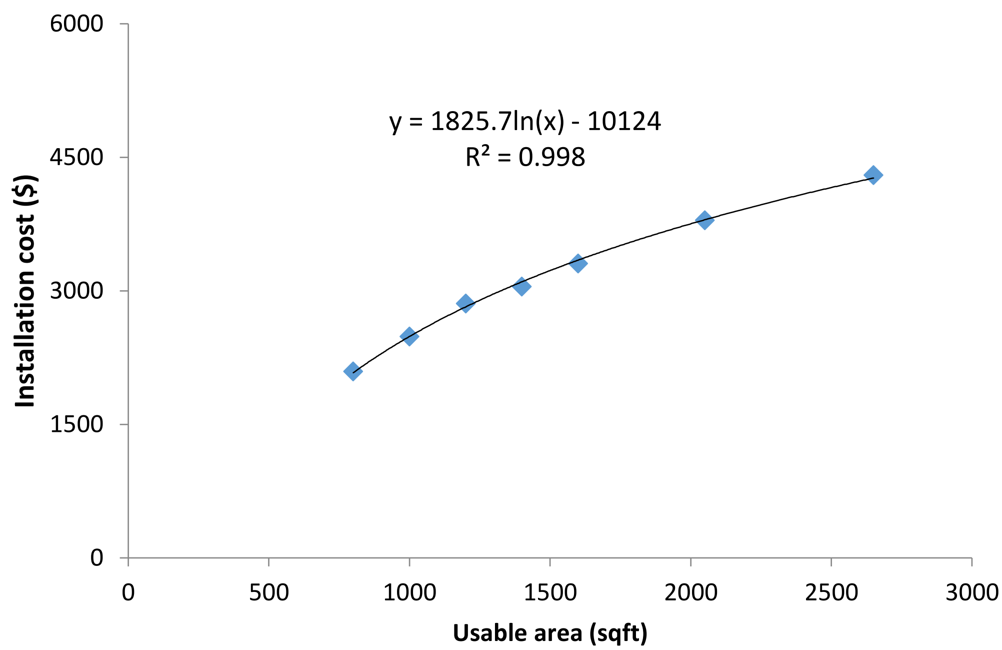

Fig. 3.5: Usable area vs installation cost for residential houses

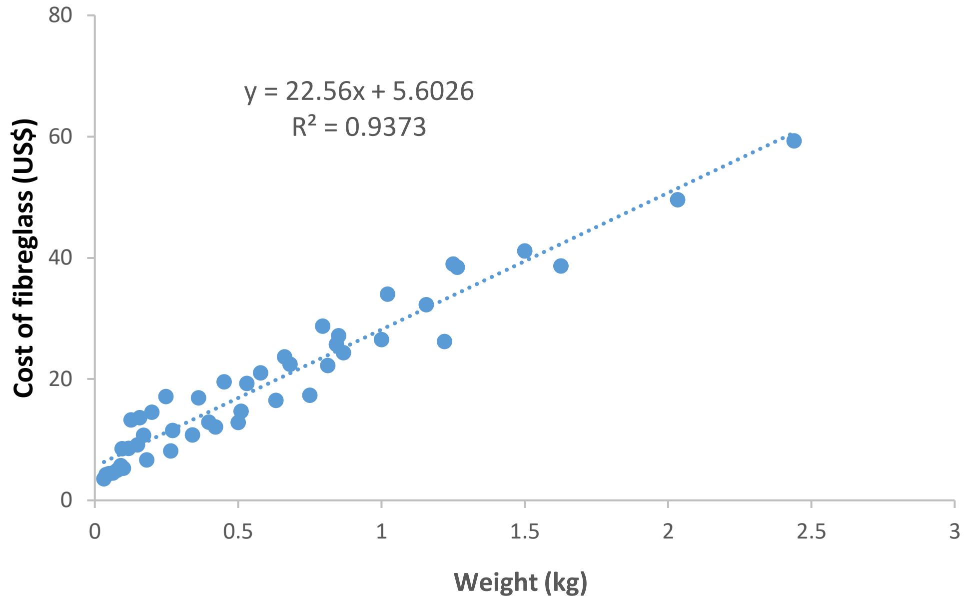

Fig. 3.6: Weight vs cost per weight for fibreglass

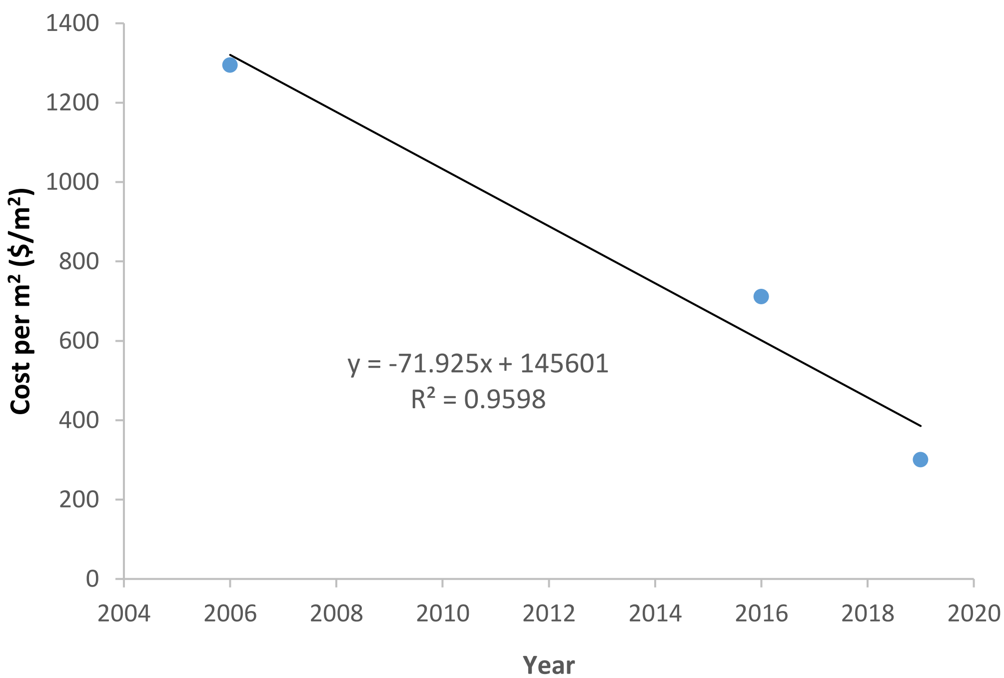

Fig. 3.7: Year vs cost per m^2 of solar collectors

The capital cost of a solar collector system including PV modules, air circulation system (air ducts and fan), glazed cover, reflectors, and installation was obtained from literature Tripanagnostopoulos et al. (2006). Glazed solar collector costs from different years were collected from literature (Tripanagnostopoulos et al. 2006; Agrawal and Tiwari 2015; Tiwari 2016). A model was developed based on the data points and glazed solar collector costs were projected for the year 2019 (Fig. 3.7). The value was adjusted slightly for a system of glazed solar collectors with reflectors. The total solar collector area was found by using household heat demand and data for potential solar irradiation from solar thermal collectors with reflectors from literature. The cost of the solar collectors, therefore, is based on the solar collector area and the cost per unit area (US\$/m^2). The lifetime of the system was considered to be 20 years in order to compare it to a natural gas furnace, the most common furnace in North America (Reliable Home Advice 2018; Petro Home Services 2020). There are three annual costs in the cash flow model: maintenance, water, and electricity. We assumed the heating system did not require major maintenance during its lifetime, but the annual maintenance cost for small components such as filters and valves or cleaning system was assumed to be US\$150 per year (Costimates 2020). The water cost consists of a fixed monthly amount of 6.63 CAD and volume of 1.94 CAD per m^3 (EPCOR 2020). The electricity price was assumed to be around 0.09 CAD per kWh (Alberta Utilities Commission 2020). All costs were inflated to 2019 dollars unless the cost models were developed from 2019 data. The discount rate was taken to be 10% annually. Additionally, Canadian dollars were converted to USD (0.75 CAD = 1 USD).

Table 3. 2: Excel model inputs for operating costs

COMPONENT	UNITS	VALUE	REFERENCE/NOTES
Yearly maintenance cost	150	US$	(Costimates 2020)
Water cost	6.63 + 1.94*(water volume)	CAD	(EPCOR 2020)
Electricity price	0.09	CAD per kWh	(Alberta Utilities Commission 2020)
Discount rate	10	%	(Thaker et al. 2017)

COMPONENT	UNITS	VALUE	REFERENCE/NOTES
Inflation rate	2	%	(Macrotrends 2020)
US -> Canada conversion rate	0.75	CAD/US$	(Bank of Canada 2020)

2.4 Sensitivity and uncertainty analysis

Sensitivity analysis assists in finding input parameters that have significant influence on the outcomes, and uncertainty analysis provides a possible range of outcomes from the given range of inputs. Our model used Morris sensitivity analysis to identify the most sensitive input data. Uncertainty analysis is performed by running a Monte Carlo simulation through thousands of runs depending on the accuracy needed (Liu 2017; Thaker et al. 2017; Kapila 2018; Di Lullo et al. 2020). The results provide a probable range for the model since predicted results for an undeveloped system is an extremely difficult task. Table 3.3 presents the input parameters and their range in sensitivity and uncertainty analyses.

Table 3.3: Sensitivity and uncertainty inputs

Variables	Min	Max	Unit	Reference
Zeolite energy density	106	250	kWh/m^3	(Gantenbein et al. 2001; Dawoud et al. 2007; Hauer 2007; Scapino et al. 2017a, 2017b)
Length-to-diameter ratio	0.1	2.8		(Ugur 2013; Kuznik et al. 2020)

Variables	Min	Max	Unit	Reference
Zeolite pellet diameter	0.003	0.008	m	(Zhengzhou Gold Mountain Science and Technique Co. Ltd 2019)
Pipe roughness	1967×10^{-7}	9836×10^{-7}	ft	(Ratnayaka et al. 2009)
Length of duct system	99.6	149.4	ft	Assumed
Fan efficiency	40%	84%		(Brendel 2010; Mathson and Ivanovich 2011)
Transportation distance	1100	5000	km	Assumed
Solar collector potential	806.5	1000	kWh/m^2-yr	(Tripanagnostopoulos et al. 2006; Athaudage Dona 2014)

Zeolite is the core material for the heating system so its weight, affected by energy density, is a parameter to consider. We identified the range of 106-250 kWh/m^3 by synthesizing different study results from a literature review (Gantenbein et al. 2001; Dawoud et al. 2007; Hauer 2007; Scapino et al. 2017a, 2017b). Length-to-diameter ratio is an essential variable that determines the duration of air flowing inside the vessel. Based on very limited information from literature, a range of 0.1 to 2.8 was found (Ugur 2013; Kuznik et al. 2020). Another parameter influencing the interaction between the inflow air and the contacting surface of zeolite 13X is the size of the pellet. The upper range of 3 to 8 mm was chosen to minimize the pressure drop in the system while maintaining sufficient contact surface (Zhengzhou Gold Mountain Science and Technique Co. Ltd 2019). The roughness of a galvanized steel duct network ranges from 0.0001967 to 0.0009836 ft given the operating and deteriorating conditions (Ratnayaka et al. 2009). The margin of safety for the duct length is assumed be 20% of its original value, which is derived from a correlation between the usable area and the duct length. We used values of 40-84% for the fan efficiency to understand the impact of this electric equipment on the overall economics of the system (Brendel 2010; Mathson and Ivanovich 2011). The shorter travel distance, 1100 km, represents the distance from Alberta to the west coast and the longer, 5000 km, is the distance to the east coast of Canada. Last but not least, since the solar collector is an important part of the space heating system, the uncertainty in its input was examined. The lower limit, 806.5 kWh/m^2-yr, is the amount of solar energy obtained from the solar air collectors and the upper limit is the lowest daily average solar potential in Alberta (Tripanagnostopoulos et al. 2006; Athaudage Dona 2014).

3. Results and Discussion

3.1 Heating system design output

Table 3.4 shows the results of the design phase from the simulation model. To provide 16 kW heat for 8 hours of operation, a vessel of approximately 1 m^3 containing zeolite 13X is needed. The footprint of the whole system is of reasonable dimensions to fit in the furnace room in most homes. Water and electricity are the two resources consumed continuously during the operating phase. Fan motors contribute a small share in electricity consumption, and the two humidifiers (0.68 kW and 1.13 kW) account for the largest share in both electricity and water consumption. Hence, a more efficient humidifier is key to lowering electricity consumption and operation cost. The solar collectors occupy almost 39 m^2, which is quite large for a usable area of 1350 square feet, but collectors of these dimensions can feasibly be mounted on the roof top of a single detached home.

Table 3.4: Output from the simulation model

COMPONENTS	PARAMETER	UNITS	VALUE
Stream 1	Volumetric flow rate	m^3/s	0.2933
Stream 2	Volumetric flow rate	m^3/s	0.5594
	Relative humidity	%	89
Zeolite	Volume	m^3	1.005
Container/Vessel	Diameter	m	1.086
	Length	m	1.086
	Pressure drop	Pa	250.22
	Thickness	m	0.00370
Fan	Total pressure loss	in of water	1.42
	Fan 1 power rating	HP	0.34
	Fan 2 power rating	HP	0.04
Humidifier	Humidifier 1 capacity	kg/hr	13.7
	Humidifier 1 power rating	W	683.0
	Humidifier 2 capacity	kg/hr	20.4
	Humidifier 2 power rating	W	1129.3
Insulation	Thickness	m	0.015
Solar collectors	Total area needed	m^2	38.9

3.2 Techno-economic assessment

Table 3.5: Simulation output from the techno-economic assessment

EQUIPMENT	VALUE	UNITS
Total primary investment	28444.13	US$
Total cost for 20 years with discount and inflation	37692.78	US$
Cost/kWh (heat)	0.0601	US$/kWh

Table 3.5 lists outputs from the techno-economic model. The highest cost contribution is from the solar collector system, which accounts for 67% of the total investment cost (Fig. 3.8). The most expensive components of the solar collector are the mc-Si PV modules followed by the transparent

cover for the glazed PVT (Tripanagnostopoulos et al. 2006). An earlier study performed an economic analysis of hybrid PVT collectors for a solar domestic hot water system and similarly found that the solar collector is around 50% of the total system cost (Matuska 2014). The material production cost contributes greatly to the total cost of PV module manufacturing (Fathi et al. 2009; Horowitz et al. 2017). Improvements in both efficiency and manufacturing cost per solar system area could help improve the economics of the whole space heating system. Other large portions of the investment are the operating and installation cost (11%), which was derived from the labour requirement and useable area of the building, the zeolite 13X material (9%), and the humidifiers (7%). The contributions from other components such as the duct system, transportation, fiberglass, and so on are comparatively small. Based on the analysis period of 20 years of using the system the cost is $0.06 per kWh of heat generated.

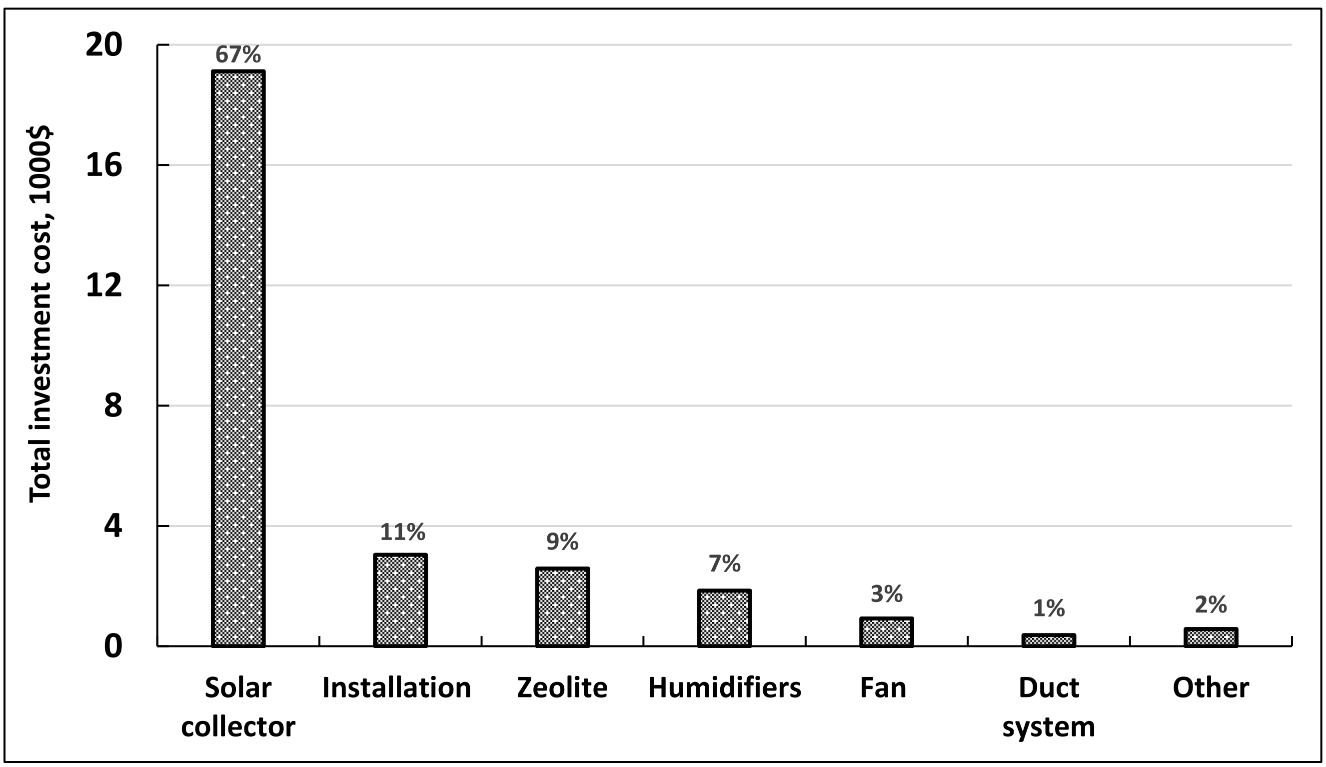

Fig. 3.8: Cost shares of the zeolite 13X space heating system

3.3 Comparisons with different heating systems

It is important to determine the proposed space heating system compares with other heating systems. Fig. 3.9 shows the cost per kWh of heat generated for 7 different heating systems. Yang et al. researched the costs of commercialized systems (i.e., electric boiler, gas-fired boiler, electric furnace, and gas-fired furnace) (2008). The values were adjusted in this research to Alberta's electricity price assumptions to make meaningful comparisons between the technologies. As can be seen from Fig. 3.9, the forced air heating (FAH) gas-fired furnace, whose cost is half that of a hot water heating (HWH) electric boiler with a heat recovery ventilator (HRV), is the most economical solution. The adsorbent system cost per kWh heat generated is smaller than the HWH electric boiler with an HRV but similar to the HWH electric boiler without an HRV and the HWH gas-fired boiler with an HRV. Given that its cost is reasonable compared to available heating systems on the market, it is worth investigating the adsorbent system further. The cost of solar collectors, which accounts for the highest investment share, is expected to decrease in the coming years because of lower installation and manufacturing costs (Smiti 2019; Fortune Business Insights 2020); this would help reduce the investment cost and cost/kWh of the proposed system. Provincial regulations and resource availability can significantly influence the cost of a space heating system.

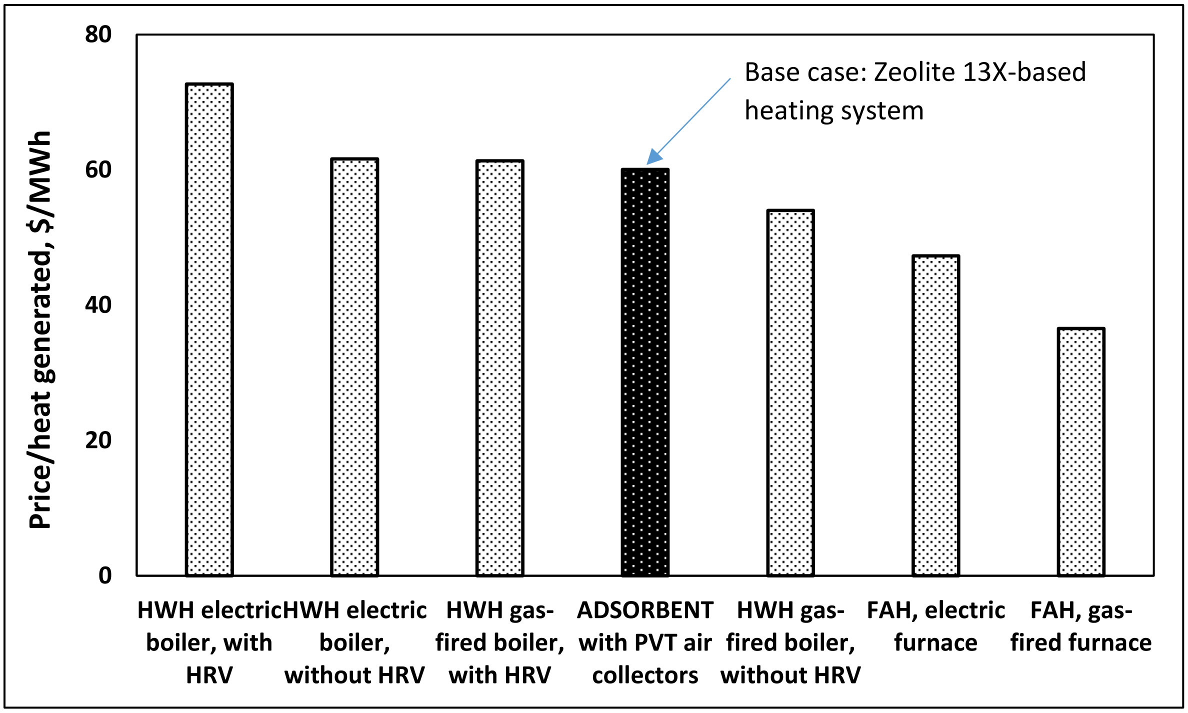

Fig. 3.9: Different space heating systems

3.4 Developed scale factor for adsorbent space heating system

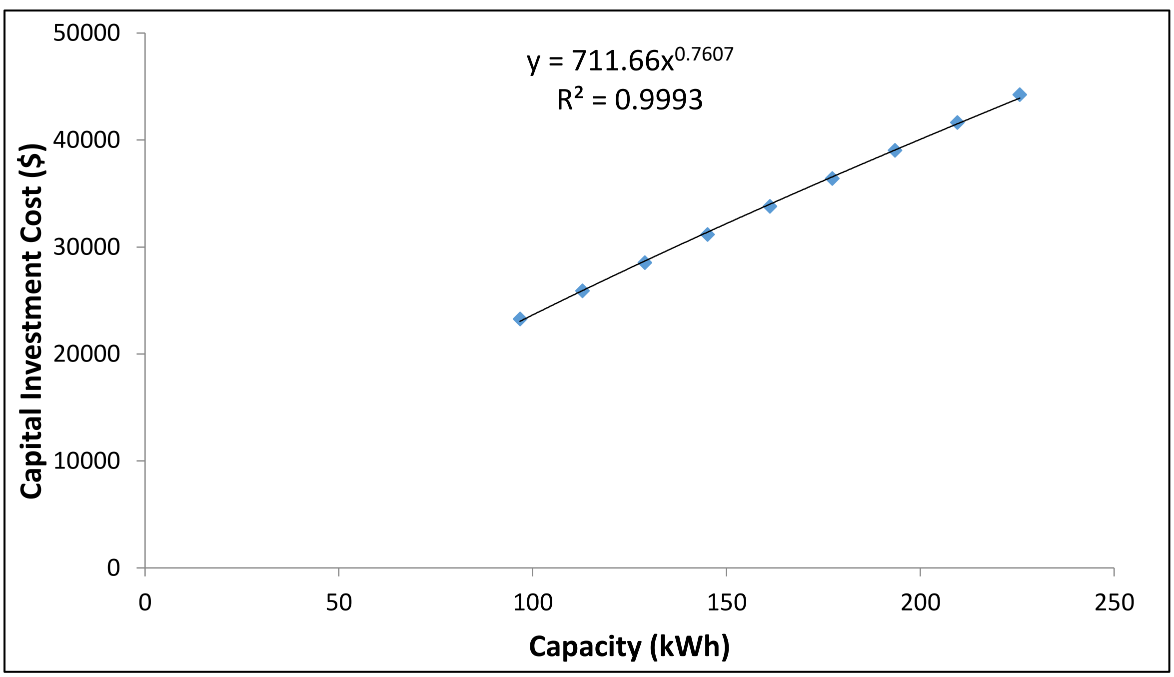

Fig. 3.10: Developed scale factor for capital cost of a furnace for the zeolite 13X space heating system

The larger the capacity, the lower the cost per unit heat generated. For instance, with a similar living space or usable area, the cost per kWh for a house in a colder climate would be lower than for one in a warmer area. Hence, studying the rate of capital investment change relative to the rate of increasing storage size would be beneificial. Fig. 3.10 shows the economies of scale benefits of decreasing incremental capital cost with the capacity of the space heating system. The figure was generated by changing the capacity through duration of discharge while keeping the other input parameters constant. The scale factor of the zeolite-based heating system is 0.761. Therefore, doubling the storage would only increase the capital investment by 69%. It is important to note that without including the solar collectors cost, the economies of scale would reduce to 0.225. The values emphasizes the importance of investigating indivdual component to improve the system capital cost.

Breaking the space heating system into components, the capital cost of each equipment can be analyzed. The duct network, fan 2, and humidifiers do not change in size when the size of storage increases. Fig. 3.11 shows the effect on different components in the system when the capacity changes. Noticibaly, fan 1 slightly decreases in size due to the fact that the system internal pressure reduces. This reduction is from the larger vessel housing the additional zeolite added. The fibreglass also has a great scaling factor since only zeolite vessel needs additional insulation in the whole system. Additionally, the zeolite vessel made of steel have great economies of scale, m = 0.488. The two components with the hishest cost, solar collectors and zeolites, have the worst economies of scale. Solar collector price, hence, should be the focus to reduce the overal cost of the system at larger scale

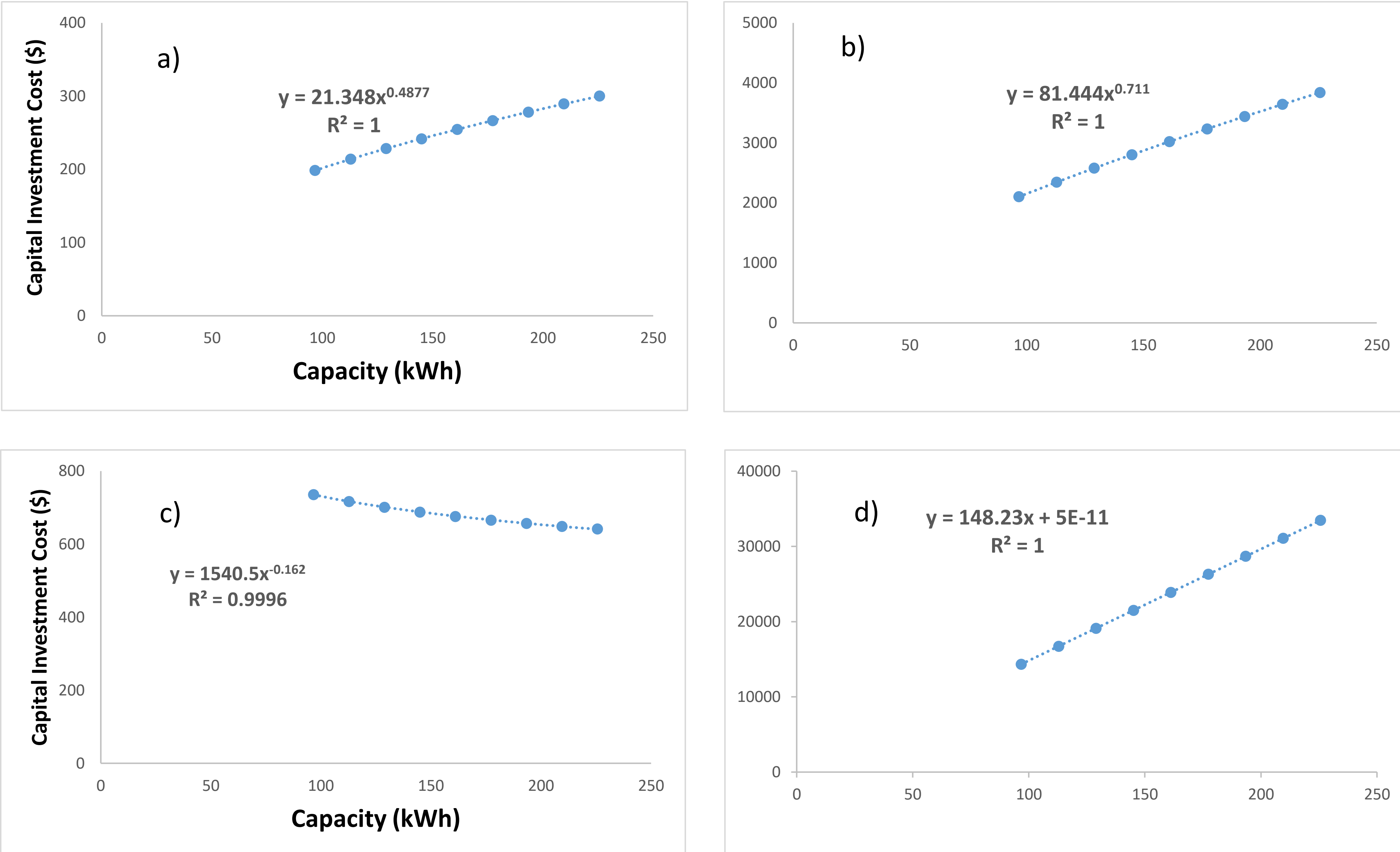
a)
y = 21.348x^0.4877
R² = 1
Capital Investment Cost ($)
Capacity (kWh)
b)
y = 81.444x^0.711
R² = 1
c)
y = 1540.5x^-0.162
R² = 0.9996
Capital Investment Cost ($)
Capacity (kWh)
d)
y = 148.23x + 5E-11
R² = 1

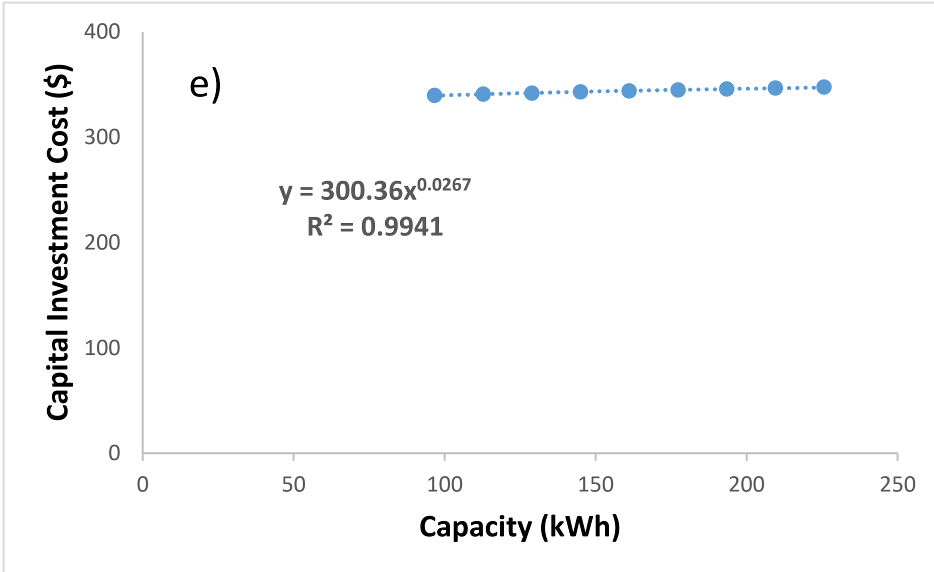

Fig. 3.11: Scale factor: a) Zeolite vessel, b) Zeolite, c) Fan 1, d) Solar collectors, e) Fibreglass

3.5 Sensitivity and uncertainty analysis

The results of the Morris sensitivity analysis are shown in Fig. 3.12 based on the methodology developed earlier (Di Lullo et al. 2020). Material properties that have great influence on the model outcomes are the length-to-diameter ratio, solar potential, pellet spherical diameter, the energy density of zeolite 13X, and fan efficiency. The length-to-diameter ratio and the pellet diameter are the factors influencing pressure loss and hence they contribute to the sizing of all other components. Therefore, the system cost would change substantially if these variables change. The efficiency of the solar collectors and the energy density of zeolite are the two properties that scientists have focussed on improving for decades. New materials and innovative manufaturing methods are improving the efficiency of the solar collectors as well as the energy density of adsorbent materials. Fans, which regulate the flow rate and allow it to surpass the internal pressure, also influence the investment cost. A conservative fan efficiency of 50% was set in the model, but fan efficiency can be above 90%.

100,000 Monte Carlo simulations were run to achieve a confident range in the output of the techno-economic model. Cost from the proposed space heating system would likely be between 5.4 cents and 6.1 cents per kWh with a mean of approximately 5.7 cents per kWh heat released, as can be seen from Fig. 3.13. Even at the high end of the range, the space heating system still requires less investment than an HWH electric boiler with an HRV. The two parameters with most uncertainty are the solar collector potential and length-to-diameter ratio. With respect to the former, there is a wide range of collectors and scant information on PVT air solar collectors, and the amount of solar irradiation that can be collected by such a system in Alberta is unknown. As for the length-to-diameter ratio of the adsorbent vessel required to optimize the stored heat, this value is being actively experimented by researchers around the world.

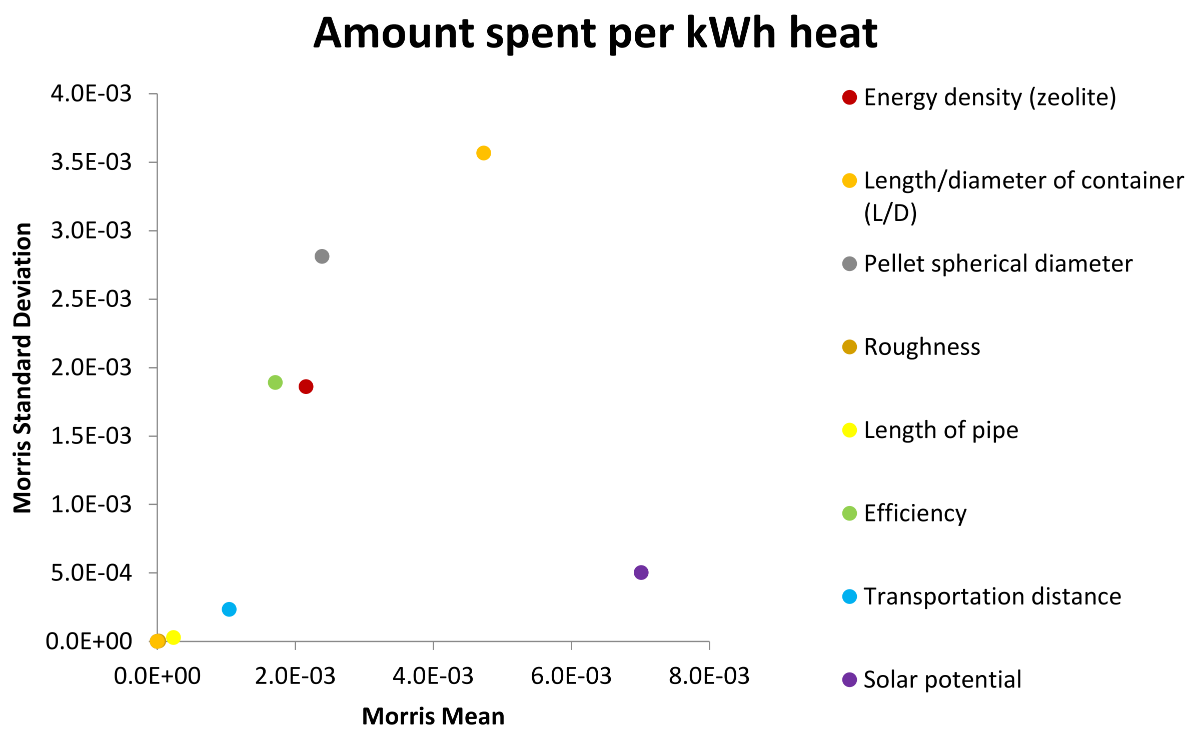

Fig. 3.12: Sensitivity analysis

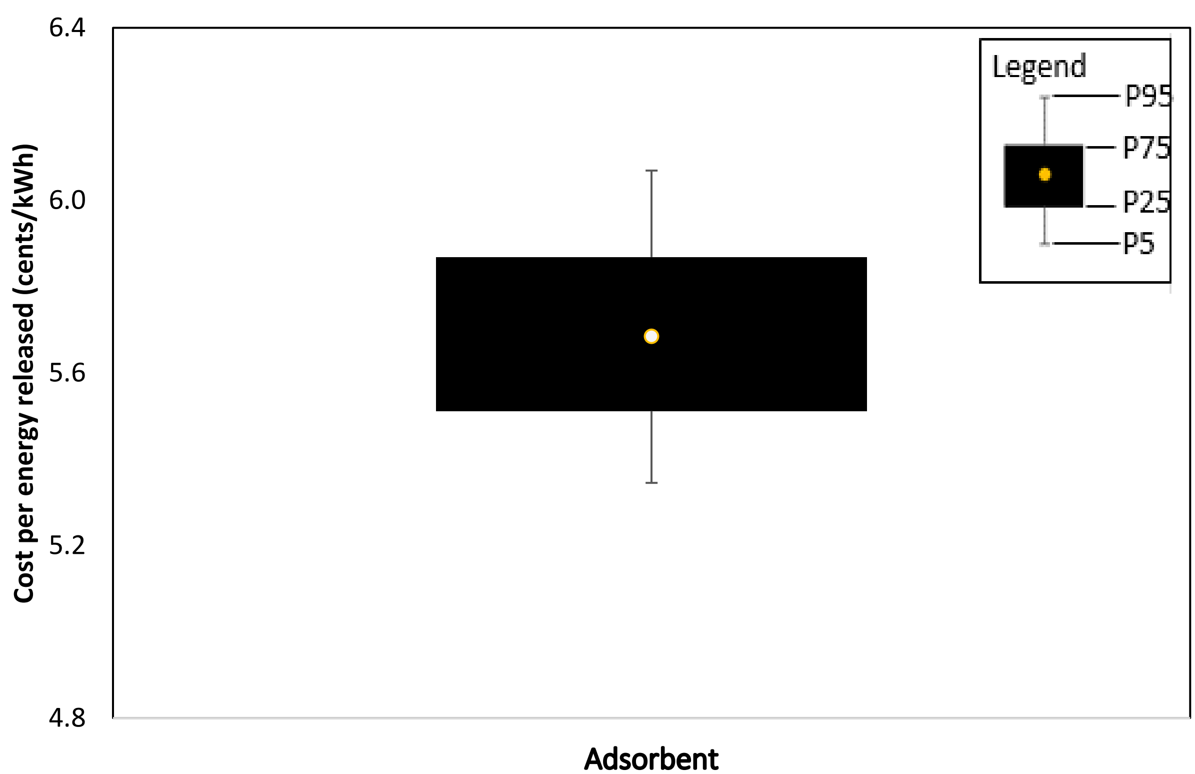

Fig. 3.13: Uncertainty analysis

4. Conclusion

In cold regions like Canada, a space heating system is an essential part of every household. Greenhouse gas emissions (GHG) emissions from natural gas consumption to provide space heating in the residential sector is a key environmental concern. There is very limited scientific research that extensively studies the economic feasibility of a zeolite 13X-based space heating system. This paper provides a novel contribution in applying engineering first principles to integrate system design and process design in techno-economic modelling to accurately estimate the life cycle cost of delivering heat energy to a residential home in a cold climate. PVT air solar collector-based zeolite 13X storage is explored through a bottom-up techno-economic model to understand its economic feasibility compared to other conventional space heating systems. An engineering design was developed for the base case of 16 kW heat output for a duration of 8 hours, intended to replace the 16 kW furnace used in the average single detached home in Canada. The cost of generating heat through the zeolite 13X space heating system is $0.06/kWh, which is slightly more expensive than an FAH electric furnace and an FAH gas-fired furnace but less than those technologies with heat recovery ventilators. Solar collectors and installation costs are the highest contributors to the total investment cost. The cost of solar collectors will likely decrease in the coming decades through the economies of scale of the solar thermal manufacturing capacity and technology improvement, and this would play a critical role in facilitating the transition to cleaner energy in the residential sector. The scale factor was determined to be 0.761, which means the system has a small economies of scale. Another point of consideration when the system is scaled up has the potential to split the system into multiple units for several zones as well as to better control heat loss. The length-to-diameter ratio, pellet diameter, and solar collector potential are the most critical parameters in the model. All of these greatly influence the sizing of the other equipment and hence the total system footprint. Even at the higher end, the price of the adsorbent is competitive compared to a FAH electric furnace and a FAH gas-fired furnace. These research highlights, broadly, that overall investment in new technology such as zeolite 13X storage for a space heating system can be competitive compared to conventional heating systems. Additionally, energy storage would be essential to improve the reliability of renewable resources, which is critical for the space heating sector. It is important to note that the proposed pace heating system would work well in regions where sufficient solar irradiation is present. The information developed in this study could be used for making investment decisions and policy formulation.

References

Acurite. 2017. Acurite. Maintaining Healthy Indoor Air Qualit. https://www.acurite.com/blog/home-monitoring-ideal-temperature-and-humidity-level-in-home (Date accessed: May 7, 2020).

Agrawal, S. and G. Tiwari. 2015. Performance analysis in terms of carbon credit earned on annualized uniform cost of glazed hybrid photovoltaic thermal air collector. Solar Energy **115**: 329-340.

Alberta Utilities Commission. 2020. Residential regulated rate option at a glance. http://www.auc.ab.ca/Pages/current-rates-electric.aspx (Date accessed: May 26, 2020).

Athaudage Dona, N. 2014. Performance of the solar thermal hot water system at the southland leisure centre. Unpublished master's thesis, University of Calgary.

Balmer, R. T. 2011. Modern Engineering Thermodynamics. United State of America, Academic Press.

Bank of Canada. 2020. Currency Converter. https://www.bankofcanada.ca/rates/exchange/currency-converter/?rangeType=dates&rangeValue=1.w&sF=Canadian+dollar&lP=lookup_currency_converter_2017.php&sR=2010-12-16&sTF=to&sT=FXUSDCAD&co=1.00&dF=2020-06-16&dT=2020-12-16 (Date accessed: Dec 17, 2020).

Bennaji, N., I. Mellouki and N. Yacoubi. 2010. Thermal properties of metals alloy by electrical pyroelectric method (EPE). Journal of Physics: Conference Series (Vol. 214, p. 012138). IOP Publishing.

Brendel, M. 2010. The Role of Fan Efficiency in Reducing HVAC Energy Consumption. https://www.amca.org/assets/resources/public/userfiles/file/AMCA_Spring2010RoleOfFE.pdf (Date accessed: April 24, 2020).

Burkes, K. 2020. 3A, 4A, 5A, 13X… What's the difference? HengYe Inc. https://hengyeinc.com/3a-4a-5a-13x-whats-the-difference/ (Date accessed: March 18, 2020).

Buy Insulation Products. 2020. Fiberglass pipe insulation. https://www.buyinsulationproductstore.com/Fiberglass-Pipe-Insulation-SSL-ASJ/ (Date accessed: July 26, 2020).

CIS GmbH Consulting Inspection Services. 2020. Some examples for allowable stress values "S" of typical carbon steels according to Section II, Part D, Table 1A, metric. https://www.cis-inspector.com/asme-code-calculation-allowable-stresses.html (Date accessed: October 7, 2019).

Climate Watch. 2016. Historical GHG Emissions. https://www.wri.org/blog/2020/02/greenhouse-gas-emissions-by-country-sector#:~:text=Global%20annual%20greenhouse%20gas%20emissions,rose%20each%20year%20since%20then. (Date accessed: December 10, 2020).

Coker, A. K. 2014. Ludwig's Applied Process Design for Chemical and Petrochemical Plants, Gulf Professional Publishing.

Costimates. 2020. January 8, 2020. Gas Furnace Tune-Up and Seasonal Maintenance Costs. https://www.costimates.com/costs/heating-air-conditioning/furnace-maintenance-tuneup/ (Date accessed: May 26, 2020).

Couper, J., W. Penney, J. Fair and S. Walas. 2010. Chapter 21-Costs of Individual Equipment. Chemical Process Equipment: 717-726.

Craig. 2019. Gas vs Electric Boilers: Pros, Cons, & Recommendations. Appliance Analysts. https://applianceanalysts.com/gas-vs-electric-boilers/ (Date accessed: May 7, 2020).

Dawoud, B., E. H. Amer and D. M. Gross. 2007. Experimental investigation of an adsorptive thermal energy storage. International Journal of Energy Research **31**(2): 135-147.

de Boer, R., S. Smeding, H. Zondag and G. Krol. 2014. Development of a prototype system for seasonal solar heat storage using an open sorption process, Petten: ECN.

Di Lullo, G., E. Gemechu, A. O. Oni and A. Kumar. 2020. Extending sensitivity analysis using regression to effectively disseminate life cycle assessment results. The International Journal of Life Cycle Assessment **25**(2): 222-239.

Dicaire, D. and F. H. Tezel. 2011. Regeneration and efficiency characterization of hybrid adsorbent for thermal energy storage of excess and solar heat. Renewable Energy **36**(3): 986-992.

Dicaire, D. and F. H. Tezel. 2013. Use of adsorbents for thermal energy storage of solar or excess heat: improvement of energy density. International Journal of Energy Research **37**(9): 1059-1068.

Direct Energy. 2019. Recommended Thermostat Settings in the Winter. Energy Efficiency. https://www.directenergy.com/learning-center/energy-efficiency/recommended-thermostat-settings-winter (Date accessed: April 22, 2020).

Direct Energy. 2020. Your Average House Temperature. https://www.directenergy.ca/learn/recommended-thermostat-settings-winter (Date accessed: Aprill 22, 2020).

Engineering ToolBox. 2003. Fans - Efficiency and Power Consumption. https://www.engineeringtoolbox.com/fans-efficiency-power-consumption-d_197.html (Date accessed: October 7, 2019).

Engineering ToolBox. 2003. Ventilation Ducts - Roughness & Surface Coefficients. https://www.engineeringtoolbox.com/surface-roughness-ventilation-ducts-d_209.html (Date accessed: October 7, 2019).

Engineering ToolBox. 2004. Density of Moist Humid Air. https://www.engineeringtoolbox.com/density-air-d_680.html (Date accessed: October 7, 2019).

EPCOR. 2020. Multi-Residential and Commercial Rates. https://www.epcor.com/products-services/water/rates-terms-conditions/Pages/commercial-multi-residential-rates.aspx (Date accessed: May 26, 2020).

Fathi, M., A. Mefoued, A. Messaoud and Y. Boukennous. 2009. Cost-effective photovoltaics with silicon material. Physics Procedia **2**(3): 751-757.

Finck, C., E. Henquet, C. van Soest, H. Oversloot, A.-J. de Jong, R. Cuypers and H. Van T'Spijker. 2014. Experimental results of a 3 kWh thermochemical heat storage module for space heating application. Energy Procedia **48**(0): 320-326.

Formisano, B. 2019. Types of Home Heating Systems. The Spruce. https://www.thespruce.com/types-of-home-heating-systems-1824772 (Date accessed: March 18, 2020).

Fortune Business Insights. 2020. Solar Thermal Market Size, Share & Amp; Industry Analysis, By Collector Type (Evacuated Tube Collector, Flat Plate Collector, Unglazed Water Collector, Air Collector), By Type of System (Thermosiphon Solar Heating Systems, Pumped Solar Heating System) By Application (Domestic Hot Water Systems, Large DHW Systems, Solar Combi Systems, Swimming Pool Heating, Others), and Regional Forecast, 2019-2026.

Gantenbein, P., S. Brunold, F. Flückiger and U. Frei. 2001. Sorbtion materials for application in solar heat energy storage. Rapperswill, Switzerland: University of Applied Science.

Ge, M. and J. Friedrich. 2020. 4 Charts Explain Greenhouse Gas Emissions by Countries and Sectors. World Resources Institute. https://www.wri.org/blog/2020/02/greenhouse-gas-emissions-by-country-sector#:~:text=Global%20annual%20greenhouse%20gas%20emissions,rose%20each%20year%20since%20then. (Date accessed: December 10, 2020).

Global Solar Atlas v2.2. 2020. https://globalsolaratlas.info/map?s=51.845617,-112.148438&m=site&c=11.609193,8.4375,3 (Date accessed: April 22, 2020).

Guangzhou Dongao Electrical Co. 2019. Air New Style Industrial Cold Storage Paper High Quality Ultrasonic Humidifier. alibaba. https://parkoo-china.en.alibaba.com/product/62279810404-212977643/2019_Air_New_Style_Industrial_Cold_Storage_Paper_High_Quality_Ultrasonic_Humidifier.html?spm=a2700.icbuShop.41413.10.302458ce7DD2HT (Date accessed: May 7, 2020).

Hammond, G. and Jones, C. 2008. Inventory of carbon & energy (ICE). http://www.viking-house.ie/downloads/ICE%20Version%201.6a.pdf (Date accessed: April 20, 2021)

Hauer, A. 2007. Adsorption systems for TES—design and demonstration projects. Thermal energy storage for sustainable energy consumption**:** 409-427, Springer.

Hauer, A. 2007. Evaluation of adsorbent materials for heat pump and thermal energy storage applications in open systems. Adsorption **13**(3-4): 399-405.

Home Guide. 2019. How Much Does a New Furnace Replacement Cost? https://homeguide.com/costs/new-furnace-replacement-cost (Date accessed: April 21, 2020).

Horowitz, K. A., R. Fu, T. Silverman, M. Woodhouse, X. Sun and M. A. Alam. 2017. An analysis of the cost and performance of photovoltaic systems as a function of module area, National Renewable Energy Lab.(NREL), Golden, CO (United States).

International Renewable Energy Agency. 2020. Renewable capacity highlights.

Jänchen, J., D. Ackermann, H. Stach and W. Brösicke. 2004. Studies of the water adsorption on zeolites and modified mesoporous materials for seasonal storage of solar heat. Solar Energy **76**(1-3): 339-344.

Kapila, S. 2018. Techno-economic and life cycle assessment of large energy storage systems.

Kerskes, H. 2016. Thermochemical Energy Storage. Storing Energy**:** 345-372, Elsevier.

Kuznik, F., D. Gondre, K. Johannes, C. Obrecht and D. David. 2020. Sensitivity analysis of a zeolite energy storage model: Impact of parameters on heat storage density and discharge power density. Renewable Energy **149**: 468-478.

Kylili, A. and P. A. Fokaides. 2016. Life cycle assessment (LCA) of phase change materials (PCMs) for building applications: a review. Journal of building engineering **6**: 133-143.

Lefebvre, D., P. Amyot, B. Ugur and F. H. Tezel. 2016. Adsorption prediction and modeling of thermal energy storage systems: a parametric study. Industrial & Engineering Chemistry Research **55**(16): 4760-4772.

Lemghalef, L. and J. Sager. 2019. The future of home heating: Hybrid home heating systems offer energy savings and reduce GHG emissions. Natural Resources Canada. https://www.nrcan.gc.ca/simply-science/future-home-heating-hybrid-home-heating-systems-offer-energy-savings-and-reduce-ghg-emissions/22236 (Date accessed: March 18, 2020).

Liu, M. 2017. Valuation Research. Optimal number of trials for Monte Carlo simulation. https://www.valuationresearch.com/wp-content/uploads/kb/SpecialReport_MonteCarloSimulationTrials.pdf (Date accessed: July 26, 2020).

Lu, J., L. Ren, S. Yao, D. Rong, M. Skare and J. Streimikis. 2020. Renewable energy barriers and coping strategies: Evidence from the Baltic States. Sustainable Development **28**(1): 352-367.

Macrotrends. 2020. Canada Inflation Rate 1960-2020. https://www.macrotrends.net/countries/CAN/canada/inflation-rate-cpi#:~:text=Canada%20inflation%20rate%20for%202019,a%200.17%25%20increase%20from%202016. (Date accessed: December 16, 2020).

Mathson, T. and M. Ivanovich. 2011. AMCA's Fan Efficiency Grades: Answers to Frequently Asked Questions. AMCA International 2011: 1-12.

https://www.amca.org/assets/resources/public/userfiles/file/Nospreads_FanEfficGrades.pdf (Date accessed: April 24, 2020).

Matuska, T. 2014. Performance and economic analysis of hybrid PVT collectors in solar DHW system. Energy Procedia **48**(0): 150-156.

Montgomery, R. 1947. Viscosity and thermal conductivity of air and diffusivity of water vapor in air. Journal of Meteorology **4**(6): 193-196.

Moore, F. T. 1959. Economies of scale: Some statistical evidence. The Quarterly Journal of Economics **73**(2): 232-245.

Mugdha, P. 2019. Psychrometric Process (with chart)|Air Conditioning|Thermal Engineering. http://www.engineeringenotes.com/mechanical-engineering/air-conditioning/psychrometric-process-with-chart-air-conditioning-thermal-engineering/50038 (Date accessed: October 3, 2019).

Natural Resources Canada. 2020. Energy and Greenhouse Gas Emissions (GHGs). https://www.nrcan.gc.ca/science-data/data-analysis/energy-data-analysis/energy-facts/energy-and-greenhouse-gas-emissions-ghgs/20063 (Date accessed: July 27, 2020).

Nienborg, B., T. Helling, D. Fröhlich, R. Horn, G. Munz and P. Schossig. 2018. Closed adsorption heat storage—A life cycle assessment on material and component levels. Energies **11**(12): 3421.

Nitkiewicz, A. and R. Sekret. 2014. Comparison of LCA results of low temperature heat plant using electric heat pump, absorption heat pump and gas-fired boiler. Energy conversion and management **87**: 647-652.

Peters, M. S., K. D. Timmerhaus, R. E. West, K. Timmerhaus and R. West. 1968. Plant Design and Economics for Chemical Engineers, McGraw-Hill New York.

Petro Home Services. 2020. When is it time to replace your oil or natural gas furnace? https://www.petro.com/heating/is-it-time-for-a-new-furnace (Date accessed: May 26, 2020).

PickHvac. 2020. HVAC Ductwork Replacement Cost & Ultimate Guide 2020. https://www.pickhvac.com/hvac-ductwork-cost/#Sample_Home_Costs (Date accessed: May 7, 2020).

Pootakham, T. and A. Kumar. 2010. Bio-oil transport by pipeline: A techno-economic assessment. Bioresource technology **101**(18): 7137-7143.

Prieto, C., P. Cooper, A. I. Fernández and L. F. Cabeza. 2016. Review of technology: Thermochemical energy storage for concentrated solar power plants. Renewable and Sustainable Energy Reviews **60**: 909-929.

Ratnayaka, D. D., M. J. Brandt and K. M. Johnson. 2009. Chapter 12 - Hydraulics. Water Supply (Sixth Edition)**:** 463-498. Boston, Butterworth-Heinemann.

Ray Barton & Associates. 2006. Estimation of Costs of Heavy Vehicle Use Per Vehicle-Kilometer.

Reliable Home Advice. 2018. Furnace Lifespan: How Many Years Does a Gas Furnace Last? https://reliablehomeadvice.ca/furnace-lifespan-how-many-years-does-a-gas-furnace-last/ (Date accessed: May 26, 2020).

Scapino, L., C. De Servi, H. A. Zondag, J. Diriken, C. C. Rindt and A. Sciacovelli. 2020. Techno-economic optimization of an energy system with sorption thermal energy storage in different energy markets. Applied Energy **258**: 114063.

Scapino, L., H. A. Zondag, J. Van Bael, J. Diriken and C. C. Rindt. 2017a. Energy density and storage capacity cost comparison of conceptual solid and liquid sorption seasonal heat storage systems for low-temperature space heating. Renewable and Sustainable Energy Reviews **76**: 1314-1331.

Scapino, L., H. A. Zondag, J. Van Bael, J. Diriken and C. C. Rindt. 2017b. Sorption heat storage for long-term low-temperature applications: A review on the advancements at material and prototype scale. Applied Energy **190**: 920-948.

Service Champions. 2018. 7 Home Heating System Types. https://www.servicechampions.net/blog/7-home-heating-system-types/ (Date accessed: March 18, 2020).

Shanghai Jiuzhou Chemicals Co. High Quality Zeolite 13X Price. alibaba. https://www.alibaba.com/product-detail/High-Quality-Zeolite-13X-Price_844340985.html?spm=a2700.details.maylikeexp.1.77226987GhTyMM&fullFirstScreen=true (Date accessed: May 7, 2020).

Smiti. 2019. Concentrated Solar Power Costs Fell 46% From 2010–2018. CleanTechnica. https://cleantechnica.com/2019/06/04/concentrated-solar-power-costs-fell-46-from-2010-2018/ (Date accessed: July 8, 2020).

Sőlken, W. 2020. Effects & Economic impact of Corrosion. Explore the World of Piping. http://www.wermac.org/materials/corrosion_allowance.html#:~:text=The%20corrosion%20allowance%20is%20a,reached%20its%20end%20of%20life. (Date accessed: October 7, 2019).

Statistics Canada. 2019. Canadian Housing Statistics Program. https://www150.statcan.gc.ca/n1/daily-quotidien/190503/dq190503b-eng.htm (Date accessed: December 16, 2020).

Sultana, A., A. Kumar and D. Harfield. 2010. Development of agri-pellet production cost and optimum size. Bioresource Technology **101**(14): 5609-5621.

Thaker, S., A. O. Oni and A. Kumar. 2017. Techno-economic evaluation of solar-based thermal energy storage systems. Energy Conversion and Management **153**: 423-434.

Tiwari, G. 2016. Analysis of series connected photovoltaic thermal air collectors partially covered by semitransparent photovoltaic module. Solar Energy **137**: 452-462.

Tripanagnostopoulos, Y., M. Souliotis, R. Battisti and A. Corrado. 2006. Performance, cost and life-cycle assessment study of hybrid PVT/AIR solar systems. Progress in Photovoltaics: Research and Applications **14**(1): 65-76.

Ugur, B. 2013. Thermal energy storage in adsorbent beds. Master of Applied Science, University of Ottawa.

UKEssays. 2018. Study into the Lifespan of Zeolites. https://www.ukessays.com/essays/sciences/study-into-the-lifespan-of-zeolites.php?vref=1 (Date accessed: December 16, 2020).

Unsdorfer, S. 2015. Managing Ideal Indoor Humidity for Maximum Comfort. Central Heating & Air Conditioning. https://www.centralhtg.com/blog/managing-home-humidity-for-maximum-comfort (Date accessed: October 7, 2019).

Van Alebeek, R., L. Scapino, M. Beving, M. Gaeini, C. Rindt and H. Zondag. 2018. Investigation of a household-scale open sorption energy storage system based on the zeolite 13X/water reacting pair. Applied Thermal Engineering **139**: 325-333.

Wallace, D. 2018. Sciencing. January 9, 2018. Price of Galvanized Steel Vs. Stainless Steel. https://sciencing.com/about-6711987-price-steel-vs--stainless-steel.html (Date accessed: May 7, 2020).

Woodford, C. 2019. Zeolites. https://www.explainthatstuff.com/zeolites.html (Date accessed: March 18, 2020).

World Steel Prices. 2019. Global Composite Steel Price and Index (US$/tonne). https://worldsteelprices.com/ (Date accessed: May 7, 2020).

Yang, L., R. Zmeureanu and H. Rivard. 2008. Comparison of environmental impacts of two residential heating systems. Building and Environment **43**(6): 1072-1081.

Zettl, B., G. Englmair and G. Steinmaurer. 2014. Development of a revolving drum reactor for open-sorption heat storage processes. Applied thermal engineering **70**(1): 42-49.

Zhengzhou Gold Mountain Science and Technique Co. Ltd. 2019. Molecular Sieve Zeolite 13X. http://www.adsorbentcn.com/13x.htm (Date accessed: April 24, 2020).

Zondag, H., V. van Essen, M. Bakker and P. Bach. 2010. An evaluation of the economical feasibility of seasonal sorption heat storage, Petten: ECN.

Chapter 4
Conclusions and recommendations

4.1 Conclusions

Global efforts are being made to reduce the impacts of climate change by transforming the energy system. Space heating is one of the main contributors to GHG emissions in the residential sector. It is necessary to rethink the way energy is sourced and used in the sector. The integration of space heating with renewable energy is among the alternative strategies. The direct use of solar energy for space heating needs an energy storage and conversion system to overcome the intermittency of solar radiation. This research focused on the use of adsorbent-based material in a thermochemical energy storage system integrated with a solar collector to deliver heating to residences in cold climates such as Canada. Most of the existing research is on understanding the physical and chemical characteristics of zeolite 13X-based adsorbent for thermochemical storage applications. There is some information available on the environmental assessment of different heating technologies, but the environmental effect of zeolite 13X for space heating has not been assessed. Moreover, the economic viability of an adsorbent-based system has only been studied for large-scale applications, not for small-scale systems in residential applications. This thesis, therefore, offers a novel contribution by developing a bottom-up life cycle assessment and a techno-economic framework based on first principles to systematically evaluate the environmental sustainability and economic feasibility of zeolite 13X storage connected to air solar collectors for space heating.

A life cycle assessment framework comprising system review, engineering design, and environmental assessment was developed to estimate the net energy ratio and life cycle GHG emissions per kWh of heat delivered. The system is designed to have a capacity of 16 kW with 8 hours of running time. We assumed a lifespan of 20 years, as for most furnaces in the market.

The system generates 0.13 kgCO_2 eq per kWh of heat delivered. The operational phase is responsible for around 71% of total emissions. Upstream emissions, because of the Alberta grid mix electricity consumption in the heating system, are the key drivers. In terms of components, humidifiers are the main component and consume high amounts of electricity to increase the relative humidity of the input air for discharging and regulating the heat throughout the house.

The operational emissions of the zeolite heating system vary significantly when the electricity mix from different provinces in Canada is considered, as shown in Fig. 4.1. In provinces with cleaner gird emissions, the overall GHG emissions could be lower.

Life cycle GHG emissions due to transportation, assembly, and other stages are negligible. Compared to other conventional heating systems in Alberta, the adsorbed-based system has the best environmental performance, as shown in Fig. 2.6. This is because it relies less on Alberta's fossil fuel-dominant electricity gird mix than the conventional system. Gas heating systems perform better than electric ones.

With a net energy ratio of 3.2, the space heating system appears to be it is energy efficient. The net energy ratio value is slightly higher than the low temperature geothermal installation and comparable to large-scale solar-based domestic hot water and space heating systems, which are already commercialized.

Finally, sensitivity and uncertainty analyses were conducted to understand the impact of input parameters of the model on the final output. The 90% confident intervals for GHG emissions and net energy ratio are 90.1-205.4 gCO_2 eq per kWh and 2.26 and 3.36, respectively. The length-to-diameter ratio and pallet diameter are the parameters that influence the results most. In order to achieve optimal results, those parameters need to be well understood and investigated.

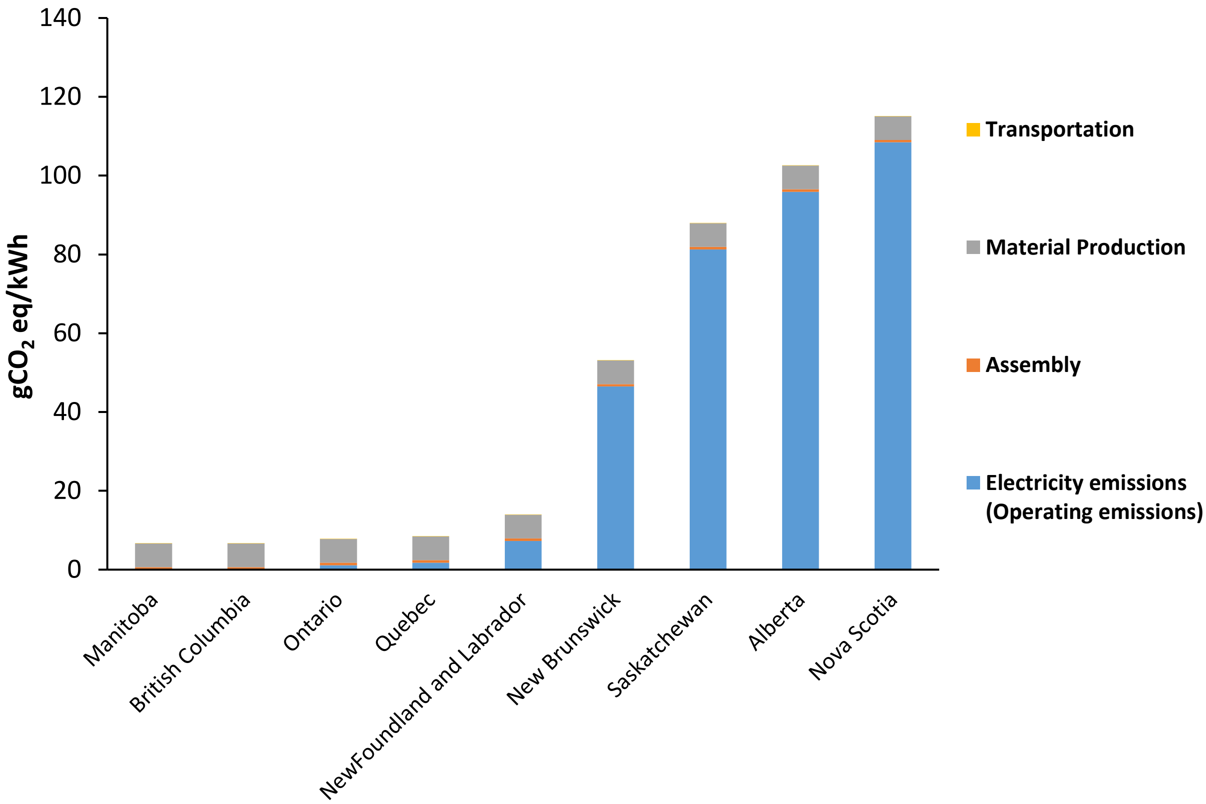

Fig. 4.1: Zeolite-based space heating systems in Canadian provinces

A similar framework was established for the techno-economic modelling. The overall cost per kWh of heat delivery was estimated to be \$0.06, as shown in Fig. 3.8. The solar collector is the main contributor to the capital investment, at 67%. Lowering the solar collector cost would significantly reduce the cost of the whole system. The contributions from the other components are similar, between 7% and 11%.

In Alberta, the zeolite 13X-based heating system costs more than the electric furnace, the gas-fired furnace, and the gas-fired boiler but less than the electric boiler, as shown in Fig. 3.9. The gas-fired furnace seems to be the most economical heating system in Alberta.

A correlation between cost and usable area in a residential house with different systems was established. A scale factor of 0.761 was found, which indicates that the system shows economies of scale. Noticeably, the solar collector is the most influential component on the scale factor. Therefore, improving the solar collector's economies of scale will not only lower the cost/kWh but also enhance the economies of scale of the proposed space heating system.

The sensitive parameters in the techno-economic model were found to be the length-to-diameter ratio, pallet diameter, and solar collector potential (including its efficiency and the solar irradiation potential by region). The 100,000-iteration Monte Carlo simulation indicated that the likely range of values for the base case is between 0.05 and 0.06$/kWh. Overall, the zeolite 13X heating system has strong economic value compared with other systems and hence shows promise.

4.2 Recommendations for future work

The following are the recommendations for future work:

- The data for the solar collector both for the life cycle assessment and techno-economic assessment is from published sources. Because the solar collector is the key component contributing to both cost and emissions, it would be important to study up-to-date solar collector technology with air as the transfer fluid for space heating.
- Experiments considering different temperatures for the input stream and its temperature lift after discharging should be done, as preheating the air before it flows through the adsorbent storage could improve results. Further, this pathway should be assessed.

- The space heating system considered in this study was open cycle. A closed cycle system could also be investigated. Additionally, different adsorbent materials could be tested for energy density, system efficiency, and compatibility with solar energy.
- A study should be conducted to understand the number of heating systems or the optimal heating system versus the larger usable area for commercial buildings.

Bibliography

Acurite. 2017. Acurite. Maintaining Healthy Indoor Air Qualit. https://www.acurite.com/blog/home-monitoring-ideal-temperature-and-humidity-level-in-home (Date accessed: May 7, 2020).

Air Turbine Propeller Co. 2015. Fan Materials & Finishes. http://www.airturbine.com/fan-materials-finishes (Date accessed: April 24, 2020).

Agrawal, S. and G. Tiwari. 2015. Performance analysis in terms of carbon credit earned on annualized uniform cost of glazed hybrid photovoltaic thermal air collector. Solar Energy **115**: 329-340.

Alberta Utilities Commission. 2020. Residential regulated rate option at a glance. http://www.auc.ab.ca/Pages/current-rates-electric.aspx (Date accessed: May 26, 2020).

Andrada, P., B. Blanqué, E. Martínez, J. Perat, J. Sánchez and M. Torrent. 2012. Environmental and life cycle cost analysis of one switched reluctance motor drive and two inverter-fed induction motor drives. IET Electric Power Applications **6**(7): 390-398.

Arrizabalaga, E., P. Hernandez, X. Oregi, L. Mabe and B. Sanchez. 2012. Net energy analysis of geothermal energy installations. Building Sustainability Assessment 2012. Portugal.

Athaudage Dona, N. 2014. Performance of the solar thermal hot water system at the southland leisure centre. Unpublished master's thesis, University of Calgary.

Balmer, R. T. 2011. Modern Engineering Thermodynamics. United State of America, Academic Press.

Bank of Canada. 2020. Currency Converter. https://www.bankofcanada.ca/rates/exchange/currency-converter/?rangeType=dates&rangeValue=1.w&sF=Canadian+dollar&lP=lookup_currency_converter_2017.php&sR=2010-12-16&sTF=to&sT=FXUSDCAD&co=1.00&dF=2020-06-16&dT=2020-12-16 (Date accessed: Dec 17, 2020).

Battisti, R. and A. Corrado. 2005. Evaluation of technical improvements of photovoltaic systems through life cycle assessment methodology. Energy **30**(7): 952-967.

Bennaji, N., I. Mellouki and N. Yacoubi. 2010. Thermal properties of metals alloy by electrical pyroelectric method (EPE). Journal of Physics: Conference Series (Vol. 214, p. 012138). IOP Publishing.

Brendel, M. 2010. The Role of Fan Efficiency in Reducing HVAC Energy Consumption. https://www.amca.org/assets/resources/public/userfiles/file/AMCA_Spring2010RoleOfFE.pdf (Date accessed: April 24, 2020).

Bull Frog Power. 2015. Canadian Emission Factors for Grid Electricity. https://www.bullfrogpower.com/wp-content/uploads/2015/09/2015_bullfrog_power_electricity_emission_calculator.pdf (Date accessed: April 24, 2020).

Burkes, K. 2020. 3A, 4A, 5A, 13X… What's the difference? HengYe Inc. https://hengyeinc.com/3a-4a-5a-13x-whats-the-difference/ (Date accessed: March 18, 2020).

Buy Insulation Products. 2020. Fiberglass pipe insulation. https://www.buyinsulationproductstore.com/Fiberglass-Pipe-Insulation-SSL-ASJ/ (Date accessed: July 26, 2020).

Cabeza, L. F. (ed.) 2014. Advances in thermal energy storage systems: Methods and applications. United Kingdom, Woodhead Publishing Series in Energy 66.

Carbon Dioxide Information Analysis Center. 2017. CDIAC Data. https://cdiac.ess-dive.lbl.gov/ (Date accessed: August 6, 2020).

Center for Climate and Energy Solutions. 2019. Global Emissions. https://www.c2es.org/content/international-emissions/#:~:text=Globally%2C%20the%20primary%20sources%20of,72%20percent%20of%20all%20emissions. (Date accessed: July 20, 2020).

Child, M., D. Bogdanov and C. Breyer. 2018. The role of storage technologies for the transition to a 100% renewable energy system in Europe. Energy Procedia **155**: 44-60.

CIS GmbH Consulting Inspection Services. 2020. Some examples for allowable stress values "S" of typical carbon steels according to Section II, Part D, Table 1A, metric. https://www.cis-inspector.com/asme-code-calculation-allowable-stresses.html (Date accessed: October 7, 2019).

Climate Watch. 2016. Historical GHG Emissions. https://www.wri.org/blog/2020/02/greenhouse-gas-emissions-by-country-sector#:~:text=Global%20annual%20greenhouse%20gas%20emissions,rose%20each%20year%20since%20then. (Date accessed: December 10, 2020).

Coker, A. K. 2014. Ludwig's Applied Process Design for Chemical and Petrochemical Plants, Gulf Professional Publishing.

Colclough, S. and T. McGrath. 2015. Net energy analysis of a solar combi system with Seasonal Thermal Energy Store. Applied Energy **147**: 611-616.

Costimates. 2020. January 8, 2020. Gas Furnace Tune-Up and Seasonal Maintenance Costs. https://www.costimates.com/costs/heating-air-conditioning/furnace-maintenance-tuneup/ (Date accessed: May 26, 2020).

Couper, J., W. Penney, J. Fair and S. Walas. 2010. Chapter 21-Costs of Individual Equipment. Chemical Process Equipment: 717-726.

Craig. 2019. Gas vs Electric Boilers: Pros, Cons, & Recommendations. Appliance Analysts. https://applianceanalysts.com/gas-vs-electric-boilers/ (Date accessed: May 7, 2020).

Dawoud, B., E. H. Amer and D. M. Gross. 2007. Experimental investigation of an adsorptive thermal energy storage. International Journal of Energy Research **31**(2): 135-147.

de Boer, R., S. Smeding, H. Zondag and G. Krol. 2014. Development of a prototype system for seasonal solar heat storage using an open sorption process, Petten: ECN.

Di Lullo, G., E. Gemechu, A. O. Oni and A. Kumar. 2020. Extending sensitivity analysis using regression to effectively disseminate life cycle assessment results. The International Journal of Life Cycle Assessment **25**(2): 222-239.

Díaz-González, F., A. Sumper, O. Gomis-Bellmunt and R. Villafáfila-Robles. 2012. A review of energy storage technologies for wind power applications. Renewable and Sustainable Energy Reviews **16**(4): 2154-2171.

Dicaire, D. and F. H. Tezel. 2011. Regeneration and efficiency characterization of hybrid adsorbent for thermal energy storage of excess and solar heat. Renewable Energy **36**(3): 986-992.

Dicaire, D. and F. H. Tezel. 2013. Use of adsorbents for thermal energy storage of solar or excess heat: improvement of energy density. International Journal of Energy Research **37**(9): 1059-1068.

Direct Energy. 2019. Recommended Thermostat Settings in the Winter. Energy Efficiency. https://www.directenergy.com/learning-center/energy-efficiency/recommended-thermostat-settings-winter (Date accessed: April 22, 2020).

Direct Energy. 2020. Recommended Thermostat Settings in the Winter. Energy Efficiency. https://www.directenergy.com/learning-center/energy-efficiency/recommended-thermostat-settings-winter (Date accessed: April 22, 2020).

Direct Energy. 2020. Your Average House Temperature. https://www.directenergy.ca/learn/recommended-thermostat-settings-winter (Date accessed: Aprill 22, 2020).

ElectricityMap Live. 2019. Climate Impact by Area. https://www.electricitymap.org/?page=map&solar=false&remote=true&wind=false (Date accessed: October 7, 2019).

Engineering ToolBox. 2003. Fans - Efficiency and Power Consumption. https://www.engineeringtoolbox.com/fans-efficiency-power-consumption-d_197.html (Date accessed: October 7, 2019).

Engineering ToolBox. 2003. Ventilation Ducts - Roughness & Surface Coefficients. https://www.engineeringtoolbox.com/surface-roughness-ventilation-ducts-d_209.html (Date accessed: October 7, 2019).

Engineering ToolBox. 2003. Fans - Efficiency and Power Consumption. https://www.engineeringtoolbox.com/fans-efficiency-power-consumption-d_197.html (Date accessed: October 7, 2019).

Engineering ToolBox. 2003. Ventilation Ducts - Roughness & Surface Coefficients. https://www.engineeringtoolbox.com/surface-roughness-ventilation-ducts-d_209.html (Date accessed: October 7, 2019).

Engineering ToolBox. 2008. Ducts - Sheet Metal Gauges. https://www.engineeringtoolbox.com/ductwork-sheet-metal-gauges-d_1157.html (Date accessed: October 8, 2019).

Engineering ToolBox. 2004. Density of Moist Humid Air. https://www.engineeringtoolbox.com/density-air-d_680.html (Date accessed: October 7, 2019).

Environment and Climate Change Canada. 2018. Canada's coal power phase-out reaches another milestone. https://www.canada.ca/en/environment-climate-change/news/2018/12/canadas-coal-power-phase-out-reaches-another-milestone.html (Date accessed: May 14, 2020).

Environment and Climate Change Canada. 2019. Government of Canada releases emissions projections, showing progress towards climate target,. https://www.canada.ca/en/environment-climate-change/news/2019/12/government-of-canada-releases-emissions-projections-showing-progress-towards-climate-target.html (Date accessed: August 6, 2020).

Environment and Natural Resources. 2020. Greenhouse gas emissions. https://www.canada.ca/en/environment-climate-change/services/environmental-indicators/greenhouse-gas-emissions.html (Date accessed: August 4, 2020).

EPCOR. 2020. Multi-Residential and Commercial Rates. https://www.epcor.com/products-services/water/rates-terms-conditions/Pages/commercial-multi-residential-rates.aspx (Date accessed: May 26, 2020).

Fathi, M., A. Mefoued, A. Messaoud and Y. Boukennous. 2009. Cost-effective photovoltaics with silicon material. Physics Procedia **2**(3): 751-757.

Finck, C., E. Henquet, C. van Soest, H. Oversloot, A.-J. de Jong, R. Cuypers and H. Van T'Spijker. 2014. Experimental results of a 3 kWh thermochemical heat storage module for space heating application. Energy Procedia **48**(0): 320-326.

Formisano, B. 2019. Types of Home Heating Systems. The Spruce. https://www.thespruce.com/types-of-home-heating-systems-1824772 (Date accessed: March 18, 2020).

Fortune Business Insights. 2020. Solar Thermal Market Size, Share & Amp; Industry Analysis, By Collector Type (Evacuated Tube Collector, Flat Plate Collector, Unglazed Water Collector, Air Collector), By Type of System (Thermosiphon Solar Heating Systems, Pumped Solar Heating System) By Application (Domestic Hot Water Systems, Large DHW Systems, Solar Combi Systems, Swimming Pool Heating, Others), and Regional Forecast, 2019-2026.

Fthenakis, V. and E. Alsema. 2006. Photovoltaics energy payback times, greenhouse gas emissions and external costs: 2004–early 2005 status. Progress in Photovoltaics: Research and Applications **14**(3): 275-280.

Fu, Y., X. Liu and Z. Yuan. 2015. Life-cycle assessment of multi-crystalline photovoltaic (PV) systems in China. Journal of Cleaner Production **86**: 180-190.

Furnace Depot. 2016. BTU Charts. http://furnacedepot.ca/btu-charts/ (Date accessed: September 26, 2019).

Gantenbein, P., S. Brunold, F. Flückiger and U. Frei. 2001. Sorbtion materials for application in solar heat energy storage. Rapperswill, Switzerland: University of Applied Science.

Ge, M. and J. Friedrich. 2020. 4 Charts Explain Greenhouse Gas Emissions by Countries and Sectors. World Resources Institute. https://www.wri.org/blog/2020/02/greenhouse-gas-emissions-by-country-sector#:~:text=Global%20annual%20greenhouse%20gas%20emissions,rose%20each%20year%20since%20then. (Date accessed: December 10, 2020).

Global Solar Atlas v2.2. 2020. https://globalsolaratlas.info/map?s=51.845617,-112.148438&m=site&c=11.609193,8.4375,3 (Date accessed: April 22, 2020).

Government of Canada. 2021. Net-Zero Emissions by 2050. https://www.canada.ca/en/services/environment/weather/climatechange/climate-plan/net-zero-emissions-2050.html (Date accessed: April 24, 2021).

Guangzhou Dongao Electrical Co. 2019. Air New Style Industrial Cold Storage Paper High Quality Ultrasonic Humidifier. alibaba. https://parkoo-china.en.alibaba.com/product/62279810404-212977643/2019_Air_New_Style_Industrial_Cold_Storage_Paper_High_Quality_Ultrasonic_Humidifier.html?spm=a2700.icbuShop.41413.10.302458ce7DD2HT (Date accessed: May 7, 2020).

Hammond, G. and Jones, C. 2008. Inventory of carbon & energy (ICE). http://www.viking-house.ie/downloads/ICE%20Version%201.6a.pdf (Date accessed: April 20, 2021)

Hauer, A. 2007. Adsorption systems for TES—design and demonstration projects. Thermal energy storage for sustainable energy consumption**:** 409-427, Springer.

Hauer, A. 2007. Evaluation of adsorbent materials for heat pump and thermal energy storage applications in open systems. Adsorption **13**(3-4): 399-405.

Heaps, C. 2012. Somerville, MA, USA. Long-range Energy Alternatives Planning (LEAP) system. Stockholm Environment Institute. [Software version 2017.0. 4.0]. http://sei-us.org/Publications_PDF/SEI-LEAP-brochure-Jan2012.pdf (Date accessed: May 5, 2019).

Home Guide. 2019. How Much Does a New Furnace Replacement Cost? https://homeguide.com/costs/new-furnace-replacement-cost (Date accessed: April 21, 2020).

Horn, R., M. Burr, D. Fröhlich, S. Gschwander, M. Held, J. P. Lindner, G. Munz, B. Nienborg and P. Schossig. 2018. Life cycle assessment of innovative materials for thermal energy storage in buildings. Procedia CIRP **69**: 206-211.

Horowitz, K. A., R. Fu, T. Silverman, M. Woodhouse, X. Sun and M. A. Alam. 2017. An analysis of the cost and performance of photovoltaic systems as a function of module area, National Renewable Energy Lab.(NREL), Golden, CO (United States).

Hua, Y., B. Ugur and F. H. Tezel. 2019. Adsorbent screening for thermal energy storage application. Solar Energy Materials and Solar Cells **196**: 119-123.

International Energy Agency. 2019. World Energy Outlook 2019. (Date accessed: August 6, 2020).

International Energy Agency. 2020. Global CO2 emissions in 2019. https://www.iea.org/articles/global-co2-emissions-in-2019 (Date accessed: June 25, 2020).

International Organization for Standardization. 2006a. ISO 14040 International Standard-Environmental Management-Life Cycle Assessment-Principles and Framework, Geneva, Switzerland. https://www.iso.org/obp/ui/#iso:std:iso:14040:ed-2:v1:en (Date accessed: September 1, 2019).

International Organization for Standardization. 2006b. Environmental Management: Life Cycle Assessment; Requirements and Guidelines. ISO Geneva. https://www.iso.org/obp/ui/#iso:std:iso:14044:ed-1:v1:en (Date accessed: September 1, 2019).

International Renewable Energy Agency. 2020. Renewable capacity highlights.

Jänchen, J., D. Ackermann, H. Stach and W. Brösicke. 2004. Studies of the water adsorption on zeolites and modified mesoporous materials for seasonal storage of solar heat. Solar Energy **76**(1-3): 339-344.

Jänchen, J., K. Schumann, E. Thrun, A. Brandt, B. Unger and U. Hellwig. 2012. Preparation, hydrothermal stability and thermal adsorption storage properties of binderless zeolite beads. International Journal of Low-Carbon Technologies **7**(4): 275-279.

Jelle, B. P. 2016. Nano-based thermal insulation for energy-efficient buildings. Start-Up Creation**:** 129-181, Elsevier.

Johannes, K., F. Kuznik, J.-L. Hubert, F. Durier and C. Obrecht. 2015. Design and characterisation of a high powered energy dense zeolite thermal energy storage system for buildings. Applied Energy **159**: 80-86.

Kalair, A., N. Abas, M. S. Saleem, A. R. Kalair and N. Khan. 2020. Role of energy storage systems in energy transition from fossil fuels to renewables. Energy Storage: e135.

Kapila, S. 2018. Techno-economic and life cycle assessment of large energy storage systems.

Kerskes, H. 2016. Thermochemical Energy Storage. Storing Energy**:** 345-372, Elsevier.

Kriegler, E., J. P. Weyant, G. J. Blanford, V. Krey, L. Clarke, J. Edmonds, A. Fawcett, G. Luderer, K. Riahi and R. Richels. 2014. The role of technology for achieving climate policy objectives:

overview of the EMF 27 study on global technology and climate policy strategies. Climatic Change **123**(3-4): 353-367.

Krishna, R., B. Smit and S. Calero. 2002. Entropy effects during sorption of alkanes in zeolites. Chemical Society Reviews **31**(3): 185-194.

Kuznik, F., D. Gondre, K. Johannes, C. Obrecht and D. David. 2020. Sensitivity analysis of a zeolite energy storage model: Impact of parameters on heat storage density and discharge power density. Renewable Energy **149**: 468-478.

Kylili, A. and P. A. Fokaides. 2016. Life cycle assessment (LCA) of phase change materials (PCMs) for building applications: a review. Journal of building engineering **6**: 133-143.

Lefebvre, D., P. Amyot, B. Ugur and F. H. Tezel. 2016. Adsorption prediction and modeling of thermal energy storage systems: a parametric study. Industrial & Engineering Chemistry Research **55**(16): 4760-4772.

Lemghalef, L. and J. Sager. 2019. The future of home heating: Hybrid home heating systems offer energy savings and reduce GHG emissions. Natural Resources Canada. https://www.nrcan.gc.ca/simply-science/future-home-heating-hybrid-home-heating-systems-offer-energy-savings-and-reduce-ghg-emissions/22236 (Date accessed: March 18, 2020).

Liu, M. 2017. Valuation Research. Optimal number of trials for Monte Carlo simulation. https://www.valuationresearch.com/wp-content/uploads/kb/SpecialReport_MonteCarloSimulationTrials.pdf (Date accessed: July 26, 2020).

Lu, J., L. Ren, S. Yao, D. Rong, M. Skare and J. Streimikis. 2020. Renewable energy barriers and coping strategies: Evidence from the Baltic States. Sustainable Development **28**(1): 352-367.

Macrotrends. 2020. Canada Inflation Rate 1960-2020. https://www.macrotrends.net/countries/CAN/canada/inflation-rate-cpi#:~:text=Canada%20inflation%20rate%20for%202019,a%200.17%25%20increase%20from%202016. (Date accessed: December 16, 2020).

Mathson, T. and M. Ivanovich. 2011. AMCA's Fan Efficiency Grades: Answers to Frequently Asked Questions. AMCA International 2011: 1-12. https://www.amca.org/assets/resources/public/userfiles/file/Nospreads_FanEfficGrades.pdf (Date accessed: April 24, 2020).

Matuska, T. 2014. Performance and economic analysis of hybrid PVT collectors in solar DHW system. Energy Procedia **48**(0): 150-156.

McDonald, A. G. and H. Magande. 2012. Introduction to Thermo-fluids Systems Design. United States of America, John Wiley & Sons.

Mehari, A., Z. Xu and R. Wang. 2020. Thermal energy storage using absorption cycle and system: a comprehensive review. Energy Conversion and Management **206**: 112482.

Melillo, J. M, T. T. C. Richmond and G. W. Yohe. 2014. Climate Change Impacts in the United States: The Third National Climate Assessment. United States of America, U.S. Global Change Research Program.

Miller, P. and A. Kumar. 2013. Development of emission parameters and net energy ratio for renewable diesel from Canola and Camelina. Energy **58**: 426-437.

Montgomery, R. 1947. Viscosity and thermal conductivity of air and diffusivity of water vapor in air. Journal of Meteorology **4**(6): 193-196.

Moore, F. T. 1959. Economies of scale: Some statistical evidence. The Quarterly Journal of Economics **73**(2): 232-245.

Mugdha, P. 2019. Psychrometric Process (with chart)|Air Conditioning|Thermal Engineering. http://www.engineeringenotes.com/mechanical-engineering/air-conditioning/psychrometric-process-with-chart-air-conditioning-thermal-engineering/50038 (Date accessed: October 3, 2019).

NASA. 2020. Climate Change: How Do We Know? National Aeronautics and Space Administration (NASA). https://climate.nasa.gov/evidence/ (Date accessed: June 27, 2019).

Natural Resources Canada. 2019. Energy Efficiency Trends in Canada 1990 to 2013. Office of Energy Efficiency. https://www.nrcan.gc.ca/energy/publications/19030 (Date accessed: October 31, 2019).

Natural Resources Canada. 2020. Energy and Greenhouse Gas Emissions (GHGs). https://www.nrcan.gc.ca/science-data/data-analysis/energy-data-analysis/energy-facts/energy-and-greenhouse-gas-emissions-ghgs/20063 (Date accessed: July 27, 2020).

Nave, R. 2017. Relative Humidity. http://hyperphysics.phy-astr.gsu.edu/hbase/Kinetic/relhum.html (Date accessed: October 4, 2019).

Nienborg, B., T. Helling, D. Fröhlich, R. Horn, G. Munz and P. Schossig. 2018. Closed adsorption heat storage—A life cycle assessment on material and component levels. Energies **11**(12): 3421.

Nitkiewicz, A. and R. Sekret. 2014. Comparison of LCA results of low temperature heat plant using electric heat pump, absorption heat pump and gas-fired boiler. Energy conversion and management **87**: 647-652.

Orlova, S., A. Rassõlkin, A. Kallaste, T. Vaimann and A. Belahcen. 2016. Lifecycle analysis of different motors from the standpoint of environmental impact. Latvian Journal of Physics and Technical Sciences **53**(6): 37-46.

Peters, M. S., K. D. Timmerhaus, R. E. West, K. Timmerhaus and R. West. 1968. Plant Design and Economics for Chemical Engineers, McGraw-Hill New York.

Petro Home Services. 2020. When is it time to replace your oil or natural gas furnace? https://www.petro.com/heating/is-it-time-for-a-new-furnace (Date accessed: May 26, 2020).

PickHvac. 2020. HVAC Ductwork Replacement Cost & Ultimate Guide 2020. https://www.pickhvac.com/hvac-ductwork-cost/#Sample_Home_Costs (Date accessed: May 7, 2020).

Pootakham, T. and A. Kumar. 2010. Bio-oil transport by pipeline: A techno-economic assessment. Bioresource technology **101**(18): 7137-7143.

Prieto, C., P. Cooper, A. I. Fernández and L. F. Cabeza. 2016. Review of technology: Thermochemical energy storage for concentrated solar power plants. Renewable and Sustainable Energy Reviews **60**: 909-929.

Ratnayaka, D. D., M. J. Brandt and K. M. Johnson. 2009. Chapter 12 - Hydraulics. Water Supply (Sixth Edition)**:** 463-498. Boston, Butterworth-Heinemann.

Ray Barton & Associates. 2006. Estimation of Costs of Heavy Vehicle Use Per Vehicle-Kilometer.

Reliable Home Advice. 2018. Furnace Lifespan: How Many Years Does a Gas Furnace Last? https://reliablehomeadvice.ca/furnace-lifespan-how-many-years-does-a-gas-furnace-last/ (Date accessed: May 26, 2020).

Rogelj, J., G. Luderer, R. C. Pietzcker, E. Kriegler, M. Schaeffer, V. Krey and K. Riahi. 2015. Energy system transformations for limiting end-of-century warming to below 1.5 C. Nature Climate Change **5**(6): 519.

Sandomierski, M., B. Strzemiecka and A. Voelkel. 2020. The influence of ion exchange in zeolite X on the properties of phenol-formaldehyde composites. International Journal of Adhesion and Adhesives: 102625.

Scapino, L., C. De Servi, H. A. Zondag, J. Diriken, C. C. Rindt and A. Sciacovelli. 2020. Techno-economic optimization of an energy system with sorption thermal energy storage in different energy markets. Applied Energy **258**: 114063.

Scapino, L., H. A. Zondag, J. Van Bael, J. Diriken and C. C. Rindt. 2017a. Energy density and storage capacity cost comparison of conceptual solid and liquid sorption seasonal heat storage systems for low-temperature space heating. Renewable and Sustainable Energy Reviews **76**: 1314-1331.

Scapino, L., H. A. Zondag, J. Van Bael, J. Diriken and C. C. Rindt. 2017b. Sorption heat storage for long-term low-temperature applications: A review on the advancements at material and prototype scale. Applied Energy **190**: 920-948.

Schumann, K., B. Unger, A. Brandt and F. Scheffler. 2012. Investigation on the pore structure of binderless zeolite 13× shapes. Microporous and Mesoporous Materials **154**: 119-123.

Sedgwick. 2020. How Long Does It Take to Replace a Furnace & When to Replace It? https://www.sedgwickheating.com/long-furnace-last-know-replace/#:~:text=The%20average%20lifespan%20of%20a,is%20approximately%2015%2D20%20years (Date accessed: December 10, 2020).

Seo, Y., M. Suzuki, T. Takagi and K. Dowaki. 2019. Life-cycle assessment of adsorbents for biohydrogen production. Resources **8**(1): 52.

Service Champions. 2018. 7 Home Heating System Types. https://www.servicechampions.net/blog/7-home-heating-system-types/ (Date accessed: March 18, 2020).

Shanghai Jiuzhou Chemicals Co. High Quality Zeolite 13X Price. alibaba. https://www.alibaba.com/product-detail/High-Quality-Zeolite-13X-Price_844340985.html?spm=a2700.details.maylikeexp.1.77226987GhTyMM&fullFirstScreen=true (Date accessed: May 7, 2020).

Sharp, A. 2019. Alberta's NDP government says emissions reductions prove carbon pricing works. The National Observer. https://www.nationalobserver.com/2019/02/20/news/albertas-ndp-government-says-emissions-reductions-prove-carbon-pricing-works (Date accessed: April 24, 2020).

Smiti. 2019. Concentrated Solar Power Costs Fell 46% From 2010–2018. CleanTechnica. https://cleantechnica.com/2019/06/04/concentrated-solar-power-costs-fell-46-from-2010-2018/ (Date accessed: July 8, 2020).

Socaciu, L. G. 2011. Seasonal sensible thermal energy storage solutions. Leonardo Electronic Journal of Practices and Technologies **19**: 49-68.

Sőlken, W. 2020. Effects & Economic impact of Corrosion. Explore the World of Piping. http://www.wermac.org/materials/corrosion_allowance.html#:~:text=The%20corrosion%20allowance%20is%20a,reached%20its%20end%20of%20life. (Date accessed: October 7, 2019).

Statistics Canada. 2011. Households and the Environment: Energy Use. https://www150.statcan.gc.ca/n1/en/pub/11-526-s/11-526-s2013002-eng.pdf?st=rCDt1deo (Date accessed: December 20, 2020).

Statistics Canada. 2019. Canadian Housing Statistics Program. https://www150.statcan.gc.ca/n1/daily-quotidien/190503/dq190503b-eng.htm (Date accessed: December 16, 2020).

Sultana, A., A. Kumar and D. Harfield. 2010. Development of agri-pellet production cost and optimum size. Bioresource Technology **101**(14): 5609-5621.

Tatsidjodoung, P., N. Le Pierrès, J. Heintz, D. Lagre, L. Luo and F. Durier. 2016. Experimental and numerical investigations of a zeolite 13X/water reactor for solar heat storage in buildings. Energy Conversion and Management **108**: 488-500.

Thaker, S., A. O. Oni and A. Kumar. 2017. Techno-economic evaluation of solar-based thermal energy storage systems. Energy Conversion and Management **153**: 423-434.

The United Nations. 2016. The Paris Agreement. https://unfccc.int/process-and-meetings/the-paris-agreement/the-paris-agreement (Date accessed: June 27, 2019).

Tiwari, G. 2016. Analysis of series connected photovoltaic thermal air collectors partially covered by semitransparent photovoltaic module. Solar Energy **137**: 452-462.

Tonkens, A. 2020. How Long Does a Furnace Last in Canada? Cansumer. https://cansumer.ca/how-long-does-a-furnace-last-canada/ (Date accessed: December 10, 2020).

Toth, A. and E. Bobok. 2016. Flow and Heat Transfer in Geothermal Systems: Basic Equations for Describing and Modeling Geothermal Phenomena and Technologies, Elsevier.

Tripanagnostopoulos, Y., M. Souliotis, R. Battisti and A. Corrado. 2006. Performance, cost and life-cycle assessment study of hybrid PVT/AIR solar systems. Progress in Photovoltaics: Research and Applications **14**(1): 65-76.

Ugur, B. 2013. Thermal energy storage in adsorbent beds. Master of Applied Science, University of Ottawa.

UKEssays. 2018. Study into the Lifespan of Zeolites. https://www.ukessays.com/essays/sciences/study-into-the-lifespan-of-zeolites.php?vref=1 (Date accessed: December 16, 2020).

Unsdorfer, S. 2015. Managing Ideal Indoor Humidity for Maximum Comfort. Central Heating & Air Conditioning. https://www.centralhtg.com/blog/managing-home-humidity-for-maximum-comfort (Date accessed: October 7, 2019).

U.S. Department of Energy. 2020. Active Solar Heating. https://www.energy.gov/energysaver/home-heating-systems/active-solar-heating (Date accessed: August 6, 2020).

U.S. Energy Information Administration. How much carbon dioxide is produced per kilowatthour of U.S. electricity generation? EIA. https://www.eia.gov/tools/faqs/faq.php?id=74&t=11 (Date accessed: April 24, 2020).

Van Alebeek, R., L. Scapino, M. Beving, M. Gaeini, C. Rindt and H. Zondag. 2018. Investigation of a household-scale open sorption energy storage system based on the zeolite 13X/water reacting pair. Applied Thermal Engineering **139**: 325-333.

Wadkar, V., S. Malgave, D. Patil, H. Bhore and P. Gavade. 2015. Design and analysis of pressure vessel using ANSYS. Journal of Mechanical Engineering and Technology (JMET) **3**(2): 01-13.

Wallace, D. 2018. Sciencing. January 9, 2018. Price of Galvanized Steel Vs. Stainless Steel. https://sciencing.com/about-6711987-price-steel-vs--stainless-steel.html (Date accessed: May 7, 2020).

Wang, M. 2018. Argonne National Laboratory. Fuel Cell GREET1 Model. Center for Transportation Research. https://greet.es.anl.gov/ (Date accessed: October 7, 2019).

Weather & Climate. 2019. Climate and Average Weather in Canada. https://weather-and-climate.com/average-monthly-Rainfall-Temperature-Sunshine-in-Canada (Date accessed: June 25, 2020).

Woodford, C. 2019. Zeolites. https://www.explainthatstuff.com/zeolites.html (Date accessed: March 18, 2020).

World Steel Prices. 2019. Global Composite Steel Price and Index (US$/tonne). https://worldsteelprices.com/ (Date accessed: May 7, 2020).

World Resources Institute. 2017. Climate Analysis Indicators Tool. http://cait.wri.org/ (Date accessed: August 6, 2020).

Yang, L., R. Zmeureanu and H. Rivard. 2008. Comparison of environmental impacts of two residential heating systems. Building and Environment **43**(6): 1072-1081.

Zettl, B., G. Englmair and G. Steinmaurer. 2014. Development of a revolving drum reactor for open-sorption heat storage processes. Applied thermal engineering **70**(1): 42-49.

Zhang, H., J. Baeyens, G. Caceres, J. Degreve and Y. Lv. 2016. Thermal energy storage: Recent developments and practical aspects. Progress in Energy and Combustion Science **53**: 1-40.

Zhengzhou Gold Mountain Science and Technique Co. Ltd. 2019. Molecular Sieve Zeolite 13X. http://www.adsorbentcn.com/13x.htm (Date accessed: April 24, 2020).

Zondag, H., V. van Essen, M. Bakker and P. Bach. 2010. An evaluation of the economical feasibility of seasonal sorption heat storage, Petten: ECN.

Appendix

$$\rho = \frac{\rho_{da}(1+x)}{1+1.609x} \quad where \quad \rho_{da} = \frac{p}{R_a T} \qquad \text{A1}$$

$$Re = \frac{\rho V D}{\mu} \qquad \text{A2}$$

$$\frac{1}{\sqrt{f}} = -2log_{10}\left(\frac{e}{3.7\,D} + \frac{2.51}{Re\sqrt{f}}\right) \qquad \text{A3}$$

$$f = \frac{64}{Re} \qquad \text{A4}$$

$$\frac{\mu}{\mu_0} = \frac{T_0 + C}{T + C}\left(\frac{T}{T_0}\right)^{\frac{3}{2}} \qquad \text{A5}$$

$$\triangle p = \frac{150\,\mu\,L}{D_p^2}\frac{(1-\epsilon)^2}{\epsilon^3}v_s + \frac{1.75\,L\,\rho}{D_p}\frac{(1-\epsilon)}{\epsilon^3}v_s^2 \qquad \text{A6}$$

$$h = f\,\frac{L\,V^2}{2\,g\,D} \qquad \text{A7}$$

Where,

ρ_{da}	is the dry air density
ρ	is the humid air density
x	is the humidity ratio
T	is the temperature
Re	is the Reynolds number
V	is the velocity
μ	is the dynamic viscosity of the air
e	is the roughness
D	is the diameter of duct
f	is the friction factor
μ	is the dynamic viscosity
μ_o	is the reference dynamic viscosity
T	is the absolute temperature
T_0	is the reference absolute temperature
C	is the Sutherland constant
V	is the velocity
$\triangle p$	is the pressure drop across packed bed
L	is the length of container

ϵ is the void fraction of the bed
ρ is the density of the air
v_s is the superficial velocity
g is the gravitational acceleration
h is the head loss

$$\text{System capacity} = (\text{Usable area}) * (\text{Heating factor due to climate}) \quad \text{A8}$$

$$\text{Air flow rate} = (\text{Usable area})*(\text{Ceiling height})*(\text{Number of air exchanges per hour}) \quad \text{A9}$$

$$\text{Total energy required} = \text{Power rating (kW)} * \text{Usage duration (hours)} \quad \text{A10}$$

$$\frac{m_1}{m_2} = \frac{h_3 - h_2}{h_1 - h_3} = \frac{w_3 - w_2}{w_1 - w_3} \quad \text{A11}$$

$$\text{Volume of container needed} = \frac{\text{Energy Required (kWh)}}{\text{Energy Density of Adsorbent (kWh/m}^3)} \quad \text{A12}$$

$$Fan\ Power = \frac{Pressure\ (Pa) * Volume\ Flowrate(m^3/s)}{Efficiency\ (\%)} \quad \text{A13}$$

$$Vapor\ Density = 5.018 + 0.32321T_C + 8.1847 * 10^{-3}T_C^2 + 3.1243 * 10^{-4}T_C^3 \quad \text{A14}$$

$$t = \frac{P\ r_i}{SE_j - 0.6\ P} + C_c \quad \text{A15}$$

Where

T_c is the temperature
t is the thickness of the container
C_c is the allowance for corrosion
P is the maximum allowable internal pressure
r_i is the inside radius
S is the maximum allowable working stress
E_j is the efficiency of joints

Table A1: Solar collector information

Parameter	**Value**	**Unit**
Energy needed	38.9	m^2
Emissions per collector area	15.9	$kgCO_2/m^2$-yr
Primary energy per m^2	4.5	GJ/m^2
Primary energy	175.1	GJ

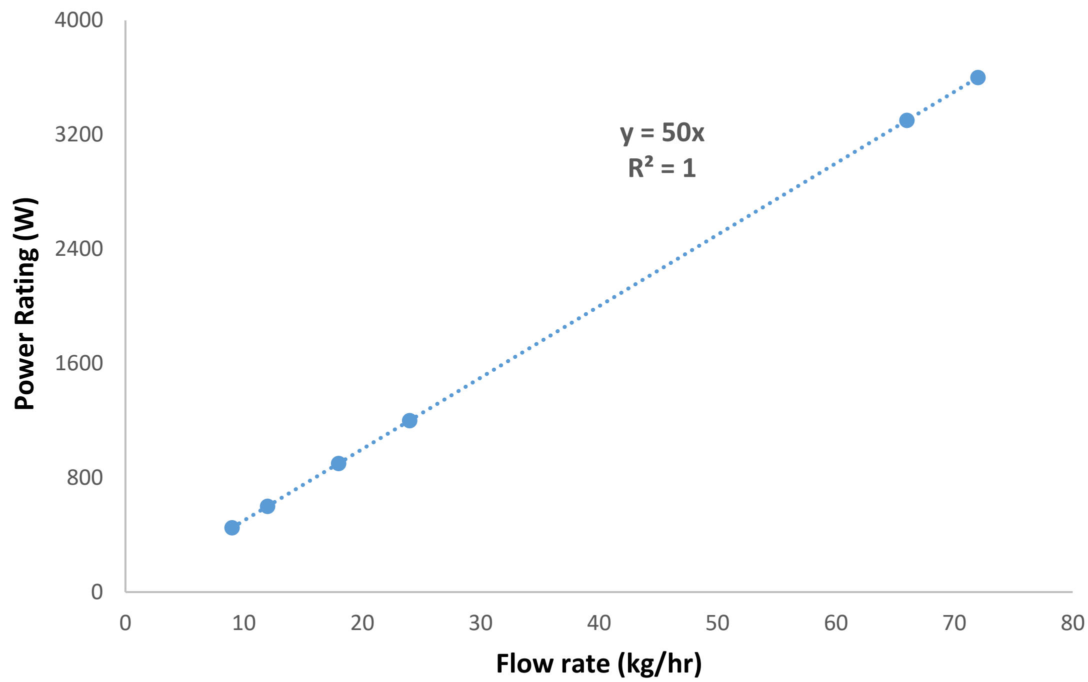

Figure A1: Flow rate versus power rating graph of humidifiers

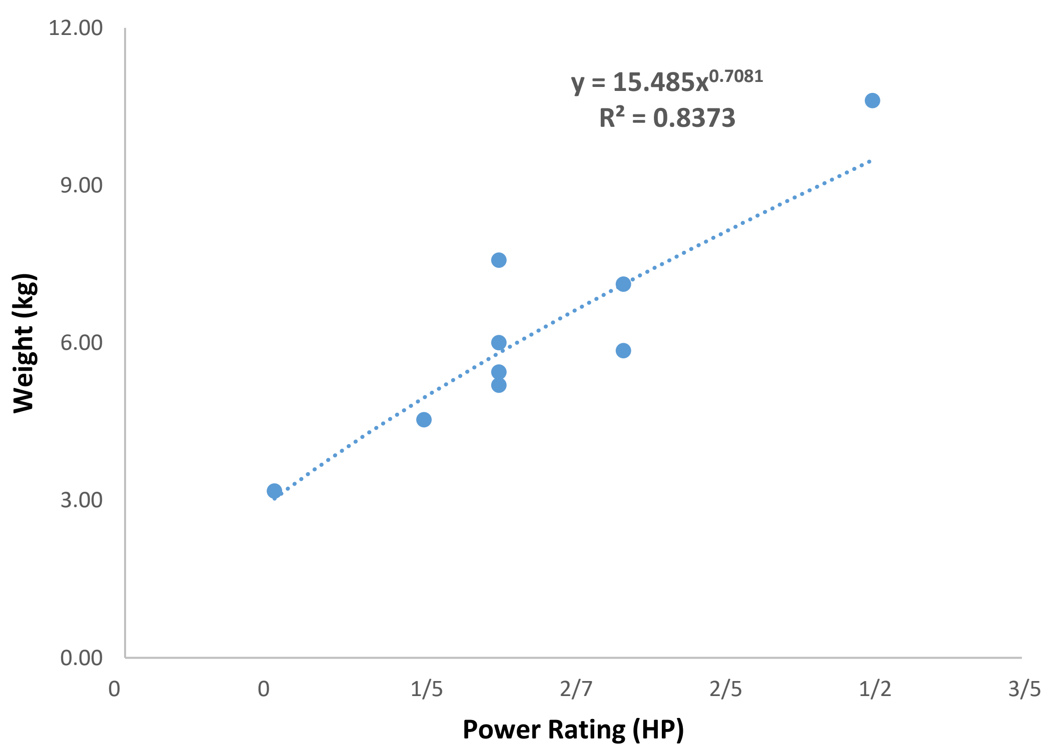

Figure A2: Power rating versus weight of fans

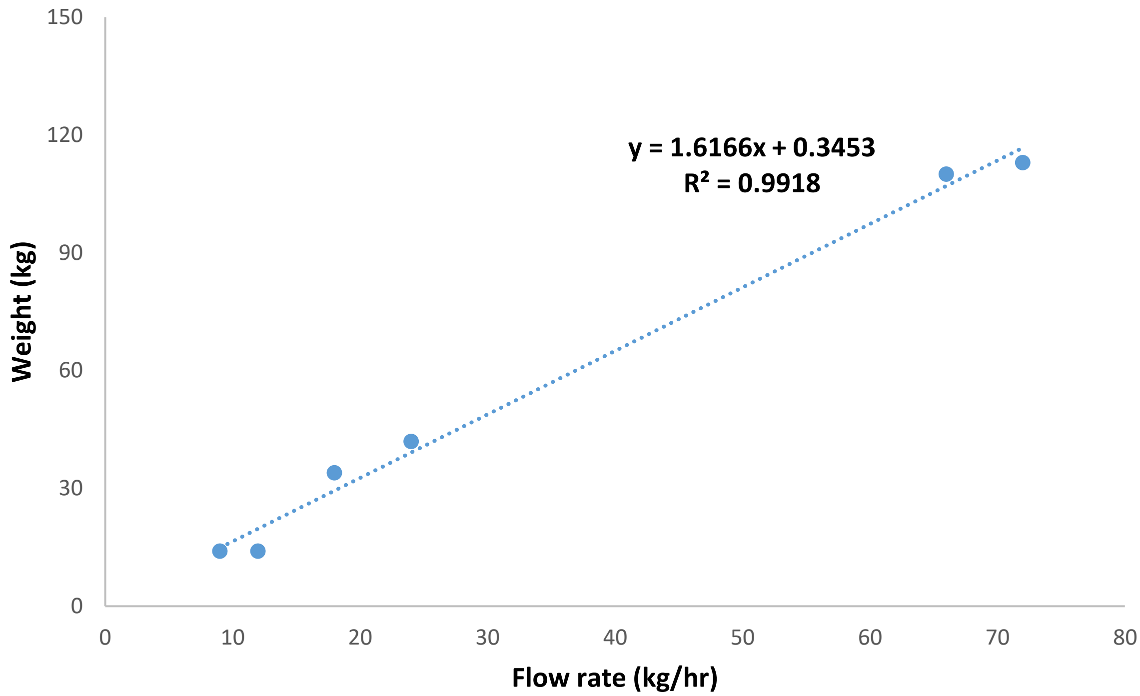

Figure A3: **Flow rate versus weight of humidifiers**

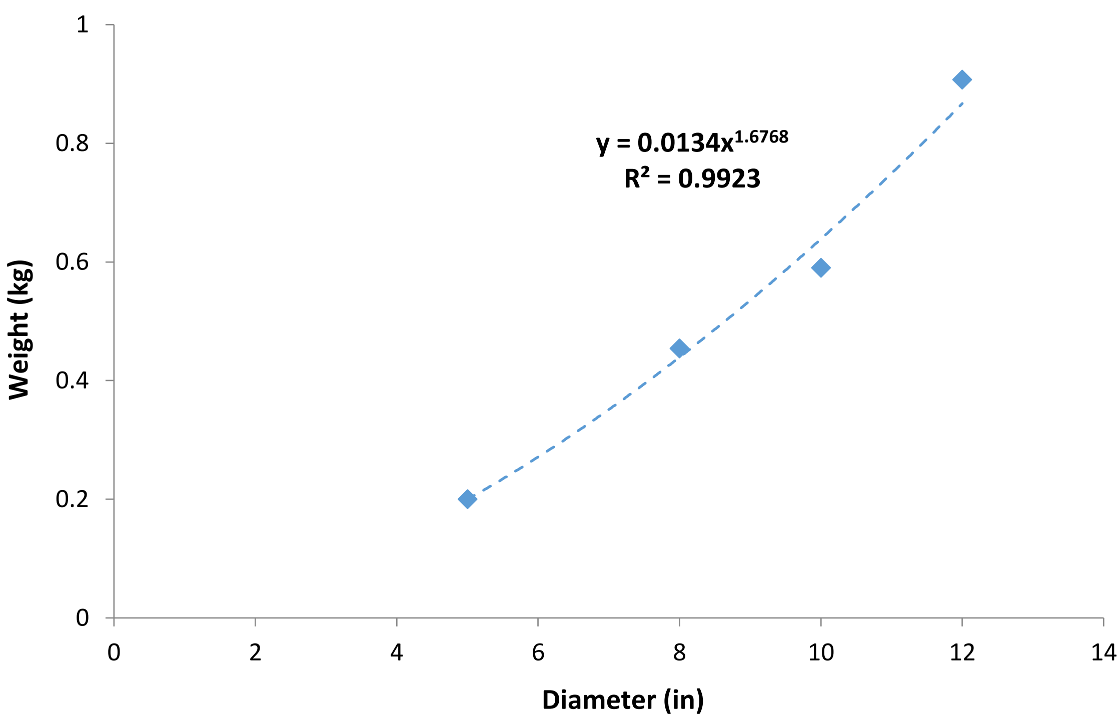

Figure A4: **Diameter versus weight of dampers (amazon.ca)**